Bournemouth University

MRes Thesis

Thesis Title:

An evaluation of Image-Based Modelling for metrically recording cultural heritage subjects suitably to enable further use in geomatics, geoinformatics, and digital humanities.

WORD COUNT **22,965**

Author:

Richard Rowley,

Faculty of Science & Technology

Submission Date:

Monday 25th January 2021

This thesis has been submitted as a partial requirement for the award of the degree Master of Research, Bournemouth University, 2021

Author's Declaration

I have read, understood, and complied with the Code of Practice of Research Degrees, issued by the Doctoral College, Bournemouth University for the academic year 2018-19. Additionally, my Research Ethics and Risk Assessments were discussed and agreed with my academic supervisor, and my Ethics Checklist was subsequently approved by Bournemouth University's Faculty of Science & Technology.

During my enrolment at Bournemouth University I have not been enrolled at any other academic institution, nor has any material in this Thesis been used in any other submission for an academic award. All material in this Thesis, where not self-generated, has been appropriately referenced both in the text and within the list of references at the end of the main text of this Thesis.

This Thesis has been submitted following a successful viva voce as a partial requirement for the award of the degree Master of Research at Bournemouth University 2017-2021. The author of this Thesis was supervised by Professor Dave Parham, Faculty of Science & Technology, Bournemouth University.

This Thesis was submitted by Richard Rowley on 25th January 2021.

Copyright Statement:

Abstract: An evaluation of Image-Based Modelling for metrically recording cultural heritage subjects suitably to enable further use in geomatics, geoinformatics, and digital humanities.

MRes Thesis submitted by Richard Rowley, Faculty of Science & Technology, Bournemouth University, 25th January 2021.

Image-Based Modelling (IBM) produces 3D models using Structure-from-Motion (SfM) to extrapolate geometry from sets of photographs in combination with additional spatial data for scaling and orientation. This project examines the extent to which such models of cultural heritage subjects may be created to quantifiable levels of accuracy to enable their further use for scientific study, archival record or wider dissemination and promotion. It also aims to further the potential impact of citizen scientists.

Demonstrably accurate datasets may also contribute to the management of at-risk in-situ material in high energy marine or coastal environments, as well as being a viable methodology for preservation by record; so long as the results can be demonstrated to be accurate. To date, much literature has considered the potential applications of such datasets, but much less research has focused on technical standards, quantitative assessments of accuracy, or the development of creator-level evaluation methodologies.

Key Words:

Photogrammetry; Image Based Modelling (IBM); Structure-from-Motion (SfM); in-situ Recording of Cultural Heritage; Quantitative Methodologies; Geomatics; Geoinformatics; Microsoft *Excel*; Direct Survey Method; Digital Humanities; Marine, Coastal and Underwater Archaeology; Citizen Science.

Table of Contents

List of Figures

Chapter 1. Project Introduction

Although written to aid volunteers and professionals alike and specifically considering divers working underwater who are engaged in recording maritime heritage subjects, the core purpose of this project relates to the production and evaluation of demonstrably accurate point-clouds of heritage subjects.

The role of professionals within archaeology, the wider cultural heritage sector, or the perhaps more academic discipline of digital humanities is evident and self-explanatory. However, especially within the maritime and underwater branches, the involvement and commitment of volunteers, now frequently referred to as citizen scientists, is perhaps less evident from the outside. Here, certainly within the United Kingdom at least, there is a well-established tradition of activities not only involving volunteers, but sometimes set-up and led by them, paying the necessary costs from their own pockets.

Perhaps the most obvious example was the underwater investigation and excavation of the Tudor warship *Mary Rose*, which sank very close to Portsmouth in the Solent in 1545. Here a small professional team led a much larger team of hundreds of volunteer divers over several years in the late 1970s and early 1980s, largely members of the British Sub-Aqua Club (BSAC), the largest diving club in the world and the National Governing Body for sport diving (SCUBA and snorkelling) in the UK.

Out of this project, and the expertise gained in training volunteer divers to participate meaningfully within a project, grew an organisation to provide such training on a longer term basis, and to further such activities: this is now known as the Nautical Archaeology Society and is still based in Portsmouth. It should also be noted that in addition to the NAS, the BSAC also provide some similar opportunities, but more importantly continue to promote the concept of "diving with a purpose" by encouraging groups to divers to undertake shipwreck or marine-life based projects – indeed the planning and management of such activities continue to form the basis of the exams needed for the award of the more advanced diving and instructor qualifications.

Whichever label may be applied to people who, it should be noted, are by no means always lacking in appropriate qualifications, skills, and experience, this project is aimed to assist them - alongside their paid, professional colleagues - in the demonstrably accurate recording of heritage subjects using digital photography, and computational 3D reconstruction and modelling.

Following the advent of digital photography and the proliferation of affordable underwater camera housings and lens ports, the additional more recent arrival of automated 3D reconstruction software, combined with the lower costs and widespread availability of the necessary computing power, has led to an explosion in the popularity of such techniques.

Such contemporary digital techniques have enormous and evident potential – especially relating to the visualisation of submerged subjects, and their presentation to the wider non-diving public. However, as this project will demonstrate then seek to address, there is a problem: difficulties arise where more is needed from these records than a visually pleasing model with no scaling or spatial reference. This may be possibly much later, possibly by other people, and quite possibly after the loss or destruction of the subject.

This project will demonstrate how little extra effort and minimal expense (if any) are needed to begin to address this problem, producing meaningful data with possibly unforeseen future applications.

After the costs incurred in delivering personnel to a subject – whether on dry land, in the inter-tidal zone, or especially underwater – the costs involved in adding scale-bars, for example, are miniscule. Suitable one metre examples, for example, may be bought or made for £10-15 and should be considered alongside the costs of vehicle fuel, car parking, accommodation, refreshments, divers' breathing gas, boat launching fees, and so on. It should also be noted that are evidently re-usable.

Alternative methods for scaling and referencing such models examined in this thesis are also reusable and again cost very small sums of money when compared to the other equipment or fieldwork costs: indeed some, such as tape-measures, are like to be present anyway during such activities.

In short, this problem is one which can be rectified with ease and with very little cost simply through a small degree of additional planning.

This project will therefore explore both how to create such records accurately and how to gauge this: it concludes with some practical recommendations, directions for future research, and some other observations about how such 3D techniques might be most appropriately applied alongside other methodologies by professionally-minded volunteers and professionals alike.

1.1 Background: 3D Recording of Cultural Heritage

Archaeologists have always needed to produce spatially accurate records. These may be of entire landscapes, more localised and specific sites or smaller subjects such as structures and artefacts. Such records must always be to scale; where appropriate, real world locations and orientations should also be provided.

The current ease of speedily producing apparently accurate and visually pleasing 3D computational models from multiple, overlapping photographs using automated processes in specialist software has led to a widespread and rapid adoption of close-range stereo-photogrammetry or simply "photogrammetry" within the cultural heritage sector, especially within its coastal and marine sub-disciplines.

Such 3D modelling from photographs used to be a laborious process, lacking automated tie-point detection, 'speed … and non-expert involvement' (Skarlatos et al 2012:1). The process was further complicated by the need to use multiple software packages for differing stages of a complex production pipeline from feature matching, to point-cloud generation, to surface modelling, to the rendering of the resulting model and finally its export for archive or further use.

The arrival of Agisoft *PhotoScan* in 2010 changed this by enabling the whole process to be automated, whilst still user determined, within a single software package - thus combining software further discounted for education and research with datasets acquired from consumer cameras (Van Damme 2015: 232; Mason ND:3; Agisoft 2016). This 'portability [and] flexibility' (Rizzi et al 2007:17) makes photogrammetry suitable for recording subjects of all scales from artefacts to landscapes (Pierrot-

Deseilligny et al 2011:297). This recording process, even at artefact level, may need to take place in-situ, in keeping with the current UNESCO recommendations (2001) for underwater cultural heritage to remain in-situ as a first-choice option.

At around the same time the increased affordability of the computing hardware needed for processing such large datasets – especially at site level using hundreds or thousands of images – enabled the production of far more ambitious models than previously envisaged.

Almost overnight, the generation of 3D digital models of cultural heritage subjects, both of objects or artefacts and at full structure or site level, became perceived almost as a requirement throughout the heritage sector, especially for publication and presentation. They may therefore be seen as 'digital surrogates': removing the risk of damage and making an interactive experience of the original subject possible for both outreach and research purposes, having 'remove[d] physical boundaries to scholarly and public access' even after it has ceased to exist (Mudge et al 2008:2-3). They may also be used as the basis for 3D printed replicas.

Such models may be used as "end products" for archiving and further analyses, or for promoting cultural heritage to the wider public through visualisation, possibly using virtual or augmented reality. Evidently, this is especially significant for underwater heritage subjects which may otherwise be outside many people's experience.

However, regardless of the subject's size and where the photographs are taken, it must be noted that images alone only enable the digital reconstruction of the subject in correct proportions if adequately captured from all angles, and also that without additional spatial data, the resulting model is unscaled. This is not always a problem, but it can hinder the further future applications of the digital record, possibly once the subject no longer exists.

1.2 Focus: Underwater and Coastal Cultural Heritage

Photogrammetry was trialled manually in the 'earliest days of modern marine archaeology' when George Bass used submarine-mounted stereo-paired cameras to record a submerged Roman shipwreck (Bass 1966:113; McCarthy and Benjamin 2014:97; Yamafune et al 2016:1).

Subsequently, it relied heavily on photo-mosaics to record beyond the limits of frequently limited underwater visibility (Muckelroy 1978). Despite the use of grids, levelled camera platforms and image rectification before combination (Martin and Martin 2002), considerable difficulties remained with ensuring 'constant height' whilst ensuring the camera remains level, in additional to the 'laborious' process of installing grids and reference data to create such photo-mosaics as the basis of a metrically recorded site-plan (Henderson et al 2013:243). Photo-mosaics also enabled people who had not dived the site to visualise what lay submerged in ways individual photographs and drawn plans cannot.

To metrically record such underwater sites in 3D, measurements were historically taken by divers using tape-measures: frequently with limited time and in challenging conditions. These tape-measurements enabled ortho-images and vertical cross-sections to be drafted with little to verify their overall accuracy other than the divers' memories and their photographs of specific parts: photo-mosaics were therefore necessary as well as desirable.

It should be noted that the current ubiquity of sonar datasets - both side-scanned and especially now multibeam - should not be regarded as making diver- or ROV-based methodologies redundant any more than the wide availability of remote-sensed datasets from satellites, and airborne photography and especially LiDAR does not negate the need for manual or drone-based field or building survey when investigating land-based sites: they may both still need to be investigated and recorded at close-range and in higher resolution.

It is arguably therefore in underwater archaeology that 'photogrammetric advances have had the greatest impact' (Historic England 2017:102). Apparently photorealistic models have an evident use in promoting and disseminating underwater sites to the wider, non-diving public (Historic England 2017:102), in addition to enabling rapid site-level recording beyond the limits of visibility.

But the question of reliable metric accuracy where the entire subject may not have been visible to the model's creators from a single vantage point due to underwater visibility - thus denying the qualitative validation of the model of their land-based counterparts - still remains an important hurdle to establishing such datasets as demonstrably metrically accurate within defined parameters, despite some enquiries (D'Amelio et al 2015; Capra et al 2015; Mertes et al 2014).

Apart from its evident utility relating to submerged subjects, those in or bordering the intertidal zone frequently have physically challenging access to sites with narrow, though predictable, windows of available time on site due to tidal flow. Such windows may be at any time of the day or night, necessitating opportunities to be identified in advance with commitments needed before access to detailed weather forecasts. Solid ground for mounting heavy equipment such as laser-scanners may also be lacking. Recording inter-tidal cultural heritage has thus also faced challenges beyond those experienced when examining similarly sized subjects on dry land: again, photogrammetry has proved an attractive option.

1.2.1 POSSIBLE FUTURE APPLICATIONS

It is in precisely such high-energy, volatile, marine and coastal environments where so much cultural heritage is being lost – perhaps without the chance for preservation through record – that metric photogrammetry could further its existing impact by becoming a demonstrably viable analytical tool for monitoring change and informing appropriate in-situ management strategies, in addition to enabling visualisation.

It is these possible applications of photogrammetry, applied alongside other optical, metrological, and geophysical technologies, to investigating and monitoring precisely such "at risk" heritage assets in-situ within these challenging environments, with a view to proposing mitigation strategies, in addition to more orthodox archaeological enquiries which form the basis of the author's longer-term research goals. However, before considering photogrammetry for such purposes, it should first be analysed in rigorous detail regarding the extent to which an individual dataset compares to the original subject.

This project, whilst aiming to contribute to wider discussions, is therefore also intended as a pilot study into how to examine the metric capabilities of photogrammetry in more quantifiable detail in the future, with this overall purpose.

1.3 Potential Shortcomings

The ease with which visually pleasing results may now be obtained from unordered sets of photographs without additional reference data has perhaps been a double-edged sword. Apparently "good" models can be achieved with minimal user input or understanding beyond acquiring and importing many photographs into an essentially automated pipeline. To illustrate this, below are models of the anchor recorded by this project. Although attractively rendered, and able to be orientated to reveal the subject from angles which may have been impossible to photograph, the spatial information is limited to the model's geometry being in correct proportion.

Figure 1: 3D models of the anchor used for this project. Image Source: The Author.

There are no indications of the anchor's dimensions – or those of the model. From an archaeological perspective, this removes any indication of the size of the vessel it came from, and thus its inferable purpose, crew, or cargo. Had it been recorded in-situ, its location and orientation would also be missing: this resulting loss of context in addition to the lack of scale would normally be regarded as totally unacceptable.

1.3.1 LACK OF SPATIAL DATA

'Image-based 3D modelling can be an excellent and suitable method for … recording, documentation and visualization of … archaeological heritage' (De Reu et al 2014:260). However, despite the origins of the term "photogrammetry" in the established science of extracting measurements from aerial photographs, many 3D computer models of heritage subjects are in fact, as the anchor example above, unscaled visualisations with arbitrary orientation (Historic England 2017:8): 'photogrammetry is not inherently scaled or measurable (Historic Environment Scotland 2018:20).

As the literature-based introduction to photogrammetry in Chapter Two will reveal, the inclusion of some forms of measurements is essential for all but simple 'visualisations', as without them the resulting models are 'scale- and orientation-free' (Historic England 2017:42,9).

It must be stressed that such models are not without their evident utility, and that such virtual visualisations of archaeological subjects may enable them to be experienced as well as seen, but problems arise when more than this is needed, possibly later and by other people. For example, unscaled models will allow change to be observed from differing models of the same subject taken over time, but scaled models would facilitate such differences to be measured and quantified.

In addition, determining the level of achieved accuracy is important to avoid giving rise to erroneous interpretations; especially where dealing with a series of similar subjects (Gnaden and Holdaway, 2000:745).

"Photogrammetric surveys" of sites are now frequently produced which lack scale-bars or North arrows present in the photographs or any other linked spatial data. Artefacts are recorded, again with scales missing from the photographs – quite possibly due to genuine misunderstanding regarding the capabilities of post-processing, or of the potential future uses of such datasets.

Even if the 3D model is not in fact produced to scale, in addition to enabling scaling by eye, the inclusion of such a datum enables subsequent scaling by post-processing. As obvious as this may sound, this does not always happen as non-aerial photogrammetry is still a developing technique, lacking detailed technical guidelines and standards.

Photogrammetry has in some ways been a victim of its own rapid and widespread application where the use of spatial data is concerned with marine and underwater applications being further hindered by additional site-specific constraints, and by having their own, possibly very different, questions to answer.

1.3.2 COMPUTATION VS MEASUREMENT

Furthermore, the geometry of these models is based on 3D point-clouds which are extracted from 2D source data – multiple overlapping photographs from differing perspectives – by automated, pixel-based feature matching based on colour and hue. Unlike laser-scans therefore, where the constant of the speed of light is used to measure distances using time, the 3D datasets here are computational extrapolations; they are *not* measurements.

These computations are themselves determined by the selected processing parameters. In other words, a model's geometry is influenced, if not determined, by choices which may subjected to undocumented and not understood trial-and-error by the user, attempting to address time or memory constraints in the current absence of detailed, published guidance outside online user forums.

This is not to say that such models cannot be made accurately - they can - but in order to be appropriate for purposes beyond visualisation, such digital models must be consistently, and demonstrably, accurate geometrically in addition to being scaled and referenced. Such accuracy may be achieved through the inclusion of spatial data alongside the photographs: ideally from the outset of processing to constrain the computation, but at the very least applied to the final product (Historic England 2017:9).

1.3.3 LACK OF TECHNICAL STANDARDS AND GUIDELINES

Other forms of recording or survey have clear technical standards not only for data collection and processing, but also for the presentation of the final dataset (Historic England 2015). For close-range stereo-photogrammetry, however, the perceived "best practices" are much vaguer.

This is not to say that no published work on this subject exists, but that as a developing field using emergent technologies and evolving techniques, even the published guidelines on the application of photogrammetry to cultural heritage by the national heritage agency for England (October 2017) lack detailed technical standards and guidance.

1.4 The Aim of this Project

This project aims to contribute to the development of technical guidelines to aid citizen scientists and paid professionals alike in the production and quantitative evaluation of 3D datasets produced from overlapping photographs of maritime heritage subjects for further application beyond un-scaled visualisation – even if that is all that is required at the time.

As such, the data acquired and presented in this thesis is intended for these purposes of experimentation and investigation of methodology rather than to be answering specific archaeological questions. The wider purpose as a pilot study is, in fact, to guide future work on how such metric datasets may be applied to answering precisely such questions, once their degrees of possible accuracy and likely error have been identified in quantitative terms.

Finally, this project hopes to contribute to wider discussions regarding technical standards for such data and guidance for its collection, production, and application within cultural heritage and the wider fields of digital humanities and citizen science. It should be noted that regarding the historic environment, professionalism is not defined by whether or not payment received, but by a commitment to 'working in the public interest' through adhering to defined standards, maintaining accountability and continued demonstration of the development of skills, knowledge and competence (Chartered Institute of Archaeologists (UK) 2020).

Although written primarily for an audience of maritime-focussed heritage professionals, researchers and citizen scientists alike, and especially for divers, although this is also intended to be relevant for a wider readership with the aim of supporting those engaged in citizen science, in keeping with the wider definition of "professionalism" outlined above.

The case studies selected (an anchor and a section of hull timbers) are not simply maritime objects; the recording methodologies selected and implemented were also designed to meet the likely needs of such enquiries, and to imitate the realities of recording such subjects in-situ, possibly by divers, and possibly by citizen scientists.

This project is also a pilot study to identify objectives for future research into the acquisition and validation of quantifiably metric 3D datasets via Image-Based Modelling with a view to their subsequent use for in-situ management of "at risk" cultural heritage within high-energy, specifically marine and coastal, environments alongside their archaeological investigation and documentation.

1.5 Scope

1.5.1 RANGE, SCALE AND ENVIRONMENT

Although historically "photogrammetry" was associated with aerial photography, this project investigates subjects recorded at much closer range using cameras mounted on tripods or held by hand. This specific approach, within a wider family of linked methods, may specially be referred to close-range stereo-photogrammetry.

3D modelling using photographs taken at varying altitudes by either manned or autonomous aircraft is beyond the scope of this project. This project is limited to recording subjects smaller than entire sites or landscapes for this reason.

Additionally, although the project was carried out indoors as an experiment, the specifics of working in a marine environment, possibly underwater, whilst investigating an historic watercraft were very much key to the design. As indicated above, the case studies and methodologies were selected and designed to mimic the realities of such enquiries.

1.5.2 SOFTWARE

Although there is a wide range of software packages at varying prices, including free and open-source options available, Agisoft *PhotoScan Professional* was used by this project due to its availability at Bournemouth University and status as the de facto "industry standard" for heritage applications.

Although during this project *PhotoScan* was superseded by *Metashape* as Agisoft's flagship product. *Metashape*, including its reported capacity for producing higher resolution datasets whilst needing less memory and reduced processing time, is also beyond the scope of this project, although evidently of interest to future studies especially those involving larger, especially aerial, subjects and datasets (Agisoft 2019).

1.5.3 LITERATURE

Although using peer-reviewed academic publications as the backbone for the literature reviewed for the project design, implementation and analyses, other publications – such as guides, online forums and websites – also needed to be consulted due to the rarity of peer-reviewed literature in some key areas: these were especially relevant to methodological details and applications.

Additional grey literature, especially university student coursework, also proved relevant: this could be considered to have been subjected to a form of review having been marked, although in most cases the grades awarded are unknown, so they must be treated with similar degrees of caution to other online material.

1.6 The Research Question

"How should Image-Based Modelling be best used for the metric recording of maritime cultural heritage subjects suitably for wider applications within heritage-based geomatics, geoinformatics and digital humanities, and to further the potential for citizen science within these fields?"

1.7 Key Terminology in the Question

1.7.1 IMAGE-BASED MODELLING

The generation of 3D computer models from a series of overlapping photographs without additional calibration data, using automated feature matching at pixel level is often referred to as "Structure-from-Motion" – the deduction of geometry based on changing perspective resulting from the movement of the camera. This can be used as the basis for a 3D visualisation of the subject which is devoid of scale, orientation or geographical location.

Image-Based Modelling differs in that the resulting 3D model combines Structure-from-Motion (to deduce the subject's 3D geometry) with additional spatial data to enable scaling: orientation and real-world location may also be achieved if appropriate data is used.

It is therefore only by using Image-Based Modelling, combining Structure-from-Motion with additional spatial data, that metric 3D digital models may be produced.

1.7.2 GEOMATICS AND GEOINFORMATICS

Geomatics is the science relating to the acquisition, storage and export of geospatial datasets. Traditionally involving field survey data, geomatics takes such datasets and combines them with other spatial data before preparing cartographic exports and suitable archives.

Geoinformatics is less concerned with the acquisition of data than with the *production* of new data from existing geospatial datasets using computation to reveal, clarify or quantify relationships. Landscape analyses such as line-of-sight or cost-surface modelling, or geodatabase interrogations relating to features, areas, distances or numbers present are examples of geoinformatics.

Image-Based Modelling may have applications to both these related disciplines – perhaps as a form of measured survey at site level (as an orthographical image from a drone flight) which is subsequently also exported as a Digital Elevation Model, allowing lines-of-sight across the site to be calculated.

1.7.3 DIGITAL HUMANITIES

This is an interdisciplinary field which applies contemporary digital technologies and approaches to the Humanities. This could involve using non-visual spectrum photography to reveal faded writing or hidden layers in paintings, possibly aiding in the conservation of artefacts or the use of virtual or augmented reality as vehicles for experiencing reconstructions of past environments.

The geoinformatics examples above, if applied to questions relating to how people may have experienced or interacted with their environment, are also examples of digital humanities.

Digital Humanities is thus an area of cross-fertilisation, using digital technology to inform our understanding, or interpretation, of human experiences, environments or material culture whilst also furthering our understanding of the technologies themselves, their capabilities and their capacity for application possibly beyond their original purpose.

1.7.4 CITIZEN SCIENCE

Essentially, this concerns training and guiding members of the public to enable them to meaningfully contribute to wider scientific enquiries.

Due to the nature of Archaeology as a discipline, it has historically proved popular with the public and maritime sites have been no exception: beachcombers and dog walkers are currently encouraged to contribute to various projects, as have divers and avocational archaeologists: the Coastal and Intertidal Zone Archaeology Network (CITiZAN), for example, released a smartphone app to enable people to photograph and upload information to a database with geographical location from their phone's satellite sensors as part of a programme to monitor at-risk heritage vulnerable to coastal erosion[1].

There have been similar initiatives in environmental and conservation sciences: Zooniverse[2] is one excellent example, where registered users across the globe participate in many active projects varying considerably across pure and applied sciences and the Humanities – again also using a smartphone app.

This may involve participation in organised group projects – sometimes of their own design – or through contributing photographs and completed pro-forma records for example, enabling a central project to crowdsource data.

By aiding the development of technical standards for the production and evaluation of heritage models using Image-Based Modelling, this project aims to further citizen science through contributing to the training and advice available to both increase the demonstrable utility of such datasets alongside enabling more productive and rewarding use of volunteering time.

1.8 Project Objectives

These intend to answer the research question by examining how demonstrable levels of appropriate accuracy can be achieved and validated, by considering:

[1] https://citizan.org.uk/
[2] www.zooniverse.org

1. What types of spatial data could be appropriate?
2. How should such spatial data be integrated?
3. Which types of spatial data are most accurate?
4. How can current technical guidelines be improved?

1.8.1 WHAT TYPES OF SPATIAL DATA COULD BE APPROPRIATE?

Literature reveals that photogrammetry-derived 3D models can compare favourably to laser-scans (Pierrot-Deseilligny et al 2011:296; Tidball 2016). However, as previously noted, these photographs need to be combined with spatial data for scaling: at the very least a scale-bar or known baseline should therefore always be present.

But what is the necessary level of spatial data needed for scaling the 3D models? A single scale-bar – thus providing two datum points and a dimension in the same plane – may prove adequate for scaling a model of an artefact, but will it suffice for a larger subject such as a site or structure? Will a full survey with on-subject detail points be required in this case? Alternatively, should multiple scale-bars in differing planes or a network of known off-subject control points be used for larger subjects? What other options exist? How does the maritime environment affect the selection and application of such methodologies?

These answers to these questions were sought from the first literature review in Chapter Three.

1.8.2 HOW SHOULD SUCH SPATIAL DATA BE INTEGRATED?

The question here is how the varying forms of spatial data identified in the literature reviewed in Chapter Three should be integrated into the model generation process. As such, answering this question required practical experimentation in addition to literature review.

On a simple level this could consist of including a scale-bar in the photographs and manually placing markers on the resulting model, labelling them as a scale-bar and assigning a measurement. The same approach may be used for on- and off-subject features surveyed with a TotalStation possibly within a real-world coordinate system or alternative survey methodologies more directly relevant to maritime subjects, such as tape-measures and levels.

However, photogrammetry software packages like *PhotoScan Professional* are also designed to identify individually numbered coded target included in the photographs – these can be assigned with real-world or arbitrary coordinates, or simply paired as scale-bars.

Manually identified markers are typically added at the end of the process, stretching the model to accommodate the new data whereas targets automatically identified from the outset of the processing pipeline constrain the geometry throughout reconstruction, if used to import spatial data rather than merely as an aid to image alignment (Historic England 2017:15).

1.8.3 WHICH TYPES OF SPATIAL DATA ARE MOST ACCURATE?

What effects do these differing forms and levels of spatial data have on the resulting model and how can this be evaluated by its creator? What contributions to technical guidance and standards can be offered as a result of this project? Answers to these questions were sought first from the second literature review of current guidance relating to model creation and evaluation in Chapter Four before metrically analysing the results of the project's practical experimentation.

Scaled models may have their features as well as their overall dimensions measured and can therefore be ground-truthed with data relating to the original subject. Such data could take various forms such as "check measurements" taken from surveys or using callipers, scaled drawings or even remote sensed data or laser-scans where appropriate.

As vector data, point-clouds constitute points with 3D coordinates. Once registered within the same coordinate system as a reference point-cloud, the differences between the two may also be extracted and examined.

Errors should be quantified in absolute terms (millimetres rather than percentages) to begin the development of a wider user-based evaluation methodology, examining the results with a view to creator-level validation: "rating" accuracy in a similar way to industry standards for surveys and survey equipment. This is of evident value to volunteers and amateurs – who need to know their time is being spent profitably - as well as paid professionals.

The critical question here is whether differing methodologies do in fact result in significantly varying outcomes, and how such outputs may be validated using the supplied spatial data as a benchmark. Consideration must not only be given to the levels of accuracy achievable from the various techniques, but also to the practicalities relating to their implementation for data collection, especially within the maritime specifics of both the environment and the likely objectives.

1.8.4 HOW CAN CURRENT TECHNICAL GUIDELINES BE IMPROVED?

The question here is to examine the extent of the current advice for creating such models and evaluating them as accurate records of the subject, with a view to improving them. It is also to bring together relevant material from a wide range of sources, alongside some experimental examples, to begin to demonstrate and explain how to do these within a single document; this is intended to aid citizen scientists and paid professional practitioners alike.

1.9 Research Methodology

The project's objectives will therefore be examined initially through reviewing the relevant academic, professional and grey literature, looking for gaps or inconsistencies relating to the linking of spatial data and photographs for 3D model generation by Image-Based Modelling and the subsequent metric evaluation of the results.

It will then move on to practical experimentation, integration and analysis of results, before looking in detail at addressing the current lack of technical guidance and evaluation.

Because this project is also intended as a pilot study, it will also be looking to identify research questions and objectives for further study.

1.10 Anticipated Significance

1. This project aims to contribute to technical guidance and standards for production and evaluation of such metric 3D models of cultural heritage, aiding professionals and citizen scientists alike.

2. This project also intends to deliver focussed objectives for further research into the production and quantitative evaluation of such 3D datasets when they are intended for further applications to the in-situ management of cultural heritage, specifically within highly dynamic marine contexts, or wider applications within digital humanities.

3. This project hopes to aid the wider application of such datasets through the ongoing development of such standards and guidance: again, this is intended to aid professionals and citizen scientists alike.

1.11 Academic Context

Initially, cultural heritage research papers focused on the wide-ranging potential applications of 3D models produced by such low-cost, easy-to-use software in combination with the ubiquity and portability of digital cameras with relatively little analysis of the results' metric accuracy.

This is not a condemnation of earlier work: Structure-from-motion is a powerful and accessible visualisation tool, and such visualisation is by no means an ephemeral novelty.

The critical concern at the heart of this thesis, however, is that the perhaps overly speedy adoption of such methods for *measured* applications, such as survey or archive, has resulted in a lack of adequate technical standards and guidance for creating and evaluating such models despite the use of additional spatial reference data now being regarded as best practice (Yamafune 2016; Historic England 2017; Bryan 2006).

By not simply using digital technology to examine cultural heritage subjects, but by considering the specific requirements of the interpretation or *in-situ* management of such subjects whilst investigating the capabilities and appropriateness of the technology and approach, this project originates more from the wider cross-disciplinary field of Digital Humanities than a purely archaeological perspective.

Chapter 2. The 3D Reconstruction Process

Having outlined the purpose, scope and context of this project, it is now important to investigate the details before designing an appropriate methodology to answer the research question. Before examining the relevant literature to explore the project's stated objectives, it is important to begin with a literature-based detailed investigative summary of the 3D reconstruction process, and its underpinning science.

2.1 Defining Photogrammetry

Photogrammetry uses photographs to reconstruct real-world subjects (Darvill 2003:321). This was historically linked to the development of aerial photographs (Wolf et al 2014:3) and their manual rectification, enabling surface features to be measured using either known dimensions contained within them.

Any straight lines in a photograph may also become scaling features if the focal lengths or a photographed dimension are known, although all such measurements are constrained within the two dimensions of the photograph. (MacDonald 2015:7). There may need to be corrections made due to inaccuracies resulting from diffraction arising from the optics, or the distances and conditions – this is a field of active research now more frequently relating to remote sensing rather than aerial photography (Wolf et al 2014:11, 101+104-113).

Photogrammetry is now associated more with 3D reconstructions of subjects as point-clouds based on 2D images, using computation to determine geometry from matching features in multiple source images. Such techniques began to appear during the 1960s to aid computers to sense their surrounding area – they are now used for geometrically accurate 3D reconstruction of subjects using 'non-contact optical methods' (Remondino in Remondino and Campana (eds.) 2014:63-64; MacDonald 2015:7).

In addition to objects and artefacts, sites and landscapes may be reconstructed using such techniques – here if the point-clouds are registered in an appropriate grid they may be combined with other such metric datasets within the 'common language' of GIS (Campana in Remondino and Campana (eds.) 2014: 10).

2.2 Close-Range Stereo-Photogrammetry

Although still used for aerial photographic 3D reconstructions, now frequently using unmanned aerial vehicles (UAVs or "drones"), these techniques are increasing being applied to objects at much closer range. Drone-based recording, with its own data collection and geographical registration challenges is an emergent field in its own right, and is beyond the scope of this project.

This thesis instead focusses on the application of such techniques to subjects much closer to the camera, and without the opportunity to gather images from high elevations. This, especially when applied to structures rather than objects and artefacts, has its own challenges and it is these which this project hopes to address, particularly considering marine and coastal subjects.

2.2.1 IMAGE-BASED MODELLING VS STRUCTURE-FROM-MOTION

Image-Based Modelling uses '2D image measurements to recover 3D object information through a mathematical model' (Rizzi et al 2007:17). Historically these needed measurements to be supplied with the photographs, either as stereo-pairs (with a known, fixed distance between the cameras) or using surveyed "control points" within the photographs (Westoby et al 2012). IBM is thus 3D model production from multiple overlapping photographs using additional spatial data, such as the distance between mounted pairs of cameras: this is best included in the calculations rather than being applied to a model at the end of the process, if possible (Historic England 2017:9).

"Structure-from-Motion" (SfM), by contrast, simply uses overlapping photographs with no additional spatial data. Geometry is deduced from feature-matching across the supplied photographs before a final, iteration-based "bundle adjustment" to calculate an overall best-fit (Westoby et al 2012). The result is a 'scale- and orientation-free … reconstruction' (Historic England 2017:9). This is not to say that they necessarily lack relative accuracy – the models should be in proportion to the subject – but that they have no quantifiable scale.

These processes will be examined in more detail, but the basic tenet must be understood from the outset because this is critical to understanding the questions of accuracy and consistency within SfM point-clouds. The point-clouds are extrapolated by a series of calculations and iterations before being subjected to further best-fit calculations: they are *not* measurements.

For these reasons, this thesis examines Image-Based Modelling, where spatial data is used alongside the photographs to reference the resulting model. The central questions examined by this thesis relate to the necessary extent of this spatial data, and how to integrate it into the modelling process, and how to evaluate the accuracy of the results.

2.3 Key Concepts: Collinearity and Coplanarity

3D geometry may be deduced from overlapping photographs by calculating the paths taken by light rays from points on the subject to the camera's sensor using common tie-points identified in the photographs.

Collinearity is the relationship between the camera's position, rotation, its focal point and length, and also the position of points on the subject. Equations can therefore determine the orientations and positions of the camera and the point on the subject using a known variable, such as focal length (MacDonald 2015:7-8).

In the below example, (xa,ya) are the coordinates for point A represented in the photograph as point A. (X_A,Y_A,Z_A) are A's real-world coordinates. (X_L,Y_L,Z_L) are the coordinates of the camera (L), f is the lens' focal length and (X_o,Y_o) are the coordinates of the lens' focal point.

Although SfM can produce 3D models simply from photographs, it must be noted that digital photographs include EXIF metadata – *indicating focal length as well as exposure settings*. Simply scanning an equivalent series of photographs processed from film may not prove adequate: in the absence of such data, Agisoft *PhotoScan* assumes a focal length of 50mm – at best this leads to further distortions, but with further departures in focal length, the processing fails as the camera orientations may not be determined (Agisoft 2016).

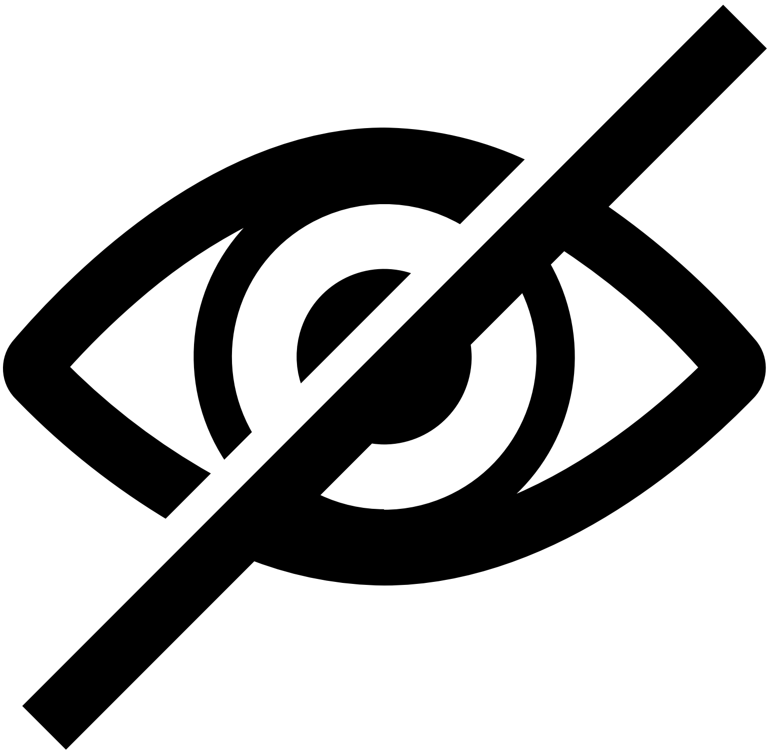

Figure 2: Collinearity diagram – Image Redacted.

Image Source: Wolf et al 2014:269.

Points A and a must be in the same plane, so the relative locations and orientations of two differing camera positions which capture the same point may be determined, using a known, constant distance. This could be the lens's focal length, or the distance between the two cameras. This distance, combined with angles, allows the calculations to be completed.

This second relationship is called coplanarity and is demonstrated in the illustration below:

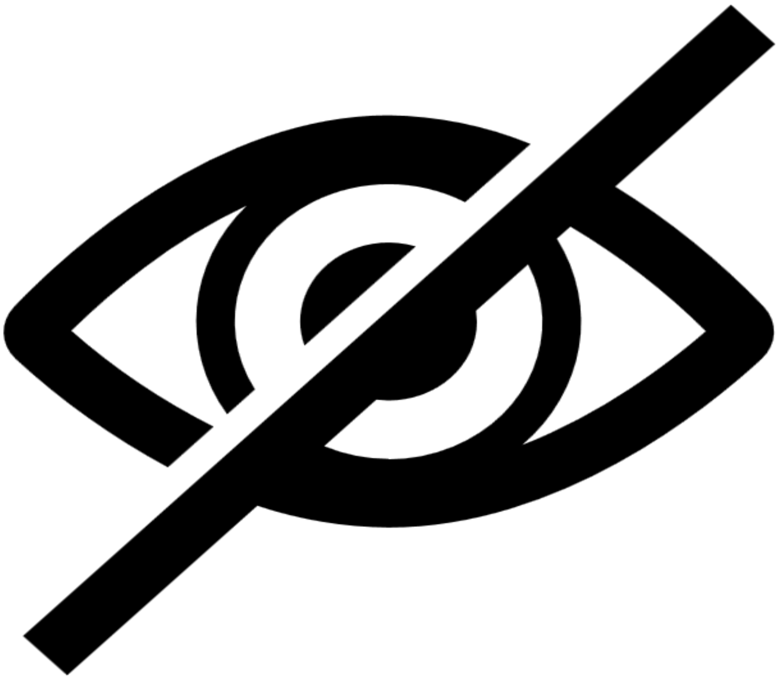

Figure 3: Coplanarity diagram - Image Redacted.

Image Source: Wolf et al 2014:270.

Photographs will therefore need to be taken from similar positions and orientations, following the plane of the object. This can prove difficult with edges, needing much overlap.

Photogrammetry is based on these two relationships, and accurate measurements may be taken, so long as the camera's settings are known (MacDonald 2015:8).

However, although Structure-from-Motion can produce results from un-calibrated cameras, it must be noted that with digital cameras it is assumed that the sensor is in the correct plane, leaving only lens-based optical distortions (Historic England 2017: 20). Unfortunately, this is not always true due to production methods, especially with cheaper cameras and camera-phones, so camera calibrations should be performed (Historic England 2017:21). With most lenses at most focal lengths, the optical distortions are most present around the edges – the high levels of overlap needed for feature-matching can overcome this problem.

2.4 Technical Workflow

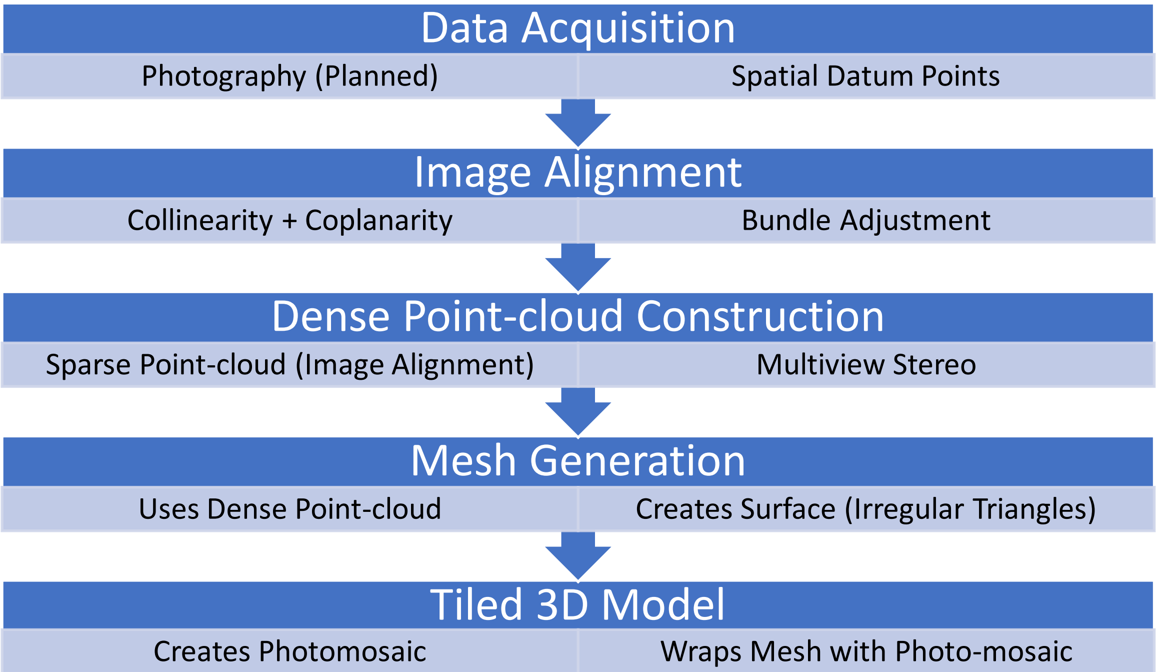

Figure 4: 3D Reconstruction process flowchart.

2.4.1 DATA ACQUISITION

Photographic Overlap

A high level of photographic overlap is needed to enable the software to project the exterior locations of the camera positions (aligning the images), having first identified common, recurring features.

Reducing the degree of overlap does not so much reduce the levels of resolution in the final dense point-clouds and meshes - thus saving processing time – as risk the software failing to align the photographs at the outset. This critical first part of the process depends entirely on the decisions made by the creator; as with other field-based techniques it is very difficult to fix problems resulting from ineffective data collection in post-processing.

360^0 Coverage

"Structure-from-motion" is the movement of the camera relative to the subject, resulting in a series of overlapping photographs with 360^0 coverage from varying elevations with considerable overlap (Re et al 2011:276). Superior results are found from well-planned datasets (Miles et al 2014:600).

This reference to 360^0 is critical to understanding the application of Structure-from-Motion. It can only deduce the 3D structure from photographs and EXIF metadata alone with any degree of unscaled geometric accuracy where the subject is photographed from as close to all these angles as possible. For artefacts or statues this is relatively straightforward but when dealing with aerial subjects this is evidently impossible, so control points will always be needed (Historic England 2017:42). This is another reason why this project has not considered aerial photogrammetry, despite the evident utility of drones within the intertidal and coastal environments.

Spatial Data

This must be collected in a way that enables its integration with the photographs in the subsequent 3D reconstruction process. This will usually mean ensuring features such as markers or scales are both present and sufficiently prominent in the original photographs, in addition to their own spatial details being recorded.

Again, as with the photography, the skill of the creator in designing and implementing an appropriate strategy is paramount here due to the limited options for subsequent actions to address shortcomings in data collection beyond repeating the exercise.

2.4.2 PROCESSING 1: IMAGE ALIGNMENT (STRUCTURE-FROM-MOTION)

The process of aligning the images to reflect their perspectives on the subject and then producing a sparse point-cloud to reconstruct the subject's overall geometry is frequently referred to as Structure-from-Motion (Historic England 2017:8-9).

Tie-Point Detection

Common features are identified in each of a series of photographs at pixel level using their colours and hues. Several such "tie-points" in each photograph enable its perspective to be deduced by projecting light rays from its focal point through each tie-point – by repeating this process for each photograph they are then aligned relative to each other and the subject (Van Damme 2015: 232).

The software generated target markers captured within the series of photographs can be used to aid this process; even when used without linked spatial data they have a potential role to play – especially where a large subject has areas of indistinguishable detail but physical considerations prevent the capture of photographs from far enough away to contain the whole subject.

SIFT and SURF

Scale-Invariant Feature Transform (SIFT) algorithms identify these tie-points even where they are captured at differing scales (McCarthy and Benjamin 2014:98; Kontogianni et al 2015:326). Newer Speeded-Up Robust Features (SURF) algorithms operate in a similar way but more quickly (Kontogianni et al 2015:326).

Bundle Adjustment

A final iterative "bundle adjustment" is then performed to ensure the image alignment is 'globally consistent' by eliminating the errors with may arise from groups of overlapping images being aligned correctly as a group but inaccurately in relation to the remaining photographs (Westoby et al 2012).

Sparse Point-Cloud

Having enabled the image alignment, these tie-points now form the basis for a best-fit sparse point-cloud, representing the overall geometry of the subject. Such combined detection and reconstruction techniques began appearing around 2000 (Pavelka and Reznícek 2011:254) enabling more detailed geometry, surfaces and textures to be modelled from additional detail in the now aligned photographs projected onto the sparse point-cloud's initial reconstruction (Miles et al 2014:146-147).

2.4.3 PROCESSING 2: THE DENSE POINT-CLOUD (MULTI-VIEW STEREO)

Having aligned the images and reconstructed the essential geometry of the subject in the sparse point-cloud, multi-view stereo now detects and matches additional features within the photographs and projects them into the sparse point-cloud adding further detail, now including 'most of the pixel data contained in [the photographs]' as 3D points (Historic England

2017:14). This results in a much higher resolution "dense point-cloud" which begins to reflect the surfaces and textures of the subject.

2.4.4 PROCESSING 3: PRODUCING THE MESH

The mesh is the surface geometry of the model created from the dense point-cloud (Yamafune 2016:62). A Triangular Irregular Network (TIN) of triangular "faces" between points selected from the dense point-cloud reconstructs the surface – this is now a 3D model with a surface, rather than a point-cloud.

2.4.5 PROCESSING 4: TEXTURING THE MESH

This maps the relevant colour and hue to each triangle in the mesh from the source photographs to provide a more 'realistic rendering of the subject' (Historic England 2017:121). It does this by wrapping the mesh with a photomosaic (Yamafune 2016:67).

2.5 The Most Critical Phase

Although software packages now largely automate the computational process, whilst still offering various degrees on control over the constraining parameters, this may be performed with minimal input from the creator beyond essentially balancing desired model complexity, time requirements, and the ability of the computer to deliver the intended outcome.

The most critical link in the 3D reconstruction process is evidently at the outset: the collection of adequate and appropriate photographs and spatial data. Mistakes and omissions here may impede the automated processes sufficiently to necessitate their repetition.

2.6 The Direction for This Project

The previous chapter explored the contribution photographic 3D reconstruction continues to make to recording, documenting and promoting maritime cultural heritage subjects, and, critically, the difficulties posed by their environments. It also highlighted the possible utility of demonstrably metrically accurate datasets to wider in-situ management strategies for such subjects, before exploring the potential shortcomings of unscaled models.

As noted at the outset, although written to aid amateurs and professionals alike, and to specifically consider divers working underwater, the purpose of this project is to examine the production and evaluation of demonstrably accurate point-clouds. This second chapter has clearly illustrated the criticality of data collection – this is evidently especially important for those working within the time and practical constraints of the marine and coastal environment.

The need for gathering sufficiently overlapping photographs in necessarily large numbers is well-known, although perhaps meticulously planning their capture is less well practiced. However, in keeping with this project's aims there emerge two areas to focus attention: *spatial* data collection and its integration with the photographic, and the subsequent evaluation of the results.

Two further literature reviews were therefore conducted: the first examined how to capture and integrate spatial data during the critical first phase of 3D reconstruction; the second considered current technical guidelines for the production of 3D data and its evaluation regarding its intended purpose. These two literature reviews are summarised in the following two chapters.

Chapter 3. Literature Review: Spatial Data for Image-Based Modelling

Following the literature-based investigation of the 3D reconstruction process in the preceding chapter, it is clear that without spatial data in addition to the photographs, Structure-from-Motion produces results which are 'in an arbitrary coordinate frame and at an arbitrary scale' (Historic England 2017:8). Such models are not without utility as visualisations, but to enable measurements to be taken – or for the results to include a geographic context, or to be integrated with other such datasets – spatial data is needed (Historic England 2017:42).

As noted in 1.8.2, this spatial data should be integrated into the processing pipeline as soon as possible following the camera alignment so that it is used as restraining features within the calculations, rather than attempting to retro-fit the coordinates to a finished model (Historic England 2017:9).

The critical questions here emerge: which forms of spatial data may be appropriate for differing envisaged purposes for the resulting 3D model, and in which contexts? How should this data be integrated into the 3D reconstruction pipeline?

This chapter, therefore, is a review of relevant literature intended to address these specific questions, which are too complex to have a catch-all solutions.

3.1 Scaling, Orientation and Referencing

Correctly proportioned 3D models may be made spatially accurate in a metric sense in three differing ways. They may be scaled, enabling measurements to be taken. When in located in a real-world setting they may also be given orientation to further capture their context. Finally, the coordinates within the model may be given real-world values to provide all the above with the additional functionality of becoming suitable for combining with other geographical datasets within a database to enable analyses to be performed and cartographic outputs created.

Because scaling is simply relative without the addition of either a known dimension or at least two x and y coordinates to enable scaling, and presented in an arbitrary orientation, this clearly necessitates the use at the very least of a scale in the photographs for all subjects.

For scaling and orientation at least three coordinates are needed. Although only two of these coordinates need to include all three dimensions, in practice most software requires all three to have x, y and z coordinates (Historic England 2017:43). Scale-bars providing known dimensions alone cannot be used for orientation.

For the model to be referenced in the real world, these x, y and z coordinates need to be within an appropriate reference system or grid, allowing 'the extraction of accurate metric information, and the computation of orthophotos and digital surface models' (De Reu et al 2014:252). For maritime subjects, the lack of familiarity 'with a site in its totality' makes such datasets, and their ease of integration into a wider geographical information database, 'especially important in underwater archaeological contexts' (Figueirido and Bernardes 2014:29).

3.2 Sources of Spatial Data

Objects and Artefacts

A scale-bar may be used to provide scale in a single dimension; an additional scale-bar parallel with an alternative principal axis may also be used.

Subjects may also be referenced within a coordinate system to scale in both the x and y axes by using scale-bars incorporating a right-angle (or two bars placed using a set square) to define an origin; placing the subject on graph paper is another option (Historic England 2017:49+76). Cubes may also be used to scale in all three dimensions, possibly combined with graph paper to form an arbitrary 3D coordinate system.

It should be noted that when dealing with such subjects outside of their original context, geographical referencing is irrelevant. All that is required here is *scaling*, as location and orientation are now arbitrary; however, it may still be important to be able to demonstrate scaling in more than a single dimension.

Structures, Sites, and Larger Artefacts

In these cases, the subject will be in a location and orientation which may also need to be recorded for context, in addition to accurately scaling the 3D model to enable metric applications beyond visualisation. Beginning with scaling, this may be may done quite adequately by using any of the techniques outlined above, or by encircling the subject with scale-bars in the X and Y axes, inputted as fixed distances within the software (Yamafune 2016:37). Alternatively, it could be 'enclosed' within four known dimensions (Yamafune 2016:35). These dimensions may also be between four encircling survey control points, rather than in physical form as scale-bars.

In addition, the tape measure methods outlined in 3.3 will also be appropriate for recording distances in two dimensions for simple scaling.

These methods will address scaling, quite possibly orientation, but in themselves are not appropriate for establishing a 3D coordinate system across the subject to demonstrably and consistently scale the model (Yamafune 2016:42). For this, a measured survey will be required.

Here, off-subject control points may be used in any reference grid or coordinate system as appropriate including local, global or arbitrary options (Historic England 2017:42). These could simply take the form of four outlying corners, although additional control points, evenly distributed within such a network, may be preferable depending on the size of the subject (Historic England 2017:43).

These control points may be established using survey-grade GNSS with localised accuracy augmentation in the form of EGNOS/WAAS[3], SmartNet[4] or base station to enable Real Time Kinematic (RTK)[5] accuracy – possibly using a TotalStation in addition (Historic England 2017:46-47). Where RTK is unavailable, a TotalStation may be used in combination with tape measures to "Grid Out" an arbitrary coordinate system: if needed this can be translated into an appropriate real-world system later.

[3] European Geostationary Navigation Overlay Service/Wide Area Augmentation Systems are GNSS accuracy augmentation systems using base stations at known locations to transmit localised correction signals.
[4] SmartNet is a similar system using mobile telephone networks to triangulate with masts at known locations.
[5] Here a base station is set up at a known point, such as an Ordnance Survey triangulation point at a known grid reference. Upon being programmed with its exact location, the base station transmits a correction signal in real-time to the RTK rover unit.

On-subject detail points may be used in addition to the external control network to increase the demonstrable accuracy of the 3D model through constraining the model's creation at such known points (Yamafune 2016:33; Tidball 2016:5; Historic England 2017:47-48). These detail points should ideally be surveyed using a TotalStation rather than RTK, due to its higher degree of accuracy[6].

These techniques may also be valid for intertidal subjects at low water depending on the site's regarding access with heavy equipment, the suitability of the ground for mounting such apparatus, and evidently the length of low water relative to the complexity of the planned recording. It should be noted that the tape measure techniques discussed below can also be used in other environments, especially where such professional equipment (and training in its use) are lacking.

3.3 Marine or Underwater Subjects

Alternative sources of spatial data are evidently required where the subject is submerged. In these cases, there are various alternatives. These options are also suitable for intertidal subjects, and for use by citizen scientists lacking access to the more professional equipment outlined above. In addition to enabling citizen science, it should be noted that in some environments, they may be the first choice of funded and well-equipped professional teams as well.

2D Survey using Tape-Measures

The techniques discussed here are summarised in Bowens (2009) in Chapter 14 (Underwater Survey). Where the subject is located on an

[6] TotalStations may record to 2mm accuracy over the distances in question, whereas RTK GNSS systems are typically accurate to 30-30mm.

essentially flat surface, especially a sandy beach or seabed, the use of tape measures to record within an arbitrary 2D coordinate system using right-angled offsets from a baseline is a simple and quite possibly adequate option.

Alternatively, a detail point's coordinates may be calculated using two tape-measurements, forming a triangle from the detail point and either two known points on a baseline, or the two ends of the baseline. These are both forms of trilateration (using distances to form triangles without needed to measure angles), although the first option is specifically referred to as ties.

These have the advantage of being simple to apply with minimal planning, preparation, or training required by using simple, cheap, and robust equipment, and relying on very basic mathematics, although as tape-measures are 'prone to being snagged' so 'should be checked … before the measurement is taken' (Bowens 2009:123).

It should be noted that although these methods will enable a 3D model to be scaled, and orientated, without the addition of additional spatial data geographical referencing is impossible. This may not necessarily be a problem, but it should be noted that such data may well be readily obtainable using equipment already available – see section 3.4.

<u>Direct Survey Method (3D Trilateration)</u>

An alternative means of surveying detail and control points is to use the Direct Survey Method (DSM) which uses only measurements of distance and elevation using tape measures and a level; underwater divers can use a dedicated depth gauge, with depths taken consecutively to avoid errors caused by changes in tidal height over time.

It was developed for diver-based use underwater during the 1970s and 1980s during the Mary Rose project. Difficulties accurately recording angles led to experimentation into recording only distances to features from marked points on a known baseline: when such 'trilateration' was taken into the third dimension using trigonometry to avoid needing plumb lines, the "Direct Survey Method" was the result (Rule 1989:157).

Any point may be located in three-dimensional space by having its distance from four other, fixed points measured when these measurements are accompanied by elevations for all five points.

The measurements may be processed using iterations to find a best fit in the *Site Recorder* software package by 3H Consulting Ltd. of Plymouth, UK. This a proprietary software package designed for underwater and intertidal archaeology projects which combines a database with a layer-based graphic user interface for survey data, illustrations and base-maps. It features "live" input of primary survey data without using intermediary file formats – including the points and measurements used for DSM.

A network of control points must first be established, and "fixed" to remove them from "best fit" calculations, before features are similarly measured from four or more control points along with their elevations – these are recorded as detail points on a separate "layer" within the software. Once each feature's measurements are added, the best fit calculate should be run and saved before continuing with the next feature. This approach allows extraneous results to be identified – possibly even whilst the measurements are taken allowing for them to be retaken.

A more detailed guide to this technique can be found in Bowens (2009) Chapter 14 on Underwater Survey, especially regarding the critical importance of the design and implementation of the survey control network, and the need for clear line-of-sight to enable to use of tape-measures.

Even when run in the free "demonstration" mode, *Site Recorder* enables these spatial coordinates to be exported in formats suitable for use alongside photographs within *Photoscan Professional*, in addition to building, computing and saving a file with unlimited DSM measurements (Holt 2019).

This spatial information is, of course, all relative, but can be made absolute on the addition of a reference coordinate system to the control points. An additional option is to scale using DSM, but instead to either lay a baseline following a cardinal bearing through the control point network to provide orientation in addition to scale (Yamafune et al 2016:10).

<u>Shallow Water Shoreline Sites</u>

It is also worth noting that additional options exist where the subject is permanently submerged in shallow water but close to the shoreline. Such sites are found in lakes and rivers as well as marine environments. Here, it may be appropriate to use RTK GNSS as above in 3.2 to establish submerged control and possibly detail points where the water depth is sufficiently shallow.

Another option is to use a TotalStation on the shore to record the coordinates of a prism, mounted on a submerged staff of known length above a submerged point of interest (Henderson et al 2013; Bowens 2009:92). The staff may be manipulated by people in wading depth, or even by divers or snorkellers, although ensuring effective communication with the TotalStation operator is evidently key.

3.4 Geographical Referencing for Submerged Subjects

When recording on dry land, the use of GNSS equipment or back-sighting from a point of known coordinates such as the corner of a building or (in the UK and Ireland) an Ordnance Survey trig point are evidently appropriate methods for geographically referencing survey control and thus the resulting 3D model. These may be performed without using professional equipment: although a smartphone or handheld satellite receiver will be less accurate than a professional device (even if it supplies coordinates to a similar degree of precision), this may not necessarily be a problem, depending on the survey requirements. The accuracy of such coordinates may also be augmented through taking additional readings to enable averaging or recording additional locations at tape measured distances apart to enable accuracy verification using check-measurements.

However, when working with submerged sites this becomes more complicated as it is evidently vital to transfer a coordinate system established above the surface underwater. In shallow sites, close to a shoreline, this may be performed using the methods discussed in the preceding section. For subjects in deeper water, or more distant locations, alternative methods for translating a coordinate system into the real world will be needed.

It may be possible to extract coordinates for key features from a geophysical dataset, depending on its resolution. Multi-beam Echo Sounder datasets (if available) may be used to easily extract such coordinates for identifiable features, because these come with 'reliable … [and] calibrated' coordinates (Ortiz Vázquez 2018:84).

However, this must also depend on how recently it was acquired, as marine sites are frequently subject to continual disruption resulting from 'scrambling devices' such the effects of underwater currents and storms on the seabed (Muckleroy 1978:175-182). As such, their site-formation processes are dynamic and continually evolving due to such physical influences (ibid.), in addition to degradation caused by biological or chemical processes.

In order to facilitate effective preservation in-situ, the effects of such factors on both the shipwreck itself as noted above and also upon the seabed itself will need mitigation (Gregory and Manders 2011:108-109): effectively aiming to halt or at least significantly decelerate these on-going processes of site-formation.

Indeed, the 3D recording methods discussed in this thesis can also be used to both monitor change over time, possibly during an archaeological excavation (De Reu et al 2014; Pascoe et al 2017). Such recording has been termed "4D" (Pacheco Ruiz et al 2018) and as also used to provide data to aid the examination of such site-formation processes (Ortiz Vázquez 2018). For these reasons, it may be preferable to apply an alternative methodology – certainly for scaling and possibly for geographical referencing if accuracy is critical, and also achievable within the circumstances.

There is an existing practice of recording the position of a buoy floating on the surface but tethered to a point of interest on the seabed (BSAC

2005:138). The position would ideally be noted at low-water slack, and the use of a second buoyed feature would also enable scaling and orientation as well as geographically locating the subject.

Traditionally, this method were used by divers or fishermen to record the locations of shipwreck sites to enable repeat visits – the buoys and the attached ropes and shot-weights could then be recovered and the sites rediscovered using coordinates in conjunction with an echo-sounder (BSAC 2010:86; RYA 2014:27). If needed, the coordinates could be marked with such a buoyed "shot-line" to form the basis for a diver-based circular or square search pattern (BSAC 2010:92-93).

These positions would be recorded either using transits from features ashore or an available GNSS device (BSAC 2000:167; RYA 2012:58-59; RYA 2014:26-27+30-31). If close enough to shore in good weather, there is no reason this could not be achieved using a prism and a shore-based TotalStation. The buoys could obviously be alternatively attached to survey control points.

Low-water slack is used to enable the buoy's rope to be pulled tight to the shortest possible length whilst not being subjected to water flow to minimise the inherent inaccuracy, possibly by suspending a "lazy shot" from the buoy (BSAC 1990:58-59; BSAC 2010:140). The depth should also be recorded to form a vertical offset to translate the position of the buoy to that of the control point.

Another method is outlined by the marine archaeologist John McCarthy in an example case-study in Historic England's guidance publication for photogrammetry for heritage subjects (Historic England 2017:102-106).

McCarthy designed an alternative approach whilst working for Wessex Archaeology (a UK-based commercial archaeology contracting company) to record a submerged cannon site at Drumbeg on Scotland's Northwest coast in 2012 and 2014.

Here, the divers' mobile position-indicating surface marker buoys (which they controlled from the seabed using a line on a reel) had their positions continually recorded, whilst the divers would have needed to record the times and depths of submerged features. During the 2012 fieldwork, the divers were themselves tracked using an acoustic positioning system (McCarthy 2012).

The use of this technique enabled a small team to rapidly survey the entire site suitably, enabling its analysis and interpretation - alongside 'typological dating' and the context of the 'known maritime archaeological resource in Scotland' - to indicate that the vessel may have been far smaller than other known examples from its time in that region of Scotland (McCarty et al 2015:206). Following further historical investigations, the potential 'national importance' of the vessel and the site led Scotland's national heritage agency, Historic Environment Scotland, to designate the area as Scotland's first Marine Protected Area in 2013 using the procedures for speedy designation established by the Marine (Scotland) Act 2010 (ibid.).

3.5 Integrating Spatial Data

Having considered the potential sources of appropriate spatial data for Image-Based Modelling, consideration must now turn to the processes by which such data is combined with the photographs into an integrated model-generation process. In essence, two methods exist: the manual marking and annotation of features or an automated process.

Manual Data Input

Features may be marked within *PhotoScan Professional*'s user interface by placing marker flags onto the model – coordinates may now be added to the marker; alternatively, pairs may be determined as scale-bars and attributed with a measurement. This method can be used for control points and detail points alike.

However, it is preferable for this spatial data to be used to constrain the calculations which produce the model not simply applied locally to the finished model, which could cause distortion. In *PhotoScan Professional* following the image alignment, a 'low-accuracy dense point-cloud and a low-resolution mesh' may be produced to enable the placement of markers and the input of their attributes before running an 'optimisation of the image alignment … using these values' before continuing with the work flow again from dense point-cloud creation because by re-running the alignment the previous dense point-cloud and mesh are 'rendered redundant' and deleted (Historic England 2017:15).

Targets

Numbered, unique photogrammetry targets may also be generated within *PhotoScan Professional* and printed copies placed on or adjacent to the subject before the photographs are taken. *PhotoScan Professional* can then automatically identify the targets in the photographs (Historic England 2017:50)

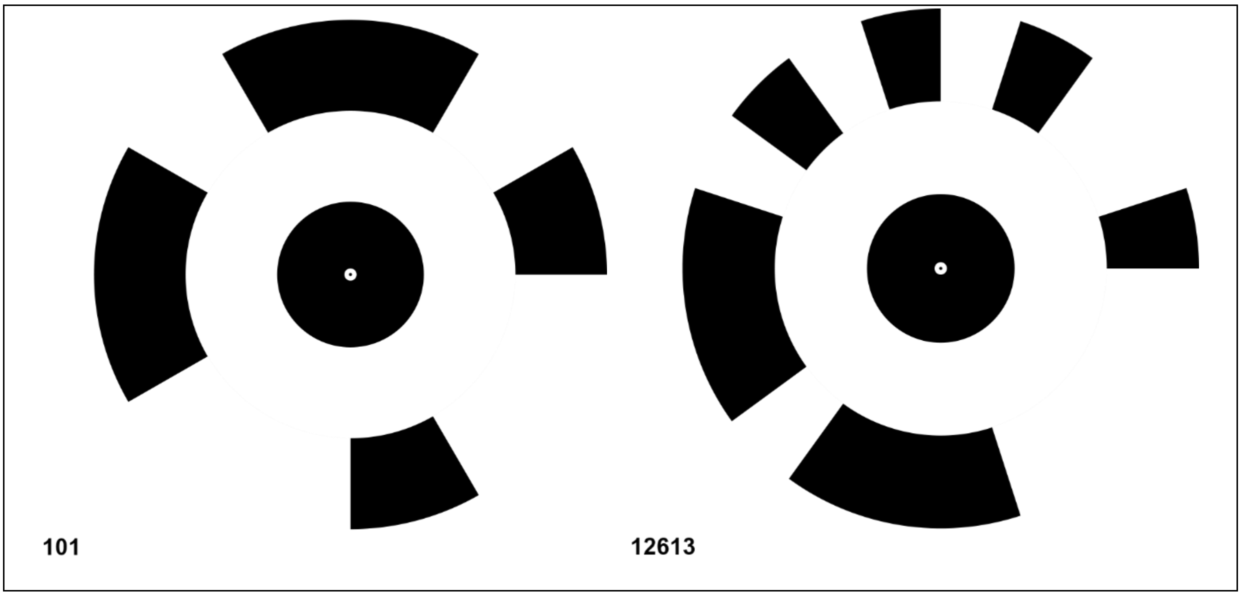

Figure 5: Two Agisoft PhotoScan *photogrammetry targets.*

Image Source: The Author.

These targets can be used for two purposes: they may be used to aid the software deducing the image alignment, but they may also have spatial data assigned to them – such as surveyed coordinates or measured distances between designated targets. Careful consideration needs to be taken to ensure they are produced in a suitable size (Yamafune 2016:20-21; Historic England 2017:50).

This method is much less laborious than using the manual approach placing markers on the model, although it requires further preparation and is evidently impossible when attempting to gain further information from existing datasets.

3.6 Chapter Conclusion

This chapter has answered the project's first objective regarding possible sources of spatial data. It has also provided the second with two methods for investigating further through practical experimentation.

Suitable sources of spatial data identified are the use of single or multiple scale-bars, or enclosure of the subject within known dimensions as possible methods of scaling Image-Based Modelling datasets. In addition, the use of on- and off-subject surveyed points are possible options for scaling, but these can also provide orientation and referencing when they are supplied as coordinates rather than linked to provide a dimension. These should be surveyed using a TotalStation within an appropriate grid, or by using the Direct Survey Method (DSM).

Two methods for linking such survey data within *PhotoScan* have been uncovered: automated targets which may be detected before aligning the photographs or manually placed markers, which can be added once the model has been constructed. Ideally, when being used for spatial data, these should be included as early in the processing pipeline as possible.

Chapter 4. Literature Review: Current Technical Guidelines

Having first examined the existing literature to investigate the details of the 3D reconstruction process, the differing sources of appropriate spatial data, and how to integrate them into the 3D reconstruction pipeline, it is now time to consider the project's third objective: which forms of spatial data produce the most accurate results?

Technical advice, possibly including specific guidelines, is evidently needed for photographic and spatial data collection, and 3D model production, but also for how the resulting 3D models should be validated. This would allow their accuracy to be "rated" in similar ways to other forms of metric recording and thus establishing the extents of their utility for further applications.

The purpose of this second formal literature review, therefore, is to explore these topics, with special consideration given to maritime or underwater subjects, how these have been recorded in the past, and to the needs of citizen scientists.

Beginning with official guidance from relevant organisations, before moving on to PhD theses and other grey literature, this chapter aims to identify gaps or inconsistencies, before examining the extent to which existing material addresses any shortcomings.

4.1 Official Organisations

Historic England (2017)

The official, published guidance for applying photogrammetry to cultural heritage from England's national heritage agency provides a clear breakdown of the production pipeline, eschewing background detail to focus on technical guidance.

From the outset it makes clear the need for spatial data to be used in tandem with photographs. Although understandably light in relation to the underlying science and history of photogrammetry, this "guide to best practice" outlines the processes involved and offers a reasonably thorough guide to photography, where relevant.

However, although this document addresses aerial photogrammetry in detail, it neglects to provide adequate coverage to recording structures and sites at closer range. There is a real shortfall are in practical guidance regarding how to plan and execute effective non-aerial data acquisition, the processing options and their implications at the varying stages of the pipeline, and how to evaluate the results beyond examining 'completeness, scale and accuracy … against the physical evidence' - in other words simple check-measurements (Historic England 2017:98).

This document refers to maximum distances between points in scaled point-clouds acceptable for use as the basis for ortho-photographs, for example, but there is no practical guidance here or in the wider body of literature reviewed as to how to achieve this (Historic England 2017:67).

The question regarding standards for production - and especially evaluation - remain not just unanswered but largely unaddressed, especially when compared to Historic England's other guidance documents; see next entry.

It is also very brief when considering objects and artefacts, to which around two pages in the main body and one three-page case-study are devoted out of a 125-page document. Commendably, two of the case studies are underwater maritime subjects, reflecting the significance of this approach within the maritime sub-discipline (Historic England 2017:102).

This is not to say that this document is not a welcome addition to the body of literature regarding the application of photogrammetry to cultural heritage: it provides a clear outline of what to do, if not adequately explaining how to do it, and underlines from the start and throughout the need for spatial data to be used alongside the photographs for all but the quickest visualisations.

<u>Historic England (2015)</u>

This publication on metric survey specifications for cultural heritage defines photogrammetric survey as 'surveys where overlapping image sets are used together *with control* to produce a three-dimensional representation of the subject from which the required detail is generated', again clearly stating the need for additional spatial data to be used alongside images (Historic England 2015:4.1.1; my emphasis[7]).

Survey design and implementation are dependent on the required levels of detail or accuracy, and this publication defines such standards for heritage

[7] This report has no page numbers only section numbers.

subjects, stipulating +/- 3mm accuracy needed for control coordinates for image-based surveys, for example (Historic England 2015:4.2.1).

This publication lists such standards for varying styles of survey including measured building and topographic surveys and terrestrial laser-scanning, as well as survey control and the presentation of such surveys for reports. However, guidance on how to achieve these standards – or to verify that such standards have been achieved – is clearly beyond the scope of this publication. This does not reduce its importance as reference document: indeed, it is referred to as 'detailed and thorough' by the next publication to be examined (Historic Environment Scotland 2018:5).

Historic Environment Scotland (2018)

This is an excellent publication written by members of Historic Environment Scotland's digital documentation team, which offers a highly readable introduction to the capabilities, uses, and implementation of a range of techniques - including Image-Based Modelling - to large subjects in-situ and structures. Additionally, there is a separate section on recording artefacts.

It is written in non-technical language, explaining the key concepts succinctly and without ambiguity, but critically also discussing how to implement such methodologies; including survey control. It underlines the critical importance of required demonstrable accuracy, considering varying outputs and deliverables, their suitability for differing purposes, and their archival requirements - differentiating this from 'storage' through the need to maintain ongoing usability rather than simply being deposited (Historic Environment Scotland 2018:8).

Photogrammetry is defined as a ‘powerful technique for producing potentially highly accurate 3D datasets’ (Historic Environment Scotland 2018:17), before going on to provide practical guidance for the photography (such as aperture for depth of focus, and the degree of overlap – here 60%) (Historic Environment Scotland 2018:18).

Of relevance to the examination of technical standards for the evaluation of such 3D datasets, this publication notes that the resolution (minimal point-to-point distance) is not determined by capture settings but from the source images (Historic Environment Scotland 2018:19). This can be calculated using a method cited from Historic England (2015) by taking the distance between the camera (presumably the sensor) and the subject, dividing that by the focal length, with the result then being multiplied by the pixel resolution of the sensor.

This “Ground Sample Distance” can also be calculated using a scale-bar or known feature of reference (presumably in the same plane as the sensor) and dividing its length in reality by its length in pixels within the image, to provide a minimum measurable distance. This is interesting because as well as being used after the event to quantify the achieved results, it could also be used at the outset in deciding either equipment requirements or achievable survey resolution.

However, again there is noticeable a lack of material regarding validation techniques for the accuracy or precision of the resulting datasets for either the creator or the end-user. This is possibly because data collection and survey control may have already been quantified in this regard, using the methods described in the text. There is also no reference to the marine or underwater environment. Despite these specific shortcomings relevant to this project, this remains an excellent and useful publication for practitioners of all levels.

4.2 Maritime and Underwater Subjects

McCarthy et al (eds.) (2019)

As McCarthy et al note in their jointly written opening chapter, there has been a 'paradigm shift … from 2D to 3D recording and interpretation techniques which becomes particularly evident in publications from 2009' and that this is not unique to archaeology (McCarthy et al (eds.) 20090:1+3). This shift towards 3D has also led to 'tensions between capturing the most accurate and objective surveys possible and the archaeologist's ultimate goal of cultural interpretation' (McCarthy et al (eds.) 2019:3).

After a thorough description of the evolving use of photogrammetry and photo-mosaics, citing the key papers relevant to the journey into the digital, and a discussion of the future uses of such data in combination with geophysical datasets, this first chapter moves to a discussion of standards.

Here the authors note the key problem which is that due to the accelerated timeframe within which these methods became mainstream, there was insufficient sharing of knowledge between individuals working alone – this has led to a 'flowering of experimentation and innovation' but also to 'duplication … [and] wasted effort' and a possible slide 'away from the rigorous standards using traditional recording techniques, which have developed over many decades' (McCarthy et al (eds.) 2019:6). They go on to note that:

> 'At the time of writing, there is no detailed formal guidance focused on underwater photogrammetry. While most of the important information is available in journal

> publications, such sources tend to present case studies with specific workflows which are still experimental in many ways' (McCarthy et al (eds.) 2019:7).

So, in the acknowledged absence of current technical standards relating to a largely emergent practice, let us turn our attention to what preceded these newer approaches.

4.2.1 HOW HAS THIS BEEN DONE BEFORE?

Underwater tape-measure surveys, alongside shallow/inter-tidal methodologies, have been discussed in the previous chapter (section 3.3). These methodologies produce 2- or 3D outputs suitable to be imported into CAD software to produce a site-plan in diagrammatic format. It should be noted that such techniques will enable the production of a site-plan created from joining a small number of accurately placed points to capture the positions of key parts of the subject.

The *details* of the subject would need to be recorded using alternative methods, such as drawing frames (double-strung to avoid parallax errors) (Bowens 2009:125-126), or alternatively from importing/tracing orthographic photographs or photo-mosaics (Martin and Martin 2002: see below). These would need to have been included within the surveyed points – though contained features, or corners of a drawing frame – to enable their localised detail to become part of wider, site-level, recording in detail.

However, although this project concerns 3D digital data in point-cloud vector format, rather than raster data derived from analogue measurements, it is still important to consider such methodologies. Not only do they offer utility as survey control: the evolution of maritime archaeological recording techniques also indicates through extension the degree of achievable accuracy in recording within such environments. Accuracy standards which are infeasible are clearly of limited value, so examining how this sort of activity has historically been performed in these environments is vital in considering relevant technical standards – or the lack thereof.

Martin and Martin (2002)

In section 3.4 the dynamic nature of submerged shipwreck sites was discussed with reference to Keith Muckelroy's publication *Maritime Archaeology* (1978). Although the techniques used have evolved far beyond the analogue methods described within this work, its introduction to the scope, environment, purpose, and theoretical framework of maritime archaeology as a discipline make it still very much a key text.

As Muckelroy notes: 'the main difficulties [in underwater archaeological recording] result from restricted visibility; it is generally impossible to get the whole of the site in one photograph, and recourse has to be made to photo-mosaics for illustrative purposes' (Muckelroy 1978:31-33). Martin and Martin (2002) discusses a methodology for avoiding some of the problems with gathering suitable photographs and then producing a mosaic whilst avoiding the frequent compound errors which can creep in from minor mistakes in scale, skew, or rotation.

Essentially the technique involves the use of a weighted frame, kept vertical using submerged buoyancy and monitored by the diver using spirit levels to take vertical photographs from a constant elevation over a flat subject. The diver decides the overlaps between the photographs, which will also capture the site's survey grid, laid-out in 5 metre squares using levelled scaffolding bars. This will produce photographs suitably to minimise the difficulties outlined earlier to aid the manual production of the photomosaic, thus enabling the entire site to be seen in a single image (which Muckelroy noted is a viewpoint usually denied to underwater archaeologists) as well as offering a visualisation of the site for other purposes.

It should be noted that such an orthographic image, if geographically referenced, would be suitable for combination with other datasets within a geographical database. Photo-mosaics could therefore be viewed in some ways as a precursor to photogrammetry and can also be key sources of legacy data.

Martin and Martin (2002) illustrates the integration of the analogue and the digital, as well as the evolution of techniques and standards within the challenges imposed by the maritime environment, as well as underlining the historic importance of photo-mosaics in underwater archaeological recording.

Campbell (2010)

In Peter Campbell's presentation to the Computing Applications and Quantitative Methods in Archaeology conference in Virginia in 2009, he describes a method for recording land-based maritime subjects, whilst also proposing how to modify the technique for submerged subjects in shallow water close to land.

A TotalStation is used to record a high-resolution survey of the subject, surveying multiple points for features and detail, rather than key vertices or dimensions. These points are all labelled with adhesive reflectors to act as prisms – this allows both higher accuracy recording than using the TotalStation in non-reflector mode and enables the coordinates to be mapped into a series of photographs to produce a scaled photogrammetric 3D model, using *Photomodeler*[8]. In addition, by using *Rhinoceros* CAD rather than *AutoCAD*, the complex curves appropriate to watercraft and accurately recorded using the TotalStation, could be more appropriately captured using NURBS (Non-Uniform Rational B-Splines), rather than the more rigid geometry found in *AutoCAD*.

Campbell's article illustrates the development of the use of digital technology not only for the collation and production of final material, but also for its capture – critically, he is aware of the capabilities and limitations of various methods, and has designed a method based on matching these as best as practicable (the article also focusses on performing such tasks using very limited funds) *based on the requirements of the analysis in question*. In other words, this method is practical and led by the required deliverables, rather than by an abstract or theoretical sense of "accuracy".

4.3 PhD Theses and Postgraduate Dissertations

Yamafune (2016)

This is a PhD thesis entitled: *Using Computer Vision Photogrammetry (Agisoft PhotoScan) to Record and Analyze Underwater Shipwrecks* submitted to Texas A&M University in May 2016 and subsequently successfully defended.

Like Historic England (2017), Yamafune highlights the importance of using spatial data in addition to the photographs. The thesis begins with an examination of photography for underwater photogrammetric data

[8] In 2009 Agisoft *Photoscan* had yet to be released, and *Photomodeler* was widely used.

collection before moving on to considerations of how to combine these with spatial data, and how to acquire both of these underwater.

During this thesis, Yamafune notes that the Agisoft user manual fails to explain the details of the various processing options at each stage of the model generation process. There is a resulting detailed third chapter in which he uses a set of photographs of two cubes with differing surface patterns to examine data processing parameters, their effects and optimal applications, considering outcome and processing time, noting that the features explored in his experiment stemmed from online software user forums (Yamafune 2016:52).

The thesis then moves into considering uses of scaled exports for further study, to promote underwater cultural heritage, and to document it. He ends with considering its utility for in-situ management of underwater cultural heritage and the use of legacy datasets.

The first two chapters were of most use to this project, considering not only data acquisition and integration but, most importantly, the effects of the processing options available in *PhotoScan Professional* – to date this is the only academic literature successfully identified and recovered by this author on this subject and was very useful in guiding the research relating to best practice for model creation.

However, the shipwreck sites considered by this thesis were largely two dimensional, following their wrecking processes. Although there was clearly an evident 3D element to them, they were largely recorded in a manner similar to aerial photogrammetry. In other words, the subject's principal axis was in the same plane as the camera's sensor – this is not the case when working on land.

Furthermore, because the coded targets used by Yamafune were again in the same plane as the camera's sensor, he only needed to consider their size to ensure they were successfully detected. This research project also had to consider their orientation in addition to their size, due to the differing perspectives resulting from working on the land.

Tidball (2016)

This is an MSc dissertation in journal format entitled: *Accuracy of Underwater Image-Based Modelling Determined Against Terrestrial Laser Scanning* submitted to Plymouth University in the UK for the degree MSc Hydrography in September 2016.

The text was made recommended to the author by one of Tidball's dissertation supervisors, Peter Holt, a contact of the author and the creator of the *Site Recorder* software package. Tidball received distinction for both this dissertation and his degree.

This dissertation used a rock on an intertidal foreshore as a case study due to its irregular geometry resembling concretion on a submerged shipwreck. The rock was surveyed within an arbitrary coordinate system using a TotalStation and the Direct Survey Method, before being photographed dry and then submerged. Image-Based Modelling was used to generate dense point-clouds which were then compared to each other and to a laser-scanned point-cloud in the same registration.

The results were that although they were less dense, contained less surface detail and had smaller volumes than the laser-scanned point-cloud, the IBM point-clouds where still very similar overall to the laser-scanned one. They were also largely consistent with each other, revealing that underwater IBM is no less accurate than dry IBM and that a well performed Direct Survey Method (DSM) survey can be comparable to one performed with a TotalStation.

An additional interesting element of this dissertation for this project was the comparison techniques used for the various point-clouds. The open source *CloudCompare* software package was used to examine cloud-cloud distance in real terms, examining their densities and the roughness of their surfaces. Volumes were also measured by adding together the intermediate volumes of cross-sections of known thicknesses, whose areas had been measured using *ArcMap.*

However, Tidball (2016) provides some very useful details on computational point-cloud validation rather than simply using check-measurements. He also indicates a possible methodology for performing several survey methodologies to a subject within the same reference coordinate system and using the same on-subject detail points for comparison. This project used a similar approach to enable comparative data to be acquired in a controlled manner.

Kjellman (2012)

This was a master's dissertation in Archaeology submitted to the University of Tromsø in Norway in spring 2012. It was entitled: *From 2D to 3D: A Photogrammetric Revolution in Archaeology?* It was recovered online by the author during research for this project. Although it can be assumed that Kjellman's dissertation passed, it is unclear how it was graded and thus needs to be treated with more caution than the earlier entries in this section.

Kjellman used a TotalStation to capture the 3D structure of the burial mounds recorded using scaled photogrammetry as case-studies for his dissertation. He then compared exported Digital Elevation Models in *ArcMap* by subtracting them from each other and dividing them by each other to quantify and represent differences respectively. He also compared resolutions, generated contour maps to avoid the 'graded representation' of the DEMs (Kjellman 2012:29) and also performed check-measurements. Although not quantified, they were consistent in capturing surface topography.

This methodology was of interest to this project partly as additional examples of user-level data evaluation methodologies. He used the TotalStation in a manner similar to Campbell (2010) for a high-resolution "scan" of the subject including its details rather than its vertices and dimensions, although he did not use reflectors.

4.4 Additional Publications

Green and Gainsford (2003)

Experiments with a purposely designed 3D structure recorded using Image-Based Modelling with a Direct Survey Method (DSM) survey as a dry control were compared to the same methodology repeated underwater. An average of 2mm deviation in the location of marked points on the structure between the two sets of measurements was found; this may, of course, have resulted from survey errors rather than integration or processing, which was performed using *Photomodeler*.

Capra et al (2015)

A similar experiment with a marked 'calibration frame' revealed a 0.5mm overall error when using a camera with reasonable quality optics (a Canon PowerShot G12) when comparing the computed value for target points to those laser-scanned in the same (local) reference frame.

Holt (2003)

Here multiple sets of tape-measurements were taken between the same points on a series of DSM surveys of a shallow underwater shipwreck; there was found to be an average standard deviation (spread) across all the measurements of 25mm which was determined to result from water movement and difficulties maintaining consistent tension on the tapes. A smaller dry experiment yielded a standard deviation of 6mm on measurements up to 12 metres.

This study illustrated the need to minimise the distances measured using tapes to avoid the introduction of increasingly significant errors. Muckelroy had noted that reduced visibility had frequently led to 'short range surveying techniques' being used 'across much greater distances than would usually be deemed acceptable … [or] even be possible on a land site, where optical instruments could be used' (Muckelroy 1978:45).

By quantifying the effective range of tape-measures for underwater surveying, Holt is in effect arguing for the use of the Direct Survey Method. Through the establishment of a control network – possible using a high number of control points – these problems may be overcome, and measurements kept within the range identified to be accurate to the defined standards.

Demonstrably accurate as this will be, it must be noted (from the author's experience) that the establishment of such a control network can easily take far more time than many project managers anticipate, and that this can result at best in compromised survey control, and at worst in many measurements taken of control and detail points, but not enough of either to enable the maths to calculate a site-plan.

This is not a criticism of the technique as impractical – in many circumstances it may well be the only viable option for a demonstrably accurate survey – but a note of caution regarding its selection and implementation. Nevertheless, Holt (2003) clearly demonstrates the effective distance limit of underwater tape-measurements as well as the range of results which can be recorded by differing people of an identical dimension.

Pascoe et al (2017)

Of relevance to this project is the method used to scale and evaluate the accuracy of the resulting models. A series of coded photogrammetry targets were used on the site: they were printed onto machine-cut boards of uniform size and placed on the subject so that each photographic "run" would include at least two of these targets. The distances between targets and their neighbours were also measured centre-to-centre using tape-measures for scaling.

Having scaled the model, the targets were then measured within software and compared to benchmark measurements taken using callipers – the targets were all a uniform size due to their construction.

These check-measurements were repeated three times to enable averaging to eliminate error from pixel selection and compared to the benchmark. These found mean errors of 2.028mm and 1.416mm in the two regions validated. By calculating the standard deviations within the measurements data for each region, and then doubling it on either side of the mean (to represent the two standard deviations either side of the mean where there can be 95% confidence with normally distributed data) this returned accuracy errors of no more than 5.7mm and 3.1mm in the areas checked.

Rule (1989)

Rule reported that during the *Mary Rose* project, it was found that 68% of tape-measurements could be expected to be 20-30mm of the correct distance.

McCarthy and Benjamin (2014)

When recording submerged two-metre cannon at Drumbeg in Scotland, scaled using a one metre bar, the longer dimensions were found to be within 10mm of check-measurements, although shorter examples such as muzzle face were found to deviate much more, and to show more variation.

4.5 Chapter Conclusion

It is clear that there is literature to support an investigation into technical standards, but that there is very little consistency between the various authors. There are evidently multiple factors involved, with both the acquisition of the spatial data and the effects it may have on the 3D model. It does appear that, despite outliers affecting the range of collected results, with these removed achievable accuracy can be higher than 20-30mm.

On balance, this project will proceed by aiming to achieve the highest accuracy possible for spatial data, both to integrate with the 3D modelling process and to use as control data to compare the results. Due to the accuracy of the measuring instruments to be used (TotalStation and tape measure) this project will use a 1mm standard of precision for recording, see 5.6.

It also appears that a large proportion of the literature refers to shipwreck sites which are essentially flat hull remains on a largely flat seabed, where the diver performs data collection "runs" in a similar fashion to how a drone would be used to record a subject of similar geometry on dry land. Historically, these may well have been recorded using photo-mosaics, and to a large degree much of the data collected may be used to produce exactly such ortho-images as site-plans.

This is significant for the development of technical guidelines, and especially for citizen scientists for two reasons. Firstly, because sport divers tend to be more interested with metal shipwrecks from the 19th and 20th Centuries, they are likely to be dealing with subjects where the geometry is typically much less flat. Even if the hulls have largely collapsed, heavier features – specifically diagnostic features which may aid identification or analysis such as boilers or other engine/armament fittings – will often remain much more intact, and frequently rise high from the seabed. This will evidently have an impact on the photographic data collection methodology.

Secondly, again due to the difference in subject geometry, because the methodologies for spatial data collection using tape-measures are reliant on line-of-site, there will be two additional problems. The first is that the subject will likely impede line-of-site, preventing the implementation of the procedures outlined above. Here, secondary (non-permanent) control points may need to be established on the subject itself to enable the line-of-site to "jump" between outlying permanent control points – in turn creating a more complex network of multiple linked networks than would be needed for an essentially flat site. This will clearly affect the time needed, and the feasibility of the survey.

The second problem is that addressing these hindrances may lead to reliance on longer tape-measurements being needed, with the increased degrees of inaccuracy identified by Holt (2003).

So, in essence, there is much useful material regarding data collection and processing, but less relating to data validation: the main method here is the use of check-measurements, possibly including averaging and standard deviation. It is also evident that much of the published work relating to archaeological shipwrecks relates to largely flat subjects. This leaves a gap for how to further the available technical guidance to aid citizen scientists (and paid professionals alike) in recording the more varied geometries of metal subjects from later periods.

Chapter 5. Experimental Methodology

5.1 Case Studies

5.1.1 SELECTION

A section of the keel and lower planking from the bow of a motor fishing vessel (MFV *Sanu*), left over from a previous Bournemouth University Maritime Archaeology project and more recently used for training MSc students, was selected as the main case study of this project. Two additional datasets were acquired from an unrelated anchor recorded twice with either a one metre scale-bar parallel to its principal axis or staged with two approximately $0.5m^3$ cube-shaped gardening plant boxes, to enable further measurements to be extracted from the resulting 3D models.

These case studies were selected not simply as maritime objects, but as suitable examples for trialling the recording methodologies selected realistically and in-situ, possibly by divers, and possibly by citizen scientists. They were also chosen as examples of the sorts of material that would be recorded with a view to answering archaeological questions relating to construction techniques, evidence of modification or use, and typology.

Additionally, they were chosen as features to record in detail to answer precisely such questions, whilst being metrically recorded suitably to enable their inclusion in wider site-level surveys, performed to lower resolution; this is in keeping with the proposal for Image-Based Modelling to be applied more selectively to features rather than entire sites, especially when being performed by citizen scientists.

5.1.2 IMPLEMENTATION

The subjects were placed on placed on pallets which had been covered with neutral coloured cotton sheets. As well as evidently being of maritime origin, and recorded using appropriate techniques for such material in-situ, these case studies had the advantage of being large enough to pose interesting challenges, especially to photographic data collection, without being so large their size would cause additional problems. This prevented lack of access to elevated camera angles, or the need for much larger numbers of photographs: this would impact both the computer processing time needed, as well as the feasibility of the methodology being used by unpaid groups without specialised computing facilities.

These relatively compact sizes also negated the need for repetitive recording of recurring features or construction details in the way larger heritage subjects would be recorded in reality; this project is a pilot study investigating the effects of differing data collection methodologies and their potential applications and utility, rather than to answer specific archaeological questions relating to the subject in question. Their size thus allowed proof-of-concept to be investigated in a reasonable straightforward fashion, identifying areas for further enquiry.

5.1.3 REFLECTION

The case studies selected proved appropriate for the experiments: suitable data was gathered, processed, and analysed. Each stage did not take excessive periods of time, although data collection and processing were time-consuming. It may be found that in some environments the methodologies would not be directly replicable due to time constraints. However, they were indicative of the sorts of materials and techniques that may well be used within this field of enquiry and should not be beyond the capabilities of a reasonably trained and prepared team of citizen scientists.

5.1.4 THE CASE STUDIES

Figure 5: 3D model of Case Study 1: The Anchor and Scale-Bar. Image Source: The Author.

Figure 6: 3D model of Case Study 2: The Anchor and Boxes. Image Source: The Author.

Figure 7: 3D model of Case Study 3: MFV Sanu*. Image Source: The Author.*

These case studies were selected as appropriate examples of the sorts of maritime heritage material that may be recorded in-situ by citizen scientists or by professional teams alike: these may be underwater or found in the inter-tidal zone, having been driven ashore and wrecked.

For the purpose of this investigation, they have been treated as inter-tidal and recorded appropriately: the effects and practicalities of underwater photography and diver-based recording were beyond the scope of this pilot study, although still included within the literature reviews and proposed method statement.

5.2 Methodology Overview

The case studies were surveyed within an arbitrary reference coordinate system using a Leica TS06 TotalStation, orientated by resection. These surveys included encircling the subject with four secondary control points at the upper corners of the sheet-wrapped pallet base (which also enabled enclosure measurements to be calculated and applied for scaling), and on-subject detail points.

These points were usually marked using photogrammetry target markers generated by Agisoft *Photoscan Professional*. The secondary control points were surveyed using the TotalStation's mini-prism, although the on-subject detail points had to be recorded using reflector-less mode which is not quite as accurate as using the mini-prism but was all that was possible when working alone with a non-robotic TotalStation.

In addition, scale-features were present alongside the subjects, parallel with a principal axis. The subjects were then photographed suitably to enable 3D models to be generated and scaled/referenced using the varying methodologies identified in Chapter Three, before being measured within *Photoscan*.

Check-measurements were also recorded using tape measures. These were used as benchmark data for ground-truthing when compared to those taken from the various computational models. Some further check-measurements were generated using *Site Recorder* from TotalStation coordinates.

Discrepancies between the scaled and/or referenced 3D models in *PhotoScan* and the benchmark survey data were expressed and evaluated in absolute terms as distances in millimetres, rather than as percentages. This was achieved though importing, processing and comparing the various metric datasets using MS *Excel*. These necessitated comparisons of both measurements and Cartesian coordinates.

This methodology was designed to compare the results of not only the differing sources of spatial data from the range identified from the literature review in Chapter Three, but also to explore the potential contribution of citizen scientists to metrically recording maritime heritage subjects. To this end, the methodology was designed in effect to compare the results of differing levels of project resources, considering *who* may be recording the subject as well as *how* they should do it.

5.3 Methodology Details

5.3.1 LOCATION

The empty floor space of an industrial unit in Poole, vacated by Bournemouth University Maritime Archaeology during summer 2018 for the excavation of HMS *Invincible* (1758), was used for this project. This provided the physical space to carry out a surveying exercise, but also to be able to leave equipment set up overnight.

Although this may well not be replicable on a real site, or underwater, it did enable a degree of experimental control: this is important because it meant that the results of the various methodologies could be compared having so far as practicable isolated them as the sole variables during the data collection.

In a real-world environment this would not have been possible, but also it should be noted that on a real project it is unlikely that so many differing methodologies would be used. It is far more likely that one or two approaches would be selected, and this project sought to aid in their selection from the alternatives: it was thus important to ensure an empirical, if perhaps unrealistic, comparison.

Figure 8: Data collection location. Image source: The Author.

Figure 9: Data collection equipment. Image Source: The Author.

This approach enabled the author to carry out a laboratory experiment, gathering more data and having an extended period of continued access to a secure site to trial more alternative approaches than could have been possible working in the field; especially where access to and from the site were constrained by the tide. This also avoiding leaving positioned survey markers in a public place at risk of interference, or misunderstandings regarding the purpose of the activity.

5.3.2 THE SURVEY CONTROL GRID

A survey control grid was set up as an arbitrary coordinate system with a control point at each corner of a five metre square. This was established on the floor of the industrial unit using tape measures, a level and a set square; this was marked using crosses made with cloth tape and fibre-tipped permanent marker pens.

The tape measures used for this were pre-checked over 15 metres to ensure any over-stretched tapes were eliminated – this distance was chosen as it was longer than any measurements required for this project. In addition, the tapes were checked against a retractable metal tape measure for accuracy and consistency over the five metres needed to establish the control grid, whose accuracy would be critical for these experiments.

This methodology was chosen partly to provide an appropriate arbitrary coordinate system, but also to be replicable by well-prepared citizen scientists (or paid professionals) working intertidally without specialist survey-grade GNSS equipment, or on an underwater site.

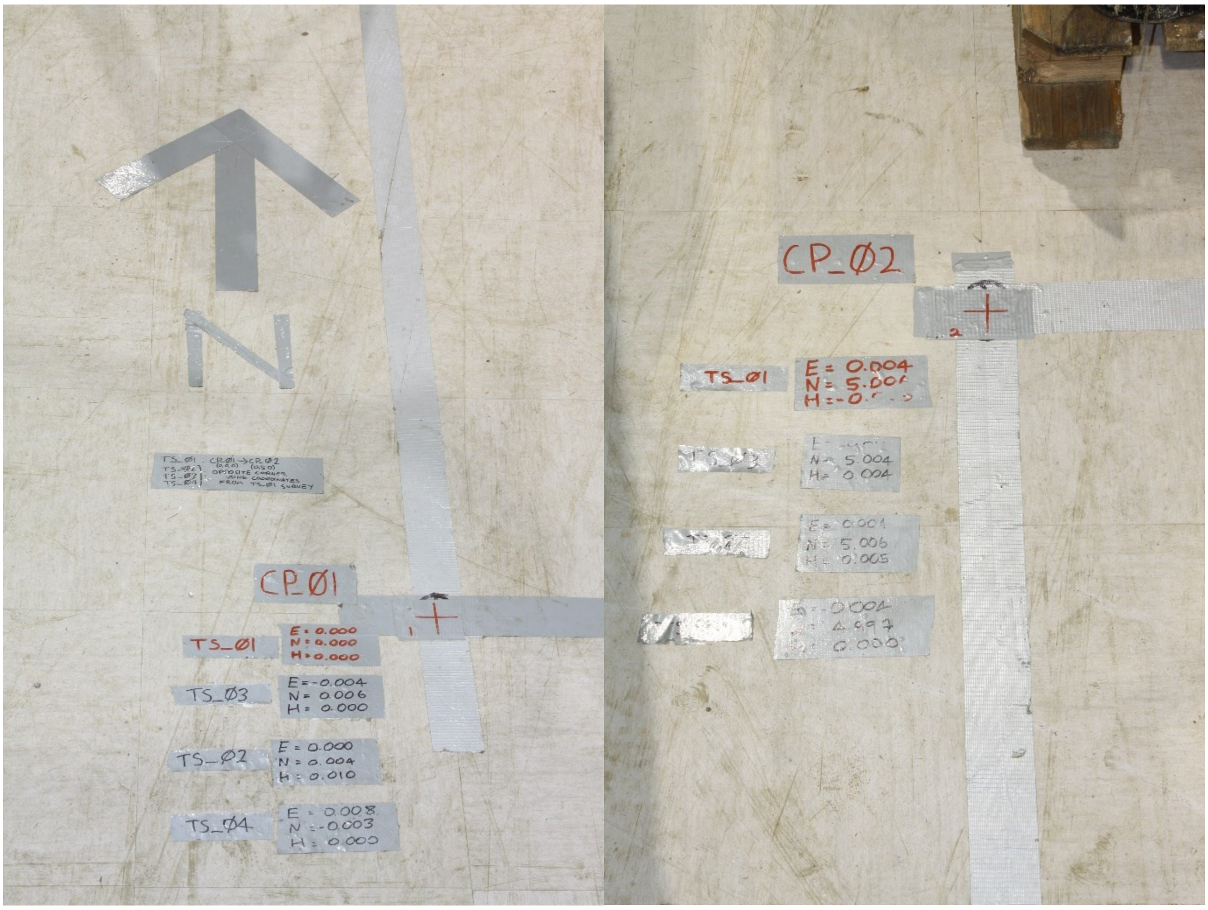

Figure 10: Survey grid control points 1+2. Image Source: The Author.

The four points were marked on the floor and repeatedly measured and adjusted using both the set square and the tape measure to enable points to be marked five metres apart but also at right angles – these were than checked with a Leica TS06 TotalStation used for this project with additional coordinates noted, to provide empirical oversite.

Once orientated over the grid origin corner by back-sight from another corner using a reflector prism and the tape-measured coordinates, all three corners were surveyed and a computed position for the origin was determined. These four measured coordinates were noted down as the grid's surveyed coordinates. These surveyed coordinates were then validated by repeating the process, back-sighting the TotalStation from corners of the grid using the first set of surveyed coordinates to locate and orientation.

The results of the three additional sets of coordinates were compared to the first set to ensure an overall consistency of within 20mm – this figure was selected due the precision of RTK GNSS equipment. In fact, a coordinate grid with a higher accuracy rating of around 10mm was achieved: the details may be found in Appendix 1. When subjected to a final check by TotalStation resection at a random point within this grid, apart from two points, all the coordinates were confirmed to be within 5mm, with most being between 1 and 3mm.

The four corners were also linked with cloth tape runs along each of the four sides of the square: these were intended to be used as enclosing baselines for right-angled offset measurements to be taken within the survey grid, to simulate the tape-measure survey methodologies outlined in 3.3, although these were never in fact used. This decision due to the more likely implementation of the Direct Survey Method either inter-tidally or underwater for tape-measure surveys.

5.3.3 TOTALSTATION SURVEYS

It should be noted that these were performed partly to provide benchmark coordinates from a calibrated instrument (in this case a Leica TS06), but also because the low costs of their hire (circa £100 per week in the UK at the time of writing) compared to other costs incurred in travel and fieldwork, combined with the speedy acquisition of quality data, make them highly suitable for use by appropriately trained citizen scientists.

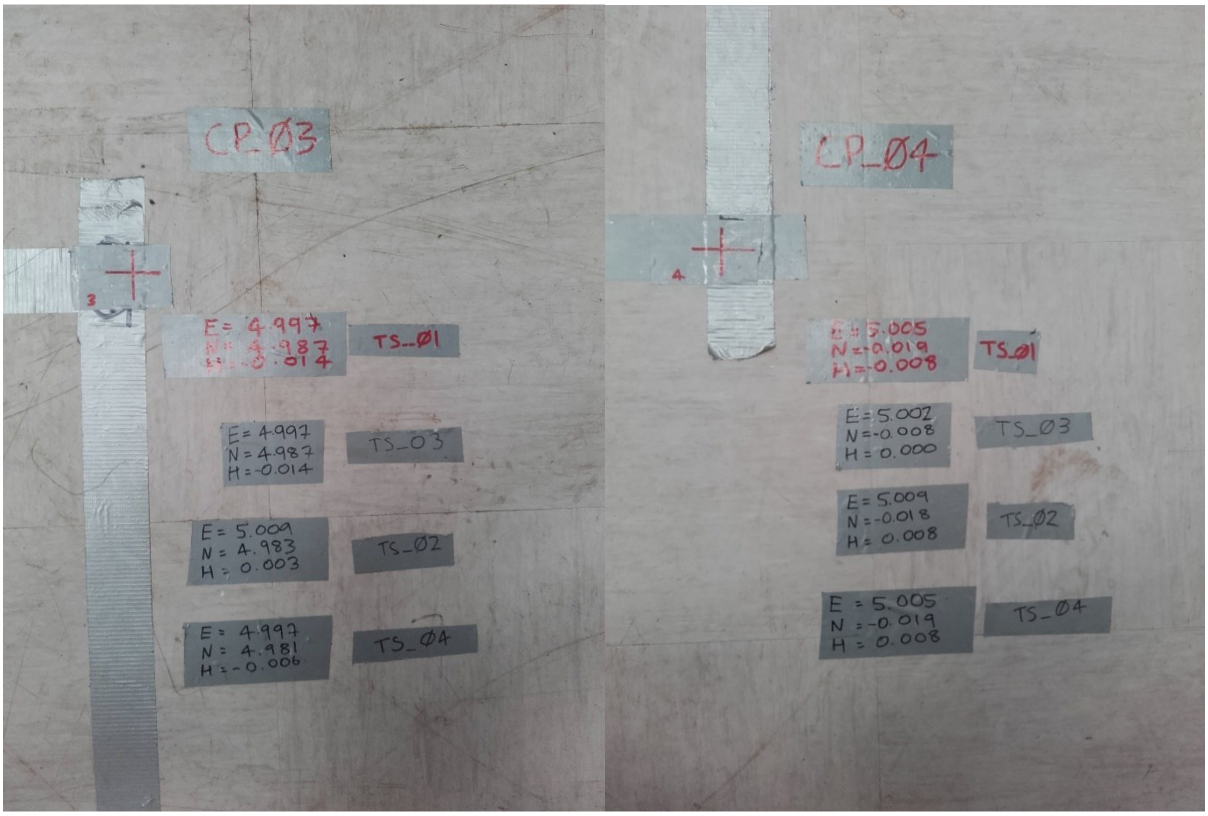

Figure 11: Survey grid control points 3+4. Image Source: The Author.

5.3.4 PHOTOGRAPHY

The photographs were taken with a Canon EOS 50D semi-professional digital SLR camera mounted on a tripod with the lens kept at a fixed focal length. Additional lighting was needed – this was set up and trialled using experimentation. Planned "runs" were made along the taped sides of the grid, taking overlapping panoramas of photographs from pre-defined, equally spaced positions. These were trialled and checked for sufficient overlap using a laptop running *PhotoScan Professional* in demonstration mode to ensure alignment whilst still able to retake the photographs if needed.

Numbers of photographs taken from each "station" were kept constant to enable predictable and consistent numbers of photographs to be captured from each location – this had the added advantage of aiding keeping track of where very similar looking photographs had been taken, based on their consecutive file numbers. A low and high elevation panorama was taken from each position.

As well as "runs" along the taped grid, at each point as well as two panoramas of photographs taken from the extent of the square, the tripod was also moved in to enable an additional panorama to be taken from a closer position with a higher elevation.

5.4 Case Studies 1 and 2: The Anchor

This was recorded twice as described above with on-subject detail points at three key places on the anchor. The only photogrammetry targets used were to mark the secondary control points at the four corners of the sheet-wrapped pallet; these were surveyed by TotalStation using a mini-prism within the arbitrary grid. The on-subject detail points were recorded in reflector-less mode out of necessity.

A single scale-bar was present, in-line with the anchor, for Case Study 1; the diagonals of the two gardening boxes were used as scale-features for Case Study 2 - the metre long scale-bar could not be accommodated in this set-up due to space constraints.

5.5 Case Study 3: MFV *Sanu*

The same recording methodology was used again here, although using two scale-bars, this time each parallel to the key dimensions of the supporting pallet. An additional section of planking was placed astern of the main section, to simulate a shipwreck. On-subject detail points were this time marked in the same fashion as the four corner secondary control points using photogrammetry targets taped in place, but again recorded using reflector-less mode.

These targets were also surveyed by setting up an additional network of control points outside the square to enable a tape-measured Direct Survey Method (DSM) survey to be performed – see section 3.3 for details on this technique.

Heights for the DSM survey were measured above the floor (which had been found to be very nearly level during "gridding out" using a level) at each point using a plumb bob. This is unlikely to prove any less accurate than using a level and staff for an inter-tidal or coastal site, or a dive computer underwater – these typically only record depth to 100mm precision.

These control points were surveyed in using the TotalStation in addition: although this would not be usually used in a DSM survey, this enabled the DSM survey to be translated into the same reference system as the other datasets for comparison.

A series of check-measurements were also taken between the centre points of the targets, as well as clearly identifiable features such as protruding nails.

The following colour plate illustrates the additional control points established for the DSM survey: Top row (L-R) are CP_01 and CP_02; second row are CP_03 and CP_04; third row are CP_05, CP_06 and CP_07; bottom row are CP_07 and C_08.

Figure 12: DSM control points. Image Source: The Author.

5.6 Project Recording and Data Standards

5.6.1 1MM PROJECT PRECISION STANDARD

Due to the use of tape measures for check-measurements or Direct Survey Method (DSM) data collection, this project recorded measurements to 1mm precision. This is higher than the accuracy of the Leica TS06 TotalStation used by this project (2mm) and considerably higher than the Leica survey grade RTK GNSS equipment, although they both offer data exports within Cartesian coordinate systems at 1mm precision (metres with three decimal places).

Due to this 1mm precision offered by the TotalStation and the tape measures used as benchmark data for this project, there would be no way to meaningfully evaluate any output data at higher levels of precision; even if it were in fact possible to record to higher levels of accuracy.

For this reason, although outputs were recorded to the full extent of available decimal places for import into MS *Excel*, they were ultimately displayed and exported to this thesis in millimetres using positive integer values only.

5.6.2 POSITIVE INTEGER VALUES

This project chose to use positive values only to avoid positive and negative differences cancelling each other out when added together to calculate total or mean errors. Ranges were determined by simply identifying the highest error positive integer value: “range” here is thus the highest individual inaccuracy, rather than the widest spread, within a dataset.

The shortcoming of this method is that, although recorded in the spreadsheets as raw data, the analysis cannot identify consistent over- or under-measuring in relation to a single variable. However, the outweighing advantage here is that for simple sets of measurements the range calculations represent the range of the variation from the benchmark (accuracy) rather than the overall spread of results regardless of the benchmark (precision): this project set out to examine accuracy.

For each criterion, the individual errors, as well as error sums and means were calculated by applying formulae to cells containing data in higher degrees of precision than the integer values displayed in this thesis, or the *Excel* spreadsheets contained in Appendices 2-4.

5.7 Computational Processing and Comparison

The sets of photographs were processed in Agisoft *PhotoScan Professional* 1.4.5 with processing parameters noted and kept consistent. 3D models were produced before the various features selected for measuring were marked with flags on the model – this was necessary in all cases due to the failure of the software to identify the coded targets – see Chapter 8 for a discussion of the results.

These markers were placed to coincide with the centre-points of photogrammetry target markers wherever practical, but also to correlate with check-measurements taken from the original subjects or extracted from surveyed coordinates.

The models were then duplicated with the markers intact before the addition of the various options for spatial data into differing copies of the original model – this was done to ensure an identical model would be measured from identical points to ensure an objective comparison between the results of the varying scaling and referencing methodologies.

The coordinates and scaling information were then incorporated into these different copies of the original models, depending on the technique in question, before measurements were taken within *PhotoScan.* Where the supplied spatial data affected the coordinates within *PhotoScan* these too were extracted.

Despite the time-intensive nature of the data collection needed for this exercise in addition to the processing, the resulting sample sizes were too small for meaningful statistical analysis. Additionally, all data was collected by the author, so there was minimal opportunity for repetition without deliberate attempts to achieve differing results.

This resulted in more basic descriptive details being used to expose trends not immediately apparent. These measurements and coordinates were therefore imported into a MS *Excel* spreadsheet and compared to the original survey data or check-measurements. Separate spreadsheets were produced for each model with different sheets for each form of spatial data. These are including in this thesis as Appendices 3, 4 and 5.

Such deviations were converted to millimetres to quantify each error. For each model and form of spatial data the total, mean, and ranges of the errors, again in millimetres, were also calculated. This enabled the results to be evaluated and compared to the existing technical standards for other forms of metric survey for cultural heritage.

Chapter 6. Results

6.1 Summary of Key Findings

At first glance, the series of measurements and coordinates collected appeared to be largely accurate, with the odd clear exception. The levels of accuracy apparent seemed constant, regardless of the method used.

However, it was only by performing analysis that resulting differences between the methodologies emerged, underlining the need for some degree of model validation if metric applications are intended, or foreseeable.

Differences in how best to evaluate the results between scaling and measuring dimensions on one hand and dealing with coordinates on the other only became clear following the analysis of the results, examined in detail in 7.5.

6.1.1 SUMMARY TABLE

Scaling	Case Study								
Data displayed as positive integers	Anchor (Scale-Bar)			Anchor (Boxes)			MFV *Sanu*		
Measurements	Errors (mm)			Errors (mm)			Errors (mm)		
	Sum	Mean	Range	Sum	Mean	Range	Sum	Mean	Range
One Scale-Bar	127	13	30	-	-	-	60	4	11
Two Scale-Bars	-	-	-	387	26	56	52	4	10
Enclosure	76	8	12	82	5	12	57	4	11
Control Points	78	8	12	85	6	12	64	5	13
Detail Points	78	8	12	94	6	12	66	5	13
DSM Control Points	-	-	-	-	-	-	61	4	13
DSM Detail Points	-	-	-	-	-	-	63	5	13
Coordinates									
Control Points	48	2	9	71	2	11	64	2	11
Detail Points	49	2	8	74	2	10	71	2	8
DSM Control Points	-	-	-	-	-	-	313	10	20
DSM Detail Points	-	-	-	-	-	-	397	13	30

Figure 13: Summary Data Table.

6.1.2 SCALING AND MEASUREMENTS

These conclusions are drawn from the above summary table:

1. The use of two scale-bars to scale the anchor and boxes produced very poor results, this may have been because they were simply not long enough relative to the subject to provide adequate scaling.
2. Enclosure, or the use of two appropriately sized scale-bars each parallel with one of the subject's principal axes, both appear to produce similar effects on scaling; this shows an improvement over the use of a single scale-bar.
3. Although the ranges (highest recorded inaccuracy) were largely consistent across the case studies, the sum and especially mean errors were lower with the larger subject (MFV *Sanu*). This is interesting because, when comparing absolute accuracy, the larger size should not produce such an effect.
4. Dimensional measurements of the models showed little evident deviation between methodologies in relation to error when examined by these criteria.

However, these results do indicate that for taking simple measurements of key dimensions, all these techniques are valid for scaling Image-Based Modelling with no clear grounds to recommend a specific preference, based on the data collected by this study.

6.1.3 COORDINATES

These conclusions are drawn from summary table in 7.1.1

1. The use of the TotalStation for control- or detail point coordinates to reference the model appeared to have a noticeable effect on the accuracy ratings of the coordinates subsequently calculated by

PhotoScan when compared to the results of coordinates produced from DSM.

However, this may be more due to the shortcomings in both experimental and analytic methodologies which became apparent during analyses, than resulting from the different sources of coordinate data; see 6.5 for further detail.

6.2 Case Study 1: The Anchor (Single Scale-Bar)

6.2.1 THE ANCHOR (SINGLE SCALE-BAR) – ILLUSTRATIONS

Plan View

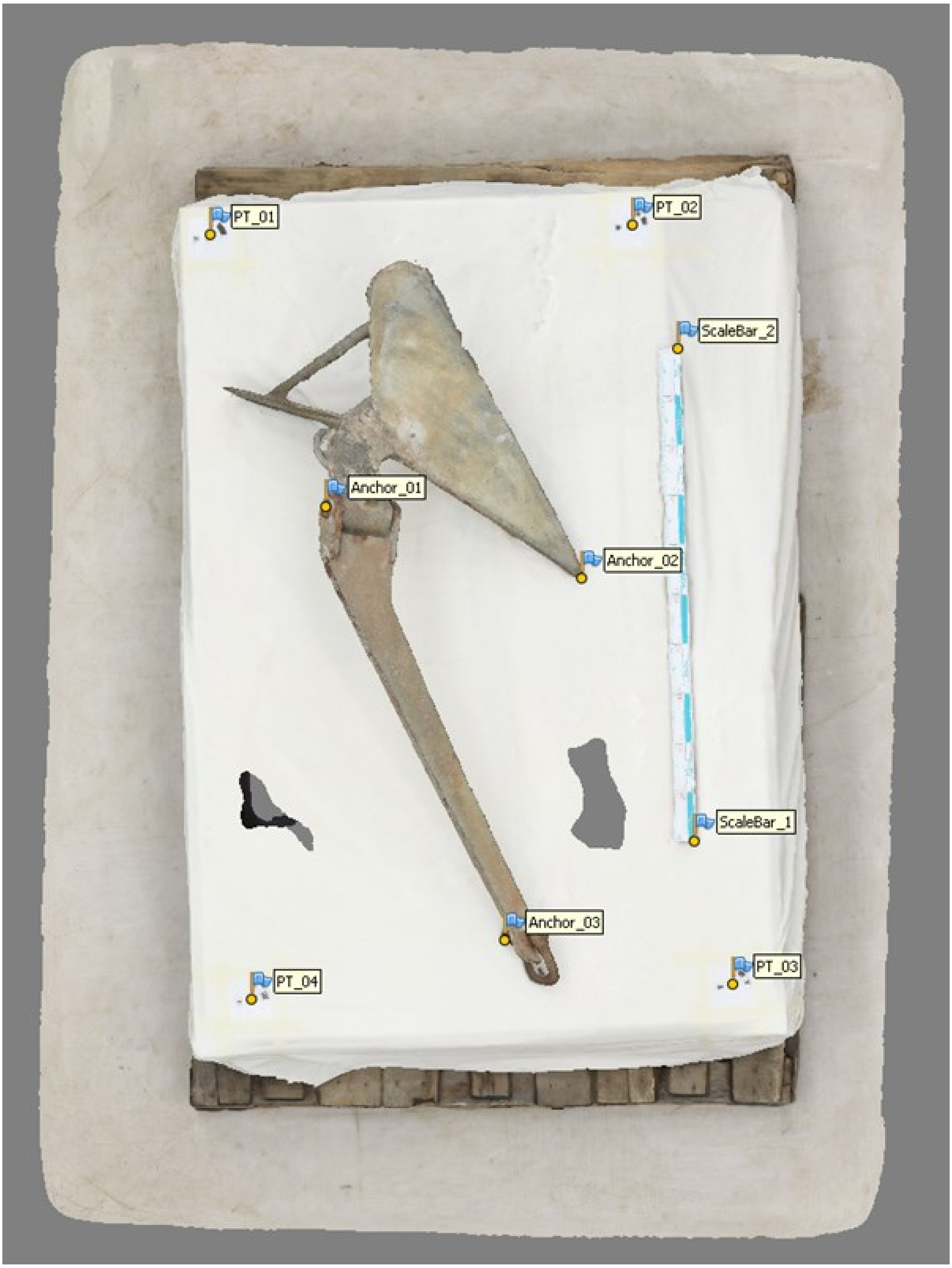

Figure 14: The Anchor and Scale-Bar with features labelled. Image Source: The Author.

Camera Locations

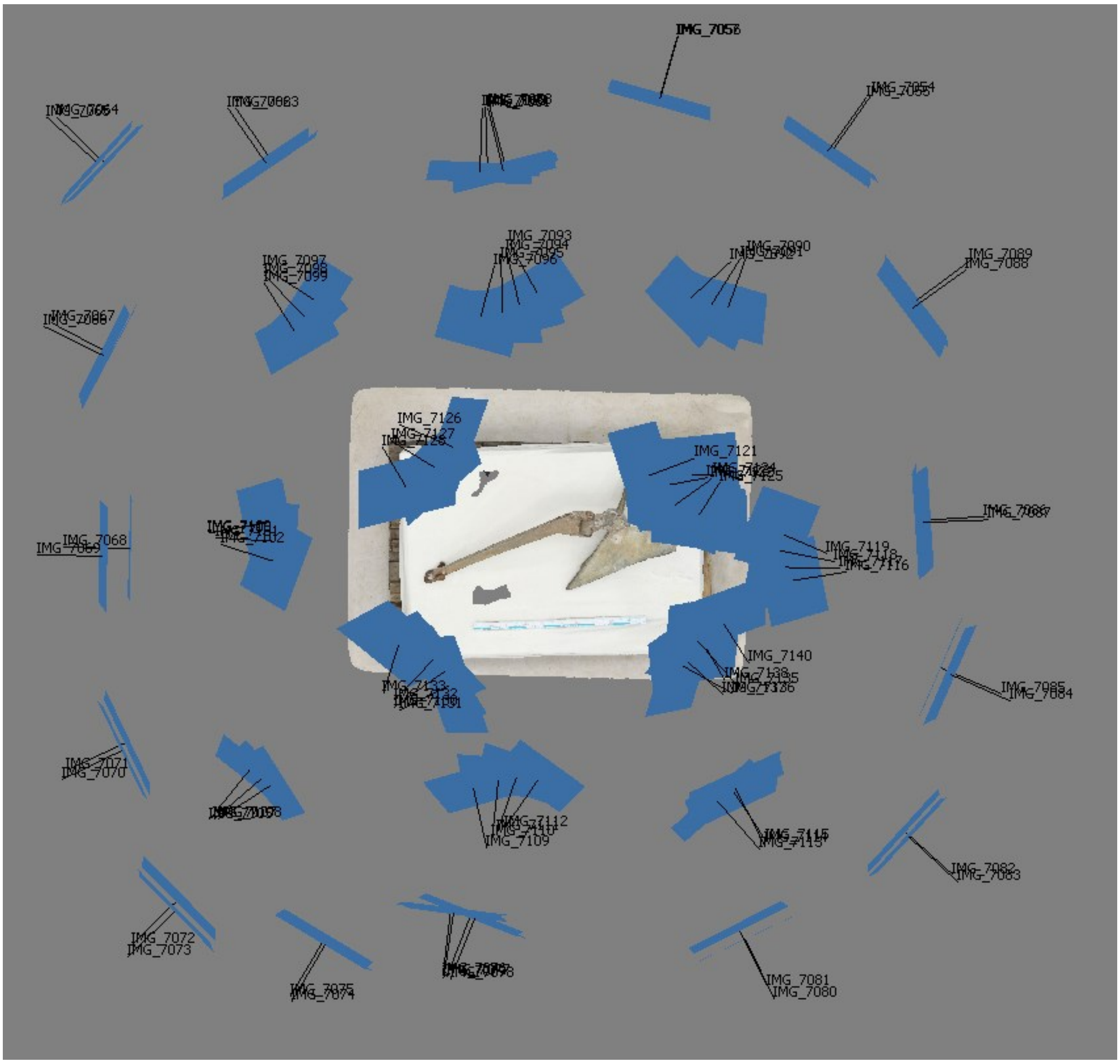

Figure 15: Anchor and Scale-Bar – Camera Locations. Image Source: The Author.

There are two holes in the mesh either side of the anchor, resulting in two apparent holes in the sheet. Aesthetically unfortunate, they do not impact on the model as an experiment, so they were not addressed.

6.2.2 THE ANCHOR (SINGLE SCALE-BAR) – SUMMARY TABLE

Number of Photographs	82		
Image Quality	Lowest	Lowest Aligned	Highest
(Agisoft Estimate)	0.425918	0.568383	0.945133

Photographs Aligned	81
Tie Points	106,924
Dense Cloud (Points)	4,864,278
3D Model (Faces)	324,285

Scaling Method	**Single Scale-Bar**	
Measurement	ScaleBar_1 to ScaleBar_2	
Scaling Method	**Enclosure**	
Measurement	PT_01 to PT_02	PT_01 to PT_04
	PT_02 to PT_03	PT_03 to PT_04
Scaling Method	**Control Points**	
Coordinates	PT_01, PT_02, PT_03, PT_04	
Scaling Method	**Detail Points**	
Coordinates	PT_01, PT_02, PT_03, PT_04	
	Anchor_01, Anchor_02, Anchor_03	

Figure 16: The Anchor and Scale-Bar - Summary Table.

6.2.3 THE ANCHOR (SINGLE SCALE-BAR) – MEASUREMENTS TABLES

Measurement		Scaling Method			
Data displayed as positive integers		Single Scale-Bar		Enclosure	
Measurement	Benchmark (mm)	Value (mm)	Error (mm)	Value (mm)	Error (mm)
ScaleBar_1 - ScaleBar_2	1000	1000	0	988	12
PT_01 - PT_02	851	862	11	851	0
PT_02 - PT_03	1539	1560	21	1540	1
PT_03 - PT_04	974	981	7	970	4
PT_01 - PT_04	1532	1550	18	1540	8
Anchor_02 - Anchor_03	732	749	17	742	10
Anchor_01 - PT_01	742	741	1	732	10
Anchor_01 - PT_02	913	913	0	904	9
Anchor_01 - PT_03	1278	1300	22	1290	12
Anchor_01 - PT_04	1050	1080	30	1060	10
	SUM ERROR (mm)		127		76
	MEAN ERROR (mm)		13		8
	ERROR RANGE (mm)		30		12

Figure 17: The Anchor and Scale-Bar - Measurements Table 1.

Measurement		Scaling Method			
Data displayed as positive integers		Control Points		Detail Points	
Measurement	Benchmark (mm)	Value (mm)	Error (mm)	Value (mm)	Error (mm)
ScaleBar_1 - ScaleBar_2	1000	988	12	989	11
PT_01 - PT_02	851	850	1	852	1
PT_02 - PT_03	1539	1540	1	1540	1
PT_03 - PT_04	974	970	4	970	4
PT_01 - PT_04	1532	1540	8	1540	8
Anchor_02 - Anchor_03	732	743	11	744	12
Anchor_01 - PT_01	742	732	10	732	10
Anchor_01 - PT_02	913	904	9	904	9
Anchor_01 - PT_03	1278	1290	12	1290	12
Anchor_01 - PT_04	1050	1060	10	1060	10
	SUM ERROR (mm)		78		78
	MEAN ERROR (mm)		8		8
	ERROR RANGE (mm)		12		12

Figure 18: The Anchor and Scale-Bar - Measurements Table 2.

6.2.4 THE ANCHOR (SINGLE SCALE-BAR) – COORDINATES

Referencing		Methodology					
Data displayed as positive integers		Control Points Errors (mm)			Detail Points Errors (mm)		
Marker	Benchmark	E	N	H	E	N	H
PT_01	TotalStation	0	1	1	2	3	0
PT_02	TotalStation	0	0	1	2	1	2
PT_03	TotalStation	2	1	1	2	1	2
PT_04	TotalStation	2	2	1	2	1	2
Anchor_01	TotalStation	2	3	1	1	1	1
Anchor_02	TotalStation	9	4	4	8	3	4
Anchor_03	TotalStation	4	2	7	5	1	6
	SUM ERROR (mm)			48			49
	MEAN ERROR (mm)			2			2
	ERROR RANGE (mm)			9			8

Figure 19: The Anchor and Scale-Bar - Coordinates Table.

6.3 Case Study 2: The Anchor (Two Boxes)

6.3.1 THE ANCHOR (TWO BOXES) – ILLUSTRATIONS

Plan View

Figure 20: The Anchor and Boxes with features labelled. Image Source: The Author.

Camera Locations

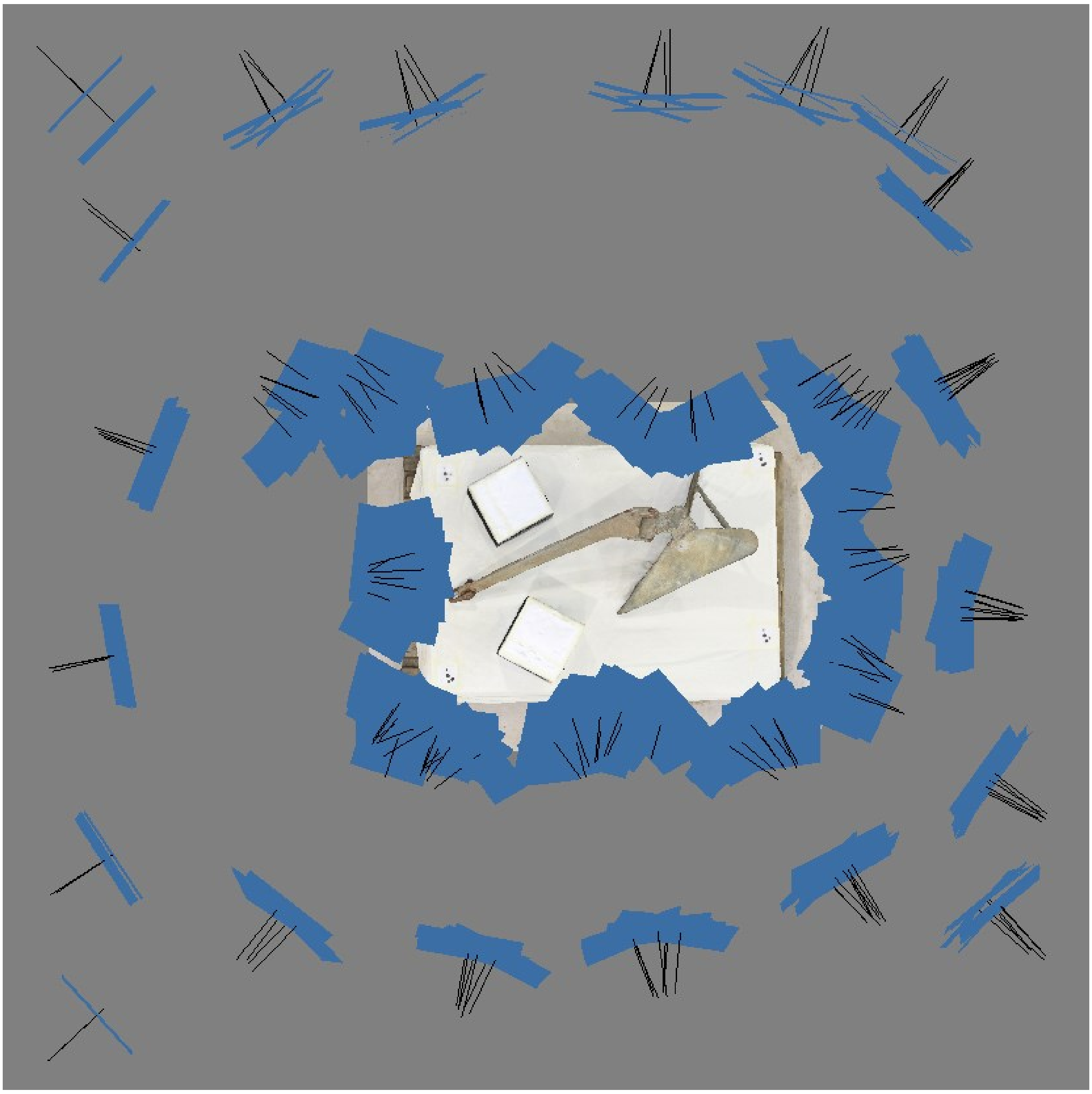

Figure 21: Anchor and Boxes – Camera Locations. Image Source: The Author.

6.3.2 THE ANCHOR (TWO BOXES) – SUMMARY TABLE

Number of Photographs	184		
Image Quality (Agisoft Estimate)	Lowest	Lowest Aligned	Highest
	0.227328	0.227328	0.828766
Photographs Aligned	184		
Tie Points	199,913		
Dense Cloud (Points)	9,435,319		
3D Model (Faces)	628,874		
Scaling Method	Two Scale-Bars		
Measurement	BOX_32_01 to BOX_32_02	BOX_38_01 to BOX_38_02	
Scaling Method	Enclosure		
Measurement	PT_01 to PT_02	PT_01 to PT_04	
	PT_02 to PT_03	PT_03 to PT_04	
Scaling Method	Control Points		
Coordinates	PT_01, PT_02, PT_03, PT_04		
Scaling Method	Detail Points		
Coordinates	PT_01, PT_02, PT_03, PT_04		
	Anchor_01, Anchor_02, Anchor_03		
	BOX_32_01, BOX_32_02, BOX_38_01, BOX_38_02		

Figure 22 : The Anchor and Boxes - Summary Table.

6.3.3 THE ANCHOR (TWO BOXES) – MEASUREMENTS TABLES

Measurement		Scaling Method			
Data displayed as positive integers		Benchmark (mm)		Enclosure	
Measurement		Value (mm)	Error (mm)	Value (mm)	Error (mm)
Box_32_01 - Box_32_02	427	427	**0**	415	**12**
Box_38_01 - Box_38_02	428	427	**0**	416	**12**
PT_01 - PT_02	851	876	**25**	852	**1**
PT_02 - PT_03	1539	1590	**51**	1540	**1**
PT_03 - PT_04	974	1000	**56**	974	**0**
PT_01 - PT_04	1532	1570	**38**	1530	**2**
Anchor_02 - Anchor_03	732	756	**24**	735	**3**
Anchor_01 - PT_01	742	755	**13**	732	**10**
Anchor_01 - PT_02	913	933	**20**	907	**6**
Anchor_01 - PT_03	1278	1320	**42**	1290	**12**
Anchor_01 - PT_04	1050	1090	**40**	1050	**0**
Anchor_01 - Box_32_01	465	479	**14**	465	**0**
Anchor_01 - Box_32_02	858	895	**37**	869	**11**
Anchor_01 - Box_38_01	626	947	**21**	630	**4**
Anchor_01 - Box_38_02	974	1010	**36**	982	**8**
	SUM ERROR (mm)		387		82
	MEAN ERROR (mm)		26		5
	ERROR RANGE (mm)		56		12

Figure 23: The Anchor and Boxes - Measurements Table 1.

Measurement		Scaling Method			
Data displayed as positive integers		Control Points		Detail Points	
Measurement	Benchmark (mm)	Value (mm)	Error (mm)	Value (mm)	Error (mm)
Box_32_01 - Box_32_02	427	415	12	416	11
Box_38_01 - Box_38_02	428	416	12	416	12
PT_01 - PT_02	851	852	1	854	3
PT_02 - PT_03	1539	1540	1	1540	1
PT_03 - PT_04	974	974	0	976	2
PT_01 - PT_04	1532	1530	2	1530	2
Anchor_02 - Anchor_03	732	738	6	734	2
Anchor_01 - PT_01	742	733	9	735	7
Anchor_01 - PT_02	913	907	6	908	5
Anchor_01 - PT_03	1278	1290	12	1290	12
Anchor_01 - PT_04	1050	1050	0	1060	10
Anchor_01 - Box_32_01	465	466	1	466	1
Anchor_01 - Box_32_02	858	869	11	870	12
Anchor_01 - Box_38_01	626	630	4	631	5
Anchor_01 - Box_38_02	974	982	8	983	9
	SUM ERROR (mm)		85		94
	MEAN ERROR (mm)		6		6
	ERROR RANGE (mm)		12		12

Figure 24: The Anchor and Boxes - Measurements Table 2.

6.3.4 THE ANCHOR (TWO BOXES) – COORDINATES

Referencing		Methodology					
Data displayed as positive integers		Control Points Errors (mm)			Detail Points Errors (mm)		
Marker	Benchmark	E	N	H	E	N	H
PT_01	TotalStation	1	2	0	0	1	1
PT_02	TotalStation	0	1	0	1	3	2
PT_03	TotalStation	0	2	0	0	2	1
PT_04	TotalStation	0	3	0	1	4	2
Anchor_01	TotalStation	3	8	0	3	5	0
Anchor_02	TotalStation	4	11	5	3	10	4
Anchor_03	TotalStation	1	2	2	1	2	2
Box_32_01	TotalStation	0	3	0	0	1	1
Box_32_02	TotalStation	3	1	5	2	2	4
Box_38_01	TotalStation	0	6	0	1	7	0
Box_38_02	TotalStation	5	1	1	5	0	1
	SUM ERROR (mm)			71			74
	MEAN ERROR (mm)			2			2
	ERROR RANGE (mm)			11			10

Figure 25: The Anchor and Boxes - Coordinates Table.

6.4 Case Study 3: MFV *Sanu*

6.4.1 MFV *SANU* – ILLUSTRATIONS

Plan View

Figure 26: MFV Sanu - Plan View. Image Source: The Author.

The four encircling photogrammetry targets (clockwise from top right) are PT_07, PT_08, PT_09 and PT_10; PT_01 to PT_06 were used on-subject. The metre rule is ScaleBar_1; the yellow levelling ruler is ScaleBar_2.

Bow Section (Labelled)

Figure 27: MFV Sanu - Bow Section with features labelled. Image Source: The Author.

Mid-Section Planking Detail (Labelled)

Figure 28: MFV Sanu - Mid Section with features labelled. Image Source: The Author.

Astern Section (Labelled)

Figure 29: MFV Sanu - Astern Section with features labelled. Image Source: The Author.

Second Section (Labelled)

Figure 30: MFV Sanu - Second Section with features labelled. Image Source: The Author.

Camera Locations

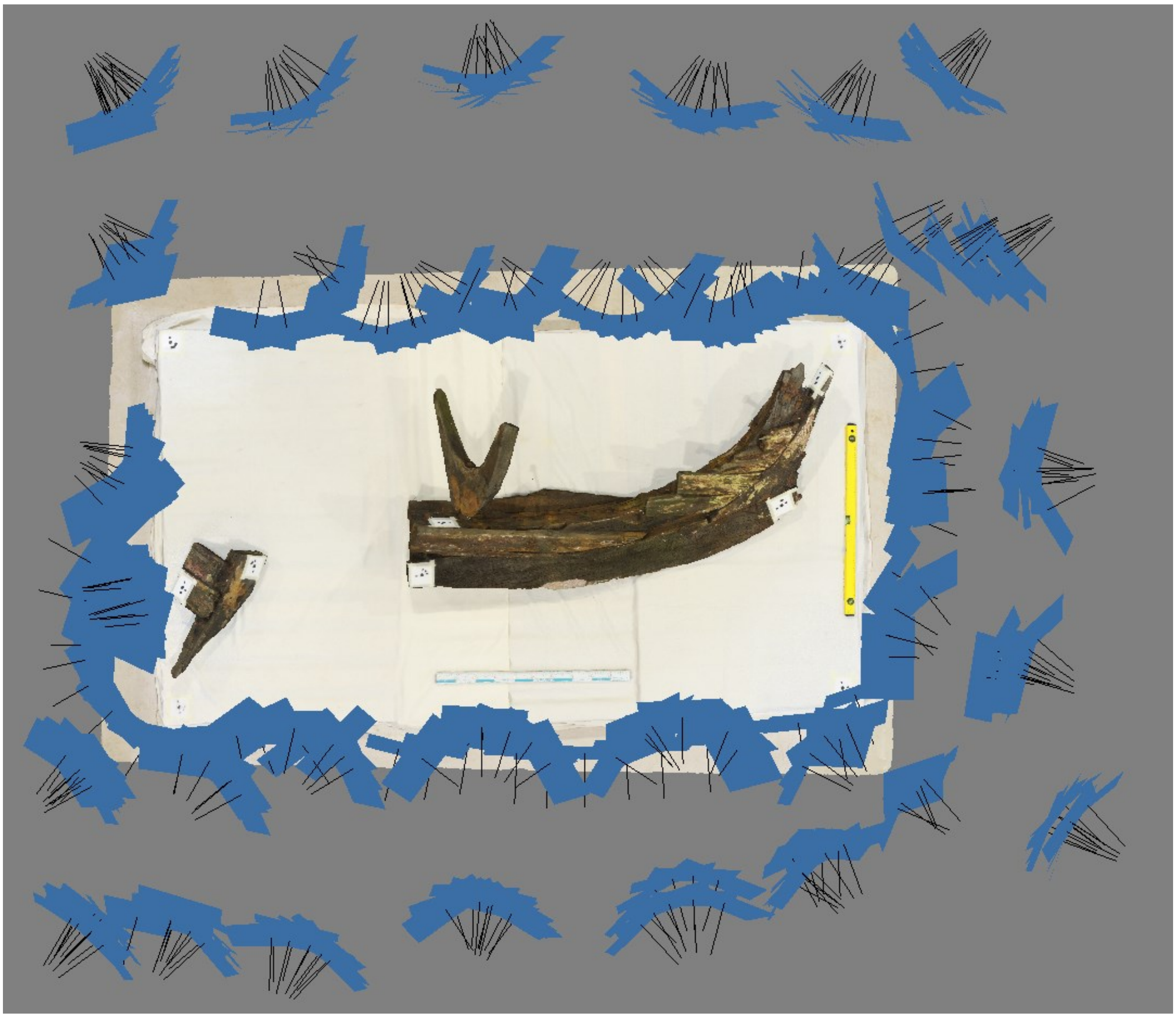

Figure 31: MFV Sanu - Camera Locations. Image Source: The Author.

6.4.2 MFV *SANU* – SUMMARY TABLE

<table>
<tr><td>Number of Photographs</td><td>349</td><td></td><td></td></tr>
<tr><td rowspan="2">Image Quality
(Agisoft Estimate)</td><td>Lowest</td><td>Lowest Aligned</td><td>Highest</td></tr>
<tr><td>0.440567</td><td>0.440567</td><td>0.919927</td></tr>
<tr><td colspan="4"></td></tr>
<tr><td>Photographs Aligned</td><td colspan="3">349</td></tr>
<tr><td>Tie Points</td><td colspan="3">213,694</td></tr>
<tr><td>Dense Cloud (Points)</td><td colspan="3">15,120,124</td></tr>
<tr><td>3D Model (Faces)</td><td colspan="3">1,008,007</td></tr>
<tr><td colspan="4"></td></tr>
<tr><td>Scaling Method</td><td colspan="3">One Scale-Bar</td></tr>
<tr><td>Measurement</td><td colspan="3">ScaleBar_1_1 to ScaleBar_1_2</td></tr>
<tr><td>Scaling Method</td><td colspan="3">Two Scale-Bars</td></tr>
<tr><td>Measurement</td><td colspan="3">ScaleBar_1_1 to ScaleBar_1_2 ScaleBar_2_1 to ScaleBar_2_2</td></tr>
<tr><td>Scaling Method</td><td colspan="3">Enclosure</td></tr>
<tr><td>Measurement</td><td>PT_07 to PT_08</td><td colspan="2">PT_07 to PT_10</td></tr>
<tr><td></td><td>PT_08 to PT_09</td><td colspan="2">PT_09 to PT_10</td></tr>
<tr><td>Scaling Method</td><td colspan="3">Control Points</td></tr>
<tr><td>Coordinates</td><td colspan="3">PT_07, PT_08, PT_09, PT_10</td></tr>
<tr><td>Scaling Method</td><td colspan="3">Detail Points</td></tr>
<tr><td rowspan="2">Coordinates</td><td colspan="3">PT_01, PT_02, PT_03, PT_04, PT_05, PT_06,</td></tr>
<tr><td colspan="3">PT_07, PT_08, PT_09, PT_10</td></tr>
</table>

Figure 32: MFV Sanu - Summary Table.

6.4.3 MFV *SANU* – MEASUREMENTS TABLES

Measurement		Scaling Method			
Data displayed as positive integers		One Scale-Bar		Two Scale-Bars	
Measurement	Benchmark (mm)	Value (mm)	Error (mm)	Value (mm)	Error (mm)
ScaleBar_1_1 - ScaleBar_1_2	1000	1000	0	999	1
ScaleBar_2_1 - ScaleBar_2_2	986	987	1	988	2
PT_07 - PT_08	3464	3470	6	3470	6
PT_08 - PT_09	1804	1810	6	1810	6
PT_09 - PT_10	3435	3440	5	3440	5
PT_07 - PT_10	1873	1870	3	1870	3
Keel_1 - Keel_2	330	329	1	330	0
U_Section_1 - U_Section_2	568	579	11	578	10
S_Plank_02_Upper_1 - S_Plank_02_Upper_2	1193	1190	3	1190	3
S_Plank_03_Recess_1 - S_Plank_03_Recess_2	112	118	6	104	8
PT_07 - PT_02	1690	1700	10	1690	0
PT_07 – PT_04	1253	1250	3	1250	3
PT_06 – PT_05	1891	1890	1	1890	1
PT_06 – PT_09	1016	1020	4	1020	4
~~Second_Section_1 – Second_Section_2~~	~~716~~	~~651~~	~~65~~	~~651~~	~~65~~
	SUM ERROR (mm)		60		52
	MEAN ERROR (mm)		4		4
	ERROR RANGE (mm)		11		10

Figure 33: MFV Sanu *- Measurements Table 1.*

Measurement		Scaling Method	
Data displayed as positive integers		**Enclosure**	
Measurement	Benchmark (mm)	Value (mm)	Error (mm)
ScaleBar_1_1 - ScaleBar_1_2	1000	999	1
ScaleBar_2_1 - ScaleBar_2_2	986	984	2
PT_07 - PT_08	3464	3470	6
PT_08 - PT_09	1804	1810	6
PT_09 - PT_10	3435	3440	5
PT_07 - PT_10	1873	1870	3
Keel_1 - Keel_2	330	329	1
U_Section_1 - U_Section_2	568	579	11
S_Plank_02_Upper_1 - S_Plank_02_Upper_2	1193	1190	3
S_Plank_03_Recess_1 - S_Plank_03_Recess_2	112	103	9
PT_07 - PT_02	1690	1690	0
PT_07 – PT_04	1253	1250	3
PT_06 – PT_05	1891	1890	1
PT_06 – PT_09	1016	1010	6
~~Second_Section_1 – Second_Section_2~~	~~716~~	~~651~~	~~65~~
	SUM ERROR (mm)		57
	MEAN ERROR (mm)		4
	ERROR RANGE (mm)		11

Figure 34: MFV Sanu - Measurements Table 2.

Measurement		**Scaling Method**			
Data displayed as positive integers		**Control Points**		**Detail Points**	
Measurement	**Benchmark (mm)**	**Value (mm)**	**Error (mm)**	**Value (mm)**	**Error (mm)**
ScaleBar_1_1 - ScaleBar_1_2	1000	999	1	998	2
ScaleBar_2_1 - ScaleBar_2_2	986	986	0	986	0
PT_07 - PT_08	3464	3470	6	3470	6
PT_08 - PT_09	1804	1810	6	1810	6
PT_09 - PT_10	3435	3440	5	3440	5
PT_07 - PT_10	1873	1860	13	1860	13
Keel_1 - Keel_2	330	327	3	327	3
U_Section_1 - U_Section_2	568	579	11	578	10
S_Plank_02_Upper_1 - S_Plank_02_Upper_2	1193	1190	3	1190	3
S_Plank_03_Recess_1 - S_Plank_03_Recess_2	112	104	8	104	8
PT_07 - PT_02	1690	1690	0	1690	0
PT_07 – PT_04	1253	1250	3	1250	3
PT_06 – PT_05	1891	1890	1	1890	1
PT_06 – PT_09	1016	1020	4	1010	6
~~**Second_Section_1 – Second_Section_2**~~	~~716~~	~~651~~	~~65~~	~~651~~	~~65~~
	SUM ERROR (mm)		**64**		**66**
	MEAN ERROR (mm)		**5**		**5**
	ERROR RANGE (mm)		**13**		**13**

Figure 35: MFV Sanu - Measurements Table 3.

Measurement		Scaling Method			
Data displayed as positive integers		DSM Control Points		DSM Detail Points	
Measurement	Benchmark (mm)	Value (mm)	Error (mm)	Value (mm)	Error (mm)
ScaleBar_1_1 - ScaleBar_1_2	1000	1000	0	998	2
ScaleBar_2_1 - ScaleBar_2_2	986	986	0	985	1
PT_07 - PT_08	3464	3460	4	3460	4
PT_08 - PT_09	1804	1800	4	1800	4
PT_09 - PT_10	3435	3440	5	3430	5
PT_07 - PT_10	1873	1860	13	1860	13
Keel_1 - Keel_2	330	327	3	328	2
U_Section_1 - U_Section_2	568	578	10	578	10
S_Plank_02_Upper_1 - S_Plank_02_Upper_2	1193	1190	3	1190	3
S_Plank_03_Recess_1 - S_Plank_03_Recess_2	112	103	9	103	9
PT_07 - PT_02	1690	1690	0	1690	0
PT_07 – PT_04	1253	1250	3	1250	3
PT_06 – PT_05	1891	1890	1	1890	1
PT_06 – PT_09	1016	1010	6	1010	6
~~Second_Section_1 – Second_Section_2~~	~~716~~	~~649~~	~~67~~	~~648~~	~~68~~
	SUM ERROR (mm)		61		63
	MEAN ERROR (mm)		4		5
	ERROR RANGE (mm)		13		13

Figure 36: MFV Sanu - Measurements Table 4.

6.4.4 MFV *SANU* – COORDINATES

Referencing		Methodology					
Data displayed as positive integers		Control Points Errors (mm)			Detail Points Errors (mm)		
Marker	Benchmark	E	N	H	E	N	H
PT_01	TotalStation	11	7	2	8	5	2
PT_02	TotalStation	8	5	0	6	3	0
PT_03	TotalStation	2	1	1	2	2	1
PT_04	TotalStation	0	4	2	0	2	2
PT_05	TotalStation	1	0	1	2	1	1
PT_06	TotalStation	1	0	0	4	1	1
PT_07	TotalStation	4	2	1	4	1	1
PT_08	TotalStation	1	1	1	2	3	2
PT_09	TotalStation	1	1	1	4	1	2
PT_10	TotalStation	5	0	1	5	1	1
	SUM ERROR (mm)			64			71
	MEAN ERROR (mm)			2			2
	ERROR RANGE (mm)			11			8

Figure 37: MFV Sanu - Coordinates Table 1.

Referencing		Methodology					
Data displayed as positive integers		DSM Control Points Errors (mm)			DSM Detail Points Errors (mm)		
Marker	Benchmark	E	N	H	E	N	H
PT_01	TotalStation	0	19	1	1	16	8
PT_02	TotalStation	1	16	9	5	11	20
PT_03	TotalStation	11	10	11	17	4	22
PT_04	TotalStation	9	15	12	16	8	23
PT_05	TotalStation	10	11	12	14	6	22
PT_06	TotalStation	13	13	7	14	9	16
PT_07	TotalStation	15	12	4	22	8	16
PT_08	TotalStation	12	11	0	13	9	10
PT_09	TotalStation	14	13	13	14	8	21
PT_10	TotalStation	5	12	20	11	4	30
	SUM ERROR (mm)			313			397
	MEAN ERROR (mm)			10			13
	ERROR RANGE (mm)			20			30

Figure 38: MFV Sanu - Coordinates Table 2.

6.5 Analysis of Results

As previously noted in 6.1, all these methods proved viable for scaling and measuring dimensions, except where scale-features were of insufficient length, as with the two boxes. There appeared to be slightly superior results when scaled using measurements rather than coordinates, although this should be treated with caution.

The more complex subject of coordinates, which would allow geographical referencing and volumetric calculation, is addressed to a lesser extent by the results of this project. This may be due in part to the same data in effect mistakenly being used as both an experimental parameter and as a control,[9] as well as the revealed inadequacies of the evaluation methodology in *Excel*.

Although *PhotoScan* has to balance the spatial data added to the markers with the proportions from the existing computations (Structure-from-Motion then Multi-View Stereo), it stands to reason that when compared to the TotalStation data as a control, its outputs based on being supplied with identical data (the TotalStation survey) will be closer to those supplied than to an alternative (the DSM survey).

It must also be noted that *PhotoScan* calculated these coordinates from those output by *Site Recorder* – which in turn had produced those by calculation based on measurements taken within the shared survey control. There are several levels of "best-fit" computing taking place here, in addition to the final bundle adjustment in Structure-from-Motion.

[9] For more discussion of this point see 8.4, bullet point 5.

However, on review of the raw data contained in Appendix Four, it became clear that some of the data processing in *Excel* may have increased the apparent nature of these errors.

By using positive integer values to avoid positive and negative values cancelling each other out within a simple series of data, for linked coordinate data this methodology increased the apparent error. Total errors arising from positive values for differences on each axis in isolation had been calculated then combined to produce an overall total error.

The methodology had negated the off-setting effect of the negative values, although even when both positive and negative results are summed and averaged in this way, the errors are still very high.

This was determined to be because *Excel* had disregarded the three-dimensional inter-dependence of these numbers which in fact represent the radius of a circle whose centre is one coordinate with the other on its circumference. The x, y and z coordinates are linked, but this method has treated them as discrete measurements.

6.6 Sources of Error

1. Virtual measurement in *PhotoScan* undoubtedly played a part in some of these errors – however accurately markers were placed on the model they can never be in exactly the same place as the check measurements. Accurate placement on scale-bars was also subject to these errors.

   Additionally, when using the measuring tool, it can be difficult to pan and zoom around the model to make an accurate selection, especially once the first point has been selected at which point panning to change perspective is no longer possible.

2. The addition of spatial data at the end of the processing pipeline meant that *PhotoScan* was having to compromise between the absolute data being inputted and the relative positions already computed – as noted earlier, best practice is to constrain the processing by including spatial data as early as possible.

   Due to the failure of the coded target identification this was not believed to be possible[10]. Future work needs to investigate why this happened and seek to rectify the errors in the methodology.

3. Although initially analysing the data in *Excel* was a productive way to evaluate the accuracy of the measurements, and this revealed patterns which were not immediately apparent, such basic mathematics proved insufficient for examining 3D vector data.

[10] See 8.4, bullet point 1.

Chapter 7. Discussion, Conclusions and Future Research

Despite the shortcomings exposed and further questions posed by these results, the project's objectives have been at least partially achieved as well as the overall aim. There has also been the development of a method statement for citizen scientists and divers, in addition to the collation of relevant information and practical examples into a single document. This will now be presented before going on to review the project's success against the stated aim and objects.

7.1 Method Statement

The critical element to successfully using Image-Based Modelling to accurately reconstruct a heritage subject in-situ is to have a coherent plan; and this plan should be formed from examining guidance material and conducting trials to hone the methodology. Such "dry-runs" must be performed before heading into the inter-tidal zone, or underwater.

This project has been written to aid citizen scientists; as noted earlier, recreational divers tend to prefer to dive on modern metal wrecks with differing geometry to wooden archaeological shipwreck sites, and are more likely to be constrained to briefer periods of fieldwork, such as a weekend.

For these reasons, it may be preferable to record important diagnostic features (such as a boiler or an anchor) in detail using photogrammetry, and to use an alternative method to generate a site-plan into which the detailed model may be integrated through coordinate data. This may be achieved in stages, allow review, and go on to produce a far superior result.

Depending on the subject, for any given focal length, a differing number of photographs will be needed to cover the subject from all angles with adequate overlap to align the images. After considering how far from the subject the camera will need to be, record a similar sized subject: how many photographs will be needed? What impact will this have on file formats or image resolution due to memory card capacity?

The capabilities of the camera and lighting need to be considered; the batteries may not hold adequate charge for the required number of exposures, especially in cold conditions, or where live view mode is used to avoid needing to look through the viewfinder. It may be necessary to switch off the last photograph review function. This is especially important for underwater sites, where batteries may evidently not be exchanged during a dive. Will two or more cameras be needed? How will similar colour balances and light temperatures be ensured to avoid software from failing to identify features?

It is critical that the photographs align to enable the reconstruction of a sparse point-cloud. If the trialled methodology fails here, it will be a waste of time and resources to go any further without finding another approach.

Also, what about the proposed spatial data collection methodology? This should not be an afterthought. How much time will it take to set up and then gather the data? Is this feasible within the available timeframe for access to the site? These additional features must be present when the photographs are taken, so will have an impact on task scheduling. How will they be integrated into the reconstruction process, and when? Are any coded targets large enough to be identified by the software?

The only answer to all these uncertainties is to practice and experiment before heading into the field. This will also enable citizen scientists to trial their computational setup: can it handle the numbers of images? How long does it take to process? Are larger coded targets needed? Or more of them?

As an example, for this project, a car was used as a subject for a trial-run. It should be noted that a car, a van, or even a small shed, may well be a similar size to a boiler or an engine, as well as being something (nearly) all people will have. The car was parked in an empty carpark at a weekend to trial both the photographic requirements of recording such a subject, but also how to integrate spatial data.

Working close to the car and taking a series of overlapping photographs from static positions, the whole car was photographed before moving to capture a differing panorama. This resulted in successful alignment and the production of an appropriate point-cloud. This approach – creating a series of overlapping panoramas, rather than individual photographs, from sequential and planned positions around the subject – was then used successfully for the two main case studies of this project.

However, this methodology resulted from various unsuccessful predecessors. The first series of photographs were found to lack adequate overlap for image alignment. When a second set with increased overlap were added, they aligned, but incorrectly producing a model of only one side of the car, projecting the other side on the modelled side's interior. An additional set of close-up photographs were taken whilst moving around the vehicle: these failed to align at all. When combined, again erroneous alignments resulted, despite experimenting with processing parameters.

7.2 Project Objectives

7.2.1 FIRST OBJECTIVE – SUITABLE SPATIAL DATA SOURCES

The first objective was achieved by the Literature Review in Chapter Three.

7.2.2 SECOND OBJECTIVE – INTEGRATION OF SPATIAL DATA

The second objective identified targets and markers with inclusion as early in the processing as possible from literature, with a further and specific investigation into the practicalities of using coded targets being required following experimentation. The use of markers was proved to be effective for scaling and dimensional measurement when added at the end of the reconstruction process.

7.2.3 THIRD OBJECTIVE – ACCURACY OF RESULTS

Is clear that all these forms of spatial data are appropriate for scaling Image-Based Modelling, that this can be applied during post-processing using markers, and that simple check-measurements can be used to validate the results.

The questions relating to referencing within a specified coordinate system are more complex. Evidently measured coordinate data will be needed for this purpose, and it appears that more work is needed here to investigate whether an alternative methodology exists which can rival the TotalStation due to its inability to operate underwater or to be used by personnel without training and access to such specialist equipment.

7.2.4 FOURTH OBJECTIVE – TECHNICAL STANDARDS

This project has contributed to the development of technical guidance and standards through collating existing material from a wide range of sources, combining this with some practical examples and experimentation, before making some methodological recommendations. It has also identified the differences between essentially flat 3D sites and those with wider ranges of variation in the subject's elevation – both in terms of photographic data collection and for the spatial data collection methodology.

Finally, it has proposed that rather pursuing Image-Based Modelling as a catch-all "new gold standard" for site-level recording, perhaps alternative methods would be better applied at site-level using Image-Based Modelling for the specific, diagnostic features, to be recorded appropriately for these models to be accurate placed within a wider site-plan.

7.3 Aims of the Project

This project set out to contribute to technical guidelines for the production and evaluation of metric photogrammetry models, to carry out a pilot study to guide future research, and to contribute to wider, relevant discussions to aid the application of Image-Based Modelling to maritime heritage subjects by citizen scientists, amateur divers and paid professionals alike.

This project has shown that such models are in fact easy to scale, and that accurate measurements of dimensions may be taken. It has also shown that some basic examinations of the data collection methodology – especially survey control – and comparisons of check-measurements for key dimensions can be a reliable, if not robust, indicator of the level of accuracy of the dimensions within the resulting models. Such analyses can be performed using basic mathematics in everyday software.

For amateurs and professionals alike, these are the two key technical points arising from this thesis: demonstrable accuracy can be achieved using simple scaling features, present in the photographs, and validated very easily - if scaling is all that is required.

However, this study has also demonstrated that the effects on point-clouds of these varying types of spatial data are much more complex and cannot be gauged by such simple procedures. It should be remembered that it is this point-cloud data which must be measured if volume and surface detail are needed in addition to dimensions, as well as geographic coordinate referencing.

This study has also highlighted the differences between essentially flat 3D subjects, and those with larger ranges of elevation: in addition to considering how to capture the photographs, there will also be differences to the spatial data collection methodology.

It has also proposed that rather than assuming the need to use Image-Based Modelling as a site-level survey technique, as the current practice may appear to suggest, it may be more appropriate to use an alternative approach for site-level recording to contain accurately located 3D models of key, diagnostic features or other artefacts, themselves produced to high degrees of demonstrable and validated accuracy.

Whilst these may only be modest contributions to the development of technical standards for model production and evaluation, they are still progress; even if the more technical elements of investigating accuracy at coordinate level to enable referencing and integration with other datasets have not been fully achieved, the difficulties in doing so have been clearly identified, as well as indicating when rudimentary analysis in everyday software is appropriate – and when it is not.

However, as a pilot study to guide future research, these results are invaluable. They have clearly identified the need to investigate the use of coded targets in much greater detail, alongside the need for a deeper understanding of the mathematics and evaluation of 3D vector datasets.

This project also aimed to contribute to wider discussions. Hopefully the further questions proposed by this investigation may prove beneficial, in addition to the evident conclusions.

7.4 Research Question

Having discussed the experimental results in relation to the project's aims and objectives, attention must now turn to the overall research question and the extent to which this project has answered its own question.

Overall, this project has achieved success in some areas, and recommended profitable directions for future work to address the areas where it was not able to reach robust, empirical conclusions.

It is evident that the question has been answered, at least when scaling 3D models and evaluating their accuracy in key dimensions is considered. Where coordinates are involved, for referencing or evaluation of overall 3D geometry, the results become much more inconclusive.

However, this project, in line with its objective as a pilot study, has identified that the criteria used to evaluate such 3D data was not entirely appropriate; indeed some of the pitfalls of such an approach were exposed, however well supported they may have appeared to be within the literature.

For subjects simply needing scaling – to enable preservation in demonstrably accurate digital form, for example – this project has answered the research question. This could be of key importance for aiding citizen scientists and professionals alike.

Where more complex further uses of data are envisaged, especially within geomatics or geoinformatics, this project has contributed to the process of finding the answer by highlighting some pitfalls to avoid and proposing new directions for exploratory work.

On the subject of how cultural heritage should be recorded to enable the future uses of data, this project has also indicated the importance of establishing and testing a control coordinate system – and the relative ease in establishing and validating one. It has also indicated how creators may evaluate and possibly rate the accuracy of their work using check-measurements and readily available software: furthering the potential citizen science applications of this approach.

Furthermore, on a related subject, this project has cast doubt on this practice of "validating" by check-measurements where point-clouds and thus volume, surface texture and detail are to be measured. This work also demonstrates the need both to expose such data to some level of quantitative analysis, but also the need to critically evaluate the outcomes of these analyses rather than to blindly accept them as "scientific".

On these bases, it is clear that this project has answered some parts of the research question, but also contributed to the process of answering the more complex and ultimately rewarding areas. This thesis should perhaps be understood as milestone report on work in progress.

7.5 Reflective Review

In retrospect, there are several methodological amendments which may have been advantageous to the outcomes and overall success of this project:

1. Target identification should have been trialled alongside camera alignment using *PhotoScan* in demonstration mode on a laptop during the data collection. Additionally, the capacity to place markers and assign attributes before optimising alignment and re-building the dense point-cloud identified in 4.3 should not have been over-looked as an alternative.
2. It would have been interesting to consider using one of boxes as 3D scaling cube – both as connecting scale-bars and as coordinates to consider scaling in the z axis. However, the difficulties exposed by using such small dimensions for scaling have already been exposed.
3. If surveyed as a pair by the TotalStation they could have introduced 3D coordinate features to the model – it would be interesting to see if this could have addressed some of the inaccuracies associated with their use in a single plane, or provided an alternative method to encircling with four single coordinates.
4. On the same subject, two scale-bars placed at a right angle using a set square can form the origin of ~~an~~ coordinate grid – admittedly

only in two dimensions. Again, this would have been interesting to trial as an alternative to the enclosure method and as a possible form of arbitrary coordinate system for subsequent registration.

5. In relation to revealed shortcomings in experimental design, to avoid simply comparing variables to other variables a benchmark independent variable should always be used – here a laser-scanned point-cloud would have been ideal, but in its absence the methodology should have been adjusted.

7.6 Future Research

This project will continue, but with some new objectives:

1. A wider literature review then practical evaluation of field survey data evaluation and validation methodologies, regardless of their apparent suitability for Image-Based Modelling.
2. Practical investigations into the use of coded targets.
3. Practical experiments into the results of the processing parameters within photogrammetric software packages.
4. Literature review and practical investigation of 3D evaluation methodologies, such as using *CloudCompare* or DEM comparison.
5. Literature and practical investigation into areas declared as beyond the scope of this project.
6. Consideration of how best to deploy an integrated recording methodology, using Image-Based Modelling alongside other established techniques, to pursue spatially accurate recording to further heritage objectives – rather than examining the levels of accuracy theoretically possible in isolation.

The first is needed because this project has revealed that basic field survey and measured recording skills and understanding are not really adequate when dealing with a research project dependent on applying them to emergent technology and techniques.

Although size may have been an issue with the coded targets, Yamafune (2016)'s experiments regarded targets in the same plane as the camera – in this project's case they were frequently presented at alternative angles appearing as ellipses rather than circles; it is possible this also needs to be examined.

The processing parameters evidently play a large role in determining the outcomes of the modelling process. However, relatively little research has explored their effects on the complex geometries of cultural heritage subjects. Yamafune (2016) was an exception, although he investigated differing surfaces on regular shapes (cubes). This will need to use non peer-reviewed material (user groups and forums) as Yamafune did.

Finally, to adequately address the use of Image-Based Modelling to geomatics and geomatics, the investigations need to be extended to aerial and underwater data collection. This is especially important to the longer-term goals relating to metric recording of at-risk cultural heritage in high energy marine and coastal locations to enable preservation by record and the proposal of in-situ management strategies based on monitoring.

7.7 Concluding Remarks

This project has indicated that especially when being performed by citizen scientists, and quite possibly by paid professionals, it may be more beneficial to use Image-Based Modelling to record specific features in sufficient detail to enable detailed analyses later within a wider, metrically accurate site-plan produced by alternative means, rather to pursue “photogrammetry” as a “gold standard”, catch-all methodology for “scanning” an entire site. The potential for large periods of time to be invested gathering data which subsequently proves to be unsuitable is very high.

This is not to say that it cannot be done – the literature reviewed in this project demonstrates clearly that it can. However, especially where citizen scientists are concerned – or even paid professionals working with minimal funding, or with short periods on-site, it may be more effective to use Image-Based Modelling as proposed here.

Perhaps, rather than being perceived as the new, “standard” methodology for recording such subjects, Image-Based Modelling should be understood to be a hugely important, and welcome, addition to an existing suite of alternative and complementary options available; all of which will need to be modified and adapted to meet the specific requirements of the deliverables within the environmental, temporal, and personnel constraints of their circumstances.

The apparently scientific and objective nature of these techniques overshadow the inherent subjectivity of the necessary choices to be made in how to implement these methodologies appropriately. For these reasons, these choices must be recorded, alongside the other technical metadata.

Finally, this project has also served as a reminder of our need to harness digital technology more effectively within the heritage sector, rather than continuing to apply analogue yardsticks to our understanding of data, its collection, and its capabilities.

One example of this, clearly demonstrated by this project, is that the thickness of a pencil at 1:20 scale (20mm) is no longer a relevant benchmark for recording accuracy or precision – it may have been appropriate when surveys were hand-drawn on drafting film, but is no longer appropriate when using digital drawings, where scale has no such effect on a line's apparent thickness.

Finally, it is also clear that measured data needs quantitative evaluation methodologies appropriate to the data forms in question. Check-measurements have their evident utility, not least for evaluating data during collection, but they are insufficient for the meaningful analysis of spatial datasets – especially those in three dimensions, or where volumetric measurements may be needed.

List of References

Agisoft (2016): Agisoft PhotoScan Professional Edition User Manual.

Retrieved 14.5.2016 from: http://www.agisoft.com/downloads/user-manuals/

Agisoft (2019): Agisoft Metashape & Agisoft PhotoScan comparison. Online pdf. St Petersburg: Agisoft.

Retrieved 25.2.2019 from: https://www.agisoft.com/pdf/metashape_comparison.pdf

Bass, G. (1966): *Archaeology Under Water*. London: Thames and Hudson.

Bowens, A. (ed.): *Underwater Archaeology: The NAS Guide to Principles and Practice.* Chichester, West Sussex, UK: John Wiley & Sons Ltd. 2nd Edition.

British Sub-Aqua Club (1990): *Advanced Sport Diving*. London: Stanley Paul & Co. Ltd.

British Sub-Aqua Club (2000): *Sport Diving: The British Sub-Aqua Club Diving Manual*. Washington, Tyne and Wear, UK: Reed Print & Design.

British Sub-Aqua Club (2005): *Seamanship: A Guide for Divers.* Richmond, Surrey, UK: Circle Publishing.

British Sub-Aqua Club (2010): *The Expedition Manual: Taking Your Diving Further*. Richmond, Surrey, UK: Circle Publishing.

Bryan, P. (2006): *User requirements for Metric Survey*. Chapter in: MacDonald, L. (ed.) (2006): *Digital Heritage: Applying Digital Imaging to Cultural Heritage*. Oxford: Elsevier.

Campana, S. (2014): *3D Modelling in Archaeology and Cultural Heritage – Theory and Best Practice*. Chapter in: Remondino, F. and S. Campana (eds.) (2014): *3D Recording and Modelling in Archaeology and Cultural Heritage: Theory and Best Practices*. Oxford: Archaeopress - BAR Monograph International Series 2598.

Campbell, P. 2010: *High Tech on a Budget: Recording Maritime Cultural Heritage Using a Total Station, RhinoPhoto, and Rhinoceros* NURBS. Proceedings from the Computing Applications in Archaeology Conference held 22-26 March 2009 in Williamsburg VA, USA.

Retrieved 26.7.2020 from:

http://archive.caaconference.org/2009/articles/Campbell_Contribution_389_final.pdf

Capra, A., M. Dubbini, E. Bertacchini, C. Castagnetti and F. Mancini (2015): *3D reconstruction of an underwater archaeological site: comparison between low cost cameras*. The International Archives of the Photogrammetry, Remote Sensing and Spatial Information Sciences, Volume XL-5/W5:73-77. Underwater 3D Recording and Modeling, April 2015, Piano di Sorrento, Italy.

Chartered Institute of Archaeologists (UK Governing Body) (2020): *Professional Archaeologists*. Online web-page. Reading, UK.

Retrieved 11.12.2020 from:

https://www.archaeologists.net/join/professional-archaeology

D'Amelio, S., V. Maggio and B. Villa (2015): *3D modeling for underwater archaeological documentation: metric verifications*. The International Archives of the Photogrammetry, Remote Sensing and Spatial Information Sciences, Volume XL-5/W5:73-77. Underwater 3D Recording and Modeling, April 2015, Piano di Sorrento, Italy.

Darvill, T. (2003): *Oxford Concise Dictionary of Archaeology*. Oxford: Oxford University Press.

De Reu, J., De Smedt, P., Herremans, D., Van Meirvenne, M., Laloo, P., and W. De Clerq (2014): *On introducing an image-based 3D reconstruction method in archaeological excavation practice*. Journal of Archaeological Science 41:251-262.

Figueirido, A. and I. Bernades (2014): *The importance of GIS in underwater archaeology*. Chapter in: Figueirido, A., Calippo, F. and G. Rambelli: (2014): *Underwater Archaeology, Coastal and Lakeside*. Proceedings of the 16th World Congress of the International Union of Prehistoric and Protohistoric Sciences, Florianópolis 4-10 September 2011. British Archaeological Reports International Series 2631. Oxford: Archaeopress.

Gnaden, D. and S. Holdaway (2000): *Understanding observer variation when recording stone artifacts*. American Antiquity 65:739-747. Article cited in: Grosman, L., O. Smikt and U. Smilansky (2008): *On the application of 3-D scanning technology for the documentation and typology of lithic artifacts*. Journal of Archaeological Science 35:3101-3110.

Green, G. and M. Gainsford (2003): *Evaluation of underwater surveying techniques*. International Journal of Nautical Archaeology 32.2:252-261.

Gregory, D. and M. Manders (2011): *In-situ Preservation of a Wreck Site.* Chapter in: Gjelstrup Björdal, C. and D. Gregory (eds.) (2011): *WreckProtect: Decay and Protection of Archaeological Wooden Shipwrecks*. Oxford: Archaeopress.

Henderson, J., O. Pizzarro, M. Johnson-Roberson and I. Mahon (2013) *Mapping submerged archaeological sites using stereo-vision* *photogrammetry*. International Journal of Nautical Archaeology 2013 42:2:243-256.

Historic England (2015): *Metric Survey Specifications for Cultural Heritage*. Third Edition. Swindon: Historic England.

Historic England (2017): *Photogrammetric Applications for Cultural Heritage. Guidance for Good Practice.* Swindon: Historic England.

Historic Environment Scotland (2018): *Applied Digital Documentation in the Historic Environment*. Short Guide 13. Edinburgh: Historic Environment Scotland.

Holt, P. (2003): *An assessment of quality in underwater archaeological surveys using tape measures.* International Journal of Nautical Archaeology 32.2:246-251.

Holt, P. (2019): *Site Recorder Exercise Book*. Online pdf. Plymouth, UK: 3H Consulting Ltd.

Retrieved 25.2.2019 from:

http://www.3hconsulting.com/Downloads/SiteRecorder4ExerciseBook.pdf

Kjellman, E. (2012): *From 2D to 3D: A Photogrammetric Revolution in Archaeology?* Unpublished Master's Thesis in Archaeology, submitted to the University of Tromsø, Norway, Spring 2012.

Kontogianni, G., E. Strathopoulou, A. Georgopoulos and A. Doulamis (2015): *HDR imaging for feature detection on detailed architectural scenes*. ISPRS-International Archives of the Photogrammetry, Remote Sensing and Spatial Information Sciences Volume XL-5/W4:325-330.

MacDonald, L. (2015): *Realistic Visualisation of Cultural Heritage Objects*. PhD Thesis in Civil and Geomatic Engineering, submitted to the University of London, UK in 2015. Available from: https://discovery.ucl.ac.uk/id/eprint/1471969/

Martin, C. and E. Martin (2002): *An underwater photomosaic technique using Adobe Photoshop*. International Journal of Nautical Archaeology 31.1:137-147.

Mason, A. (No Date): *Making 3D models with photogrammetry: getting started with Agisoft PhotoScan*. Article published online.

Retrieved 7.8.2016 from:

http://www.haskinssociety.org/resources/Documents/Tutorials/PhotogrammetrywithPhotoScanTutorial.pdf

McCarthy, J. (2012): *Unknown Wreck, Drumbeg (undesignated site assessment)*, Unpublished fieldwork report for Wessex Archaeology on behalf of Historic Scotland.

Retrieved 13.1.2021 from:

https://canmore.org.uk/collection/1319887

McCarthy, J. and J. Benjamin (2014): *Multi-image photogrammetry for underwater archaeological site recording: an accessible, diver-based approach*. Journal of Maritime Archaeology 2014 9:1:95-114.

McCarthy, J., Benjamin, J., Winton, T. and W. van Duivenvoorde (eds.) (2019): *3D Recording for Maritime Archaeology*. Open Access eBook, Coastal Research Library. Cham, Switzerland: Springer.

DOI: https://doi.org/10.1007/978-3-030-03635-5

McCarthy, J., Robertson, P. and E. Mackay (2015): *Discovery and Survey of a 17th-18th Century Shipwreck near Drumbeg, NW Scotland: an initial report.* International Journal of Nautical Archaeology 2015 44:1:202-208

Mertes, J., T. Thomsen and J. Gulley (2014): *Evaluation of Structure from Motion software to create 3D models of late Nineteenth Century Great Lakes shipwrecks using archived diver-acquired video surveys*. Journal of Maritime Archaeology 9:173-189.

Miles, J., M. Pitts, H. Pagi and G. Earl (2014): *New applications of photogrammetry and reflectance transformation imaging to an Easter Island statue*. Antiquity 88:596-605.

Muckelroy, K. (1978): *Maritime Archaeology*. Cambridge: Cambridge University Press.

Mudge, M. et al (2008): *Image-Based Empirical Information Acquisition, Scientific Reliability, and Long-Term Digital Preservation for the Natural Sciences and Cultural Heritage*. Eurographics 2008: Tutorial Notes.

CITATION PAGE NUMBERS 1-30 REFER TO ONLINE VERSION OF THIS ARTICLE AVAILABLE FROM:

http://homepages.inf.ed.ac.uk/rbf/CVonline/LOCAL_COPIES/MUDGE/EG-mudge-tutorial-notes-final.pdf

Ortiz Vázquez, R. (2018): *An Integrated Methodology to Study Site Formation Processes on Submerged Shipwrecks in the 21st Century*. PhD Thesis, University of Southampton, School of Humanities. Available from: https://eprints.soton.ac.uk/435554/

Pacheco-Ruiz, R., Adams, J. and F. Pedrotti (2018): *4D modelling of low visibility Underwater Archaeological excavations using multi-source photogrammetry in the Bulgarian Black Sea.* Journal of Archaeological Science 100:120-129.

Pascoe, D., Jones, B. and G. Cox (2017): *The use of multi-image photogrammetry to record at-risk archaeological material from the* *wreck of* Invincible. Historic England Research Report Series: 37-2017. Portsmouth, UK: Historic England.

Pavelka, K. and J. Reznícek (2011): *New low-cost automated processing of digital photos for documentation and visualisation of the cultural heritage* (sic). Reviewed papers from XXIIIrd International CIPA Symposium, Prague, Czech Republic, September 2011. Vol 6:249-258.

Pierrot-Deseilligny, M., L. De Luca and F. Remondino (2011): *Automated image-based procedures for accurate artifacts (sic) 3D modeling and orthoimage generation*. Reviewed papers from XXIIIrd International CIPA Symposium, Prague, Czech Republic, September 12-16, 2011, organized by CIPA, ISPRS and CTU in Prague with special ICOMOS section. Vol 6:291-299.

Re, C., S. Robson, R. Roncella and M. Hess (2011): *Metric accuracy evaluation of dense matching algorithms in archaeological applications.* Reviewed papers from XXIIIrd International CIPA Symposium, Prague, Czech Republic, September 12-16, 2011, organized by CIPA, ISPRS and CTU in Prague with special ICOMOS section. Vol 6:275-282.

Remondino, F. (2014): *Photogrammetry – Basic Theory*. Chapter in: Remondino, F. and S. Campana (eds.) (2014): *3D Recording and Modelling in Archaeology and Cultural Heritage: Theory and Best Practices*. Oxford: Archaeopress - BAR Monograph International Series 2598.

Rizzi, A., F. Voltolini, F. Remondino, S. Girardi and L. Gonzo (2007): *Optical measurement techniques for the digital preservation, documentation and analysis of cultural heritage*. Proceedings of the Optical 3-D Measurement Techniques VIII, Volume 2:16-24.

Royal Yachting Association (2012): *Day Skipper: Introduction to Navigation Theory, Safety and Seamanship*. Southampton, UK: Royal Yachting Association.

Royal Yachting Association (2014): *Yachtmaster: Advanced Navigation Theory, Safety and Seamanship*. Southampton, UK: Royal Yachting Association.

Rule, N. (1989): *The Direct Survey Method (DSM) of underwater survey, and its application underwater.* International Journal of Nautical Archaeology and Underwater Exploration 18.2:157-162.

Skarlatos, D., S. Demestiha and S. Kiparissi (2012): *An 'open' method for 3D modelling and mapping in underwater archaeological sites.* International Journal of Heritage in the Digital Era. 2012 1:1:1-24.

Tidball, J. (2016): *Accuracy of Underwater Image Based Modelling determined against Terrestrial Laser Scanning.* Unpublished MSc Hydrography Dissertation in Journal Format, submitted to Plymouth University, UK, September 2016.

Van Damme, T. (2015): *Computer vision photogrammetry for underwater archaeological site recording in a low-visibility environment*. The International Archives of the Photogrammetry, Remote Sensing and Spatial Information Sciences, Volume XL-5/W5: 231-238, 2015: Underwater 3D Recording and Modeling, 16–17 April 2015, Piano di Sorrento, Italy.

Westoby, M., J. Brasington, N. Glasser, M. Hambrey and J. Reynolds (2012): 'Structure from Motion' photogrammetry: a low-cost, effective tool for geoscience applications. Geomorphology 179:300-314.

Wolf, P., B. Dewitt and B. Wilkinson (2014*): Elements of Photogrammetry with Applications in GIS*. New York: McGraw Hill Education; 4th Edition.

Yamafune, K. (2016): *Using Computer Vision Photogrammetry (Agisoft PhotoScan) to Record and Analyze Underwater Shipwreck Sites.* PhD Thesis in Anthropology, submitted to the University of Texas A&M, USA, May 2016.

Yamafune, K., R. Torres and F. Castro (2016): *Multi-image photogrammetry to record and reconstruct underwater shipwreck sites*. Journal of Archaeological Method and Theory 23:1:1-23.

Appendix 1: Metadata Summary

TITLE	An evaluation of Image-Based Modelling for metrically recording cultural heritage subjects suitably to enable further use in geomatics, geoinformatics, and digital humanities.
CREATOR	Richard Rowley PGR Student Faculty of Science & Technology Bournemouth University rrowley@bournemouth.ac.uk
SUBJECT	Investigating how to use spatial data alongside photographs for 3D reconstruction of cultural heritage subjects to create demonstrably accurate records suitably for further metric applications.
DESCRIPTION	MRes Thesis Produced as assessed academic work.
PUBLISHER	Not Applicable
CONTRIBUTOR	None
DATE	25 January 2021
TYPE	Post-graduate Research Thesis
WORD COUNT	22,965
FORMAT	Adobe PDF

IDENTIFIER	RR_MRes_Thesis_2021.pdf
SOURCE	Adobe Acrobat, Adobe Photoshop CS6, Microsoft Word 365, Microsoft Excel 365, Agisoft PhotoScan Professional,
FORMATS (Generic)	PDF (2D and 3D), .docx, .xlsx, .jpg, .txt.
FORMATS (Project Specific)	**.psx** (Agisoft PhotoScan Professional project)
LANGUAGE	English (United Kingdom)
RELATION	Unpublished Research Project
COVERAGE	Non-Geographic
RIGHTS	Copyright held by Author.
ADDITIONAL NOTES	This Thesis is for academic use and contains referenced images from other published works which have been used without permission.

Appendix 2: Survey Grid

Survey Grid SetUp					
PtID	**East**	**North**	**Height**		
CP_01_SetUp	0.000	0.000	0.000		
CP_02_SetUp	0.000	5.000	0.000		
CP_03_SetUp	5.000	5.000	-0.020		
CP_04_SetUp	5.000	0.000	0.000		
TS_01	0.0000	0.0000	0.0000	BACKSIGHT	CP_02_SetUp
TS_01_COMP	0.0000	0.0000	-0.0084	INST HEIGHT	1.5950
TS_01_CP_02	0.0037	5.0057	-0.0054		
TS_01_CP_03	4.9973	4.9866	-0.0142		
TS_01_CP_04	5.0054	-0.0193	-0.0078		
CP_01_1	0.000	0.000	-0.008		
CP_02_1	0.004	5.006	-0.005		
CP_03_1	4.997	4.987	-0.014		
CP_04_1	5.005	-0.019	-0.008		
TS_02	0.0040	5.0060	0.0050	BACKSIGHT	CP_01_SetUp
TS_02_COMP	0.0040	5.0060	0.0076	INST HEIGHT	1.5380
TS_02_CP_04	5.0094	-0.0177	0.0080		
TS_02_CP_03	5.0090	4.9831	0.0027		
TS_02_CP_01	0.0001	0.0042	0.0098		
CP_01_2	0.0001	0.0042	0.0098		
CP_02_2	0.0040	5.0060	0.0076		
CP_03_2	5.0090	4.9831	0.0027		
CP_04_2	5.0094	-0.0177	0.0080		
CP_01_2	0.000	0.004	0.000		
CP_02_2	0.004	5.006	-0.002		
CP_03_2	5.009	4.983	-0.007		
CP_04_2	5.009	-0.018	-0.002		
TS_03	4.9970	4.9870	-0.0140	BACKSIGHT	CP_02_SetUp
TS_03_COMP	4.9970	4.9870	-0.0103	INST HEIGHT	1.5360
TS_03_CP_01	-0.0037	0.0061	0.0001		
TS_03_CP_02	-0.0108	5.0037	0.0036		
TS_03_CP_04	5.0024	-0.0083	0.0003		
CP_01_3	-0.004	0.006	0.000		
CP_02_3	-0.011	5.004	0.004		
CP_03_3	4.997	4.987	-0.010		
CP_04_3	5.002	-0.008	0.000		

TS_04	5.0050	-0.0190	0.0080	BACKSIGHT	CP_01_SetUp		
TS_04_COMP	5.0050	-0.0190	-0.0055	INST HEIGHT	1.5190		
TS_04_CP_02	-0.0043	4.9974	0.0000				
TS_04_CP_03	4.9968	4.9811	-0.0063				
TS_04_CP_01	0.0082	-0.0032	-0.0003				
CP_01_4	0.0082	-0.0032	-0.0003				
CP_02_4	-0.0043	4.9974	0.0000				
CP_03_4	4.9968	4.9811	-0.0063				
CP_04_4	5.0050	-0.0190	-0.0055				
CP_01_4	0.008	-0.003	-0.016				
CP_02_4	-0.004	4.997	-0.016				
CP_03_4	4.997	4.981	-0.022				
CP_04_4	5.005	-0.019	-0.022				
CHECK ERROR							
EAST						**SetUp vs TS_01**	**TS_01 vs TS_02/03/04**
	SetUp	**TS_01**	**TS_02**	**TS_03**	**TS_04**	**Within 20mm?**	**Within 20mm?**
CP_01	0.000	0.000	0.000	-0.004	0.008	YES (5mm)	YES (10mm)
CP_02	0.000	0.004	0.004	-0.011	-0.004	YES (5mm)	YES
CP_03	5.000	4.997	5.009	4.997	4.997	YES (5mm)	YES
CP_04	5.000	5.005	5.009	5.002	5.005	YES (5mm)	YES (5mm)
NORTH							
	SetUp	**TS_01**	**TS_02**	**TS_03**	**TS_04**	**Within 20mm?**	**Within 20mm?**
CP_01	0.000	0.000	0.004	0.006	-0.003	YES (5mm)	YES (10mm)
CP_02	5.000	5.006	5.006	5.004	4.997	YES (10mm)	YES (10mm)
CP_03	5.000	4.987	4.983	4.987	4.981	YES	YES (10mm)
CP_04	0.000	-0.019	-0.018	-0.008	-0.019	YES	YES
HEIGHT							
	SetUp	**TS_01**	**TS_02**	**TS_03**	**TS_04**	**Within 20mm?**	**Within 20mm?**
CP_01	0.000	-0.008	0.000	0.000	-0.016	YES (10mm)	YES (10mm)
CP_02	0.000	-0.005	-0.002	0.004	-0.016	YES (5mm)	YES
CP_03	-0.020	-0.014	-0.007	-0.010	-0.022	YES (10mm)	YES (10mm)
CP_04	0.000	-0.008	-0.002	0.000	-0.022	YES (10mm)	YES
CONTROL GRID							
CP_01	0.0000	0.0000	0.0000				
CP_02	0.0040	5.0060	-0.0050				
CP_03	4.9970	4.9870	-0.0140				
CP_04	5.0050	-0.0190	-0.0080				

Appendix 3: Anchor (Scale-Bar) Exported Data

	Anchor_ScaleBar Output Data				
	Number of Photographs	**82**			
	Image Quality	Lowest	Lowest Aligned	Highest	
		0.42592	**0.568383**	**0.945133**	
	Number Aligned	**81**			
	Tie Points	**106924**			
	Dense Cloud	**4864278**			
	3D Model	**324285**			
			SUM ERROR (MM)	**MEAN ERROR (MM)**	
	Scale Bar		**127**	**13**	
	Enclosure		**76**	**8**	
	CP (Measurements)		**78**	**8**	
	CP (Coordinates)		**48**	**2**	
	DP (Measurements)		**78**	**8**	
	DP (Coordinates)		**49**	**2**	

ScaleBar								
Scaling								
ScaleBar_1 to ScaleBar_2	1.000							
Measurements			**Check Measurements**		**ERROR**		**ERROR (MM)**	**ERROR (MM) +ve**
ScaleBar_1 to ScaleBar_2	1.000		ScaleBar_1 to ScaleBar_2	1.000	0.000		0	**0**
PT_01 to PT_02	0.862		PT_01 to PT_02	0.851	0.011		11	**11**
PT_02 to PT_03	1.560		PT_02 to PT_03	1.539	0.021		21	**21**
PT_03 to PT_04	0.981		PT_03 to PT_04	0.974	0.007		7	**7**
PT_01 to PT_04	1.550		PT_01 to PT_04	1.532	0.018		18	**18**
Anchor_02 to Anchor_03	0.749		Anchor_02 to Anchor_03	0.732	0.017		17	**17**
Anchor_01 to PT_01	0.741		Anchor_01 to PT_01	0.742	-0.001		-1	**1**
Anchor_01 to PT_02	0.913		Anchor_01 to PT_02	0.913	0.000		0	**0**
Anchor_01 to PT_03	1.300		Anchor_01 to PT_03	1.278	0.022		22	**22**
Anchor_01 to PT_04	1.080		Anchor_01 to PT_04	1.050	0.030		30	**30**
							SUM ERROR (MM)	**127**
							MEAN ERROR (MM)	**13**

Enclosure								
Scaling								
PT_01 to PT_02	0.851							
PT_01 to PT_04	1.532							
PT_02 to PT_03	1.539							
PT_03 to PT_04	0.974							
Measurements			**Check Measurements**		**ERROR**		**ERROR (MM)**	**ERROR (MM) +ve**
ScaleBar_1 to ScaleBar_2	0.988		ScaleBar_1 to ScaleBar_2	1.000	-0.012		-12	**12**
PT_01 to PT_02	0.851		PT_01 to PT_02	0.851	0.000		0	**0**
PT_02 to PT_03	1.540		PT_02 to PT_03	1.539	0.001		1	**1**
PT_03 to PT_04	0.970		PT_03 to PT_04	0.974	-0.004		-4	**4**
PT_01 to PT_04	1.540		PT_01 to PT_04	1.532	0.008		8	**8**
Anchor_02 to Anchor_03	0.742		Anchor_02 to Anchor_03	0.732	0.010		10	**10**
Anchor_01 to PT_01	0.732		Anchor_01 to PT_01	0.742	-0.010		-10	**10**
Anchor_01 to PT_02	0.904		Anchor_01 to PT_02	0.913	-0.009		-9	**9**
Anchor_01 to PT_03	1.290		Anchor_01 to PT_03	1.278	0.012		12	**12**
Anchor_01 to PT_04	1.060		Anchor_01 to PT_04	1.050	0.010		10	**10**
							SUM ERROR (MM)	**76**
							MEAN ERROR (MM)	**8**

Control Points											
Scaling	**X**	**Y**	**Z**								
PT_01	2.2573	3.5643	0.4190								
PT_02	3.1077	3.5331	0.4166								
PT_03	3.2264	1.9996	0.4265								
PT_04	2.2531	2.0315	0.4236								
Measurements					**Check Measurements**		**ERROR**		**ERROR (MM)**	**ERROR (MM) +ve**	**SUM ERROR (MM)**
ScaleBar_1 to ScaleBar_2	0.988				ScaleBar_1 to ScaleBar_2	1.000	-0.012		-12	12	**78**
PT_01 to PT_02	0.850				PT_01 to PT_02	0.851	-0.001		-1	1	
PT_02 to PT_03	1.540				PT_02 to PT_03	1.539	0.001		1	1	**MEAN ERROR (MM)**
PT_03 to PT_04	0.970				PT_03 to PT_04	0.974	-0.004		-4	4	**8**
PT_01 to PT_04	1.540				PT_01 to PT_04	1.532	0.008		8	8	
Anchor_02 to Anchor_03	0.743				Anchor_02 to Anchor_03	0.732	0.011		11	11	
Anchor_01 to PT_01	0.732				Anchor_01 to PT_01	0.742	-0.010		-10	10	
Anchor_01 to PT_02	0.904				Anchor_01 to PT_02	0.913	-0.009		-9	9	
Anchor_01 to PT_03	1.290				Anchor_01 to PT_03	1.278	0.012		12	12	
Anchor_01 to PT_04	1.060				Anchor_01 to PT_04	1.050	0.010		10	10	
Coordinates (Agisoft)	**X**	**Y**	**Z**		**ERROR**	**X**	**Y**	**Z**			
Anchor_01	2.4985	2.9915	0.8051		ANCHOR_01	-0.0021	-0.0029	0.0013			
Anchor_02	2.9674	2.8310	0.4277		ANCHOR_02	-0.0095	-0.0041	0.0039			
Anchor_03	2.7698	2.1161	0.4352		ANCHOR_03	0.0041	-0.0020	-0.0072			
PT_01	2.2576	3.5653	0.4196		PT_01	0.0003	0.0010	0.0006			
PT_02	3.1080	3.5335	0.4160		PT_02	0.0003	0.0004	-0.0006			
PT_03	3.2240	2.0003	0.4270		PT_03	-0.0024	0.0007	0.0005			
PT_04	2.2549	2.0294	0.4231		PT_04	0.0018	-0.0021	-0.0005			
					ERROR	**X (+ve)**	**Y (+ve)**	**Z (+ve)**			
TS Coordinates	**X**	**Y**	**Z**		ANCHOR_01	0.0021	0.0029	0.0013			
ANCHOR_01	2.5006	2.9944	0.8038		ANCHOR_02	0.0095	0.0041	0.0039			
ANCHOR_02	2.9769	2.8351	0.4238		ANCHOR_03	0.0041	0.0020	0.0072			
ANCHOR_03	2.7657	2.1181	0.4424		PT_01	0.0003	0.0010	0.0006			
PT_01	2.2573	3.5643	0.4190		PT_02	0.0003	0.0004	0.0006			**SUM ERROR (MM)**
PT_02	3.1077	3.5331	0.4166		PT_03	0.0024	0.0007	0.0005			**48**
PT_03	3.2264	1.9996	0.4265		PT_04	0.0018	0.0021	0.0005			
PT_04	2.2531	2.0315	0.4236								**MEAN ERROR (MM)**
					ERROR (SUM)	0.0205	0.0133	0.0147	48	48	**2**

Detail Points										
Scaling	**X**	**Y**	**Z**							
PT_01	2.2573	3.5643	0.4190							
PT_02	3.1077	3.5331	0.4166							
PT_03	3.2264	1.9996	0.4265							
PT_04	2.2531	2.0315	0.4236							
ANCHOR_01	2.5006	2.9944	0.8038							
ANCHOR_02	2.9769	2.8351	0.4238							
ANCHOR_03	2.7657	2.1181	0.4424							
Measurements				**Check Measurements**		**ERROR**		**ERROR (MM)**	**ERROR (MM) +ve**	**SUM ERROR (MM)**
ScaleBar_1 to ScaleBar_2	0.989			ScaleBar_1 to ScaleBar_2	1.000	-0.011		-11	11	**78**
PT_01 to PT_02	0.852			PT_01 to PT_02	0.851	0.001		1	1	
PT_02 to PT_03	1.540			PT_02 to PT_03	1.539	0.001		1	1	**MEAN ERROR (MM)**
PT_03 to PT_04	0.970			PT_03 to PT_04	0.974	-0.004		-4	4	**8**
PT_01 to PT_04	1.540			PT_01 to PT_04	1.532	0.008		8	8	
Anchor_02 to Anchor_03	0.744			Anchor_02 to Anchor_03	0.732	0.012		12	12	
Anchor_01 to PT_01	0.732			Anchor_01 to PT_01	0.742	-0.010		-10	10	
Anchor_01 to PT_02	0.904			Anchor_01 to PT_02	0.913	-0.009		-9	9	
Anchor_01 to PT_03	1.290			Anchor_01 to PT_03	1.278	0.012		12	12	
Anchor_01 to PT_04	1.060			Anchor_01 to PT_04	1.050	0.010		10	10	
Coordinates (Agisoft)	**X**	**Y**	**Z**	**ERROR**	**X**	**Y**	**Z**			
Anchor_01	2.5001	2.9937	0.8051	ANCHOR_01	-0.0005	-0.0007	0.0013			
Anchor_02	2.9686	2.8320	0.4276	ANCHOR_02	-0.0083	-0.0031	0.0038			
Anchor_03	2.7703	2.1171	0.4367	ANCHOR_03	0.0046	-0.0010	-0.0057			
PT_01	2.2593	3.5671	0.4186	PT_01	0.0020	0.0028	-0.0004			
PT_02	3.1098	3.5345	0.4143	PT_02	0.0021	0.0014	-0.0023			
PT_03	3.2245	2.0009	0.4283	PT_03	-0.0019	0.0013	0.0018			
PT_04	2.2551	2.0308	0.4252	PT_04	0.0020	-0.0007	0.0016			
				ERROR	**X (+ve)**	**Y (+ve)**	**Z (+ve)**			
TS Coordinates	**X**	**Y**	**Z**	ANCHOR_01	0.0005	0.0007	0.0013			
ANCHOR_01	2.5006	2.9944	0.8038	ANCHOR_02	0.0083	0.0031	0.0038			
ANCHOR_02	2.9769	2.8351	0.4238	ANCHOR_03	0.0046	0.0010	0.0057			
ANCHOR_03	2.7657	2.1181	0.4424	PT_01	0.0020	0.0028	0.0004			
PT_01	2.2573	3.5643	0.4190	PT_02	0.0021	0.0014	0.0023			**SUM ERROR (MM)**
PT_02	3.1077	3.5331	0.4166	PT_03	0.0019	0.0013	0.0018			**49**
PT_03	3.2264	1.9996	0.4265	PT_04	0.0020	0.0007	0.0016			
PT_04	2.2531	2.0315	0.4236							**MEAN ERROR (MM)**
				ERROR (SUM)	0.0215	0.0110	0.0169	49	49	**2**

Appendix 4: Anchor (Boxes) Exported Data

	Anchor_Boxes Output Data				
	Number of Photographs	**184**			
	Image Quality	Lowest	Lowest Aligned	Highest	
		0.22733	**0.227328**	**0.828766**	
	Number Aligned	**184**			
	Tie Points	**199913**			
	Dense Cloud	**9435319**			
	3D Model	**628874**			
			SUM ERROR (MM)	**MEAN ERROR (MM)**	
	Scale Bar (2)		**387**	**26**	
	Enclosure		**82**	**5**	
	CP (Measurements)		**85**	**6**	
	CP (Coordinates)		**71**	**2**	
	DP (Measurements)		**94**	**6**	
	DP (Coordinates)		**74**	**2**	

ScaleBar_1+2								
Scaling								
BOX_32_01 to BOX_32_02	0.427							
BOX_38_01 to BOX_38_02	0.428							
Measurements			**Check Measurements**		**ERROR**		**ERROR (MM)**	**ERROR (MM) +ve**
PT_01 to PT_02	0.876		PT_01 to PT_02	0.851	0.025		25	25
PT_02 to PT_03	1.590		PT_02 to PT_03	1.539	0.051		51	51
PT_03 to PT_04	1.000		PT_03 to PT_04	0.974	0.026		26	26
PT_01 to PT_04	1.570		PT_01 to PT_04	1.532	0.038		38	38
Anchor_02 to Anchor_03	0.756		Anchor_02 to Anchor_03	0.732	0.024		24	24
Anchor_01 to PT_01	0.755		Anchor_01 to PT_01	0.742	0.013		13	13
Anchor_01 to PT_02	0.933		Anchor_01 to PT_02	0.913	0.020		20	20
Anchor_01 to PT_03	1.320		Anchor_01 to PT_03	1.278	0.042		42	42
Anchor_01 to PT_04	1.090		Anchor_01 to PT_04	1.050	0.040		40	40
BOX_32_01 to BOX_32_02	0.427		BOX_32_01 to BOX_32_02	0.427	0.000		0	0
BOX_38_01 to BOX_38_02	0.428		BOX_38_01 to BOX_38_02	0.428	0.000		0	0
Anchor_01 to BOX_32_01	0.479		Anchor_01 to BOX_32_01	0.465	0.014		14	14
Anchor_01 to BOX_32_02	0.895		Anchor_01 to BOX_32_02	0.858	0.037		37	37
Anchor_01 to BOX_38_01	0.647		Anchor_01 to BOX_38_01	0.626	0.021		21	21
Anchor_01 to BOX_38_02	1.010		Anchor_01 to BOX_38_02	0.974	0.036		36	36
							SUM ERROR (MM)	**387**
							MEAN ERROR (MM)	**26**

Enclosure								
Scaling								
PT_01 to PT_02	0.851							
PT_01 to PT_04	1.532							
PT_02 to PT_03	1.539							
PT_03 to PT_04	0.974							
Measurements			**Check Measurements**		**ERROR**		**ERROR (MM)**	**ERROR (MM) +ve**
PT_01 to PT_02	0.852		PT_01 to PT_02	0.851	0.001		1	1
PT_02 to PT_03	1.540		PT_02 to PT_03	1.539	0.001		1	1
PT_03 to PT_04	0.974		PT_03 to PT_04	0.974	0.000		0	0
PT_01 to PT_04	1.530		PT_01 to PT_04	1.532	-0.002		-2	2
Anchor_02 to Anchor_03	0.735		Anchor_02 to Anchor_03	0.732	0.003		3	3
Anchor_01 to PT_01	0.732		Anchor_01 to PT_01	0.742	-0.010		-10	10
Anchor_01 to PT_02	0.907		Anchor_01 to PT_02	0.913	-0.006		-6	6
Anchor_01 to PT_03	1.290		Anchor_01 to PT_03	1.278	0.012		12	12
Anchor_01 to PT_04	1.050		Anchor_01 to PT_04	1.050	0.000		0	0
BOX_32_01 to BOX_32_02	0.415		BOX_32_01 to BOX_32_02	0.427	-0.012		-12	12
BOX_38_01 to BOX_38_02	0.416		BOX_38_01 to BOX_38_02	0.428	-0.012		-12	12
Anchor_01 to BOX_32_01	0.465		Anchor_01 to BOX_32_01	0.465	0.000		0	0
Anchor_01 to BOX_32_02	0.869		Anchor_01 to BOX_32_02	0.858	0.011		11	11
Anchor_01 to BOX_38_01	0.630		Anchor_01 to BOX_38_01	0.626	0.004		4	4
Anchor_01 to BOX_38_02	0.982		Anchor_01 to BOX_38_02	0.974	0.008		8	8
							SUM ERROR (MM)	**82**
							MEAN ERROR (MM)	**5**

Control Points										
Scaling	**X**	**Y**	**Z**							
PT_01	2.2573	3.5643	0.4190							
PT_02	3.1077	3.5331	0.4166							
PT_03	3.2264	1.9996	0.4265							
PT_04	2.2531	2.0315	0.4236							
Measurements				**Check Measurements**			**ERROR**	**ERROR (MM)**	**ERROR (MM) +ve**	**SUM ERROR (MM)**
PT_01 to PT_02	0.852			PT_01 to PT_02	0.851		0.001	1	1	**85**
PT_02 to PT_03	1.540			PT_02 to PT_03	1.539		0.001	1	1	
PT_03 to PT_04	0.974			PT_03 to PT_04	0.974		0.000	0	0	**MEAN ERROR (MM)**
PT_01 to PT_04	1.530			PT_01 to PT_04	1.532		-0.002	-2	2	**6**
Anchor_02 to Anchor_03	0.738			Anchor_02 to Anchor_03	0.732		0.006	6	6	
Anchor_01 to PT_01	0.733			Anchor_01 to PT_01	0.742		-0.009	-9	9	
Anchor_01 to PT_02	0.907			Anchor_01 to PT_02	0.913		-0.006	-6	6	
Anchor_01 to PT_03	1.290			Anchor_01 to PT_03	1.278		0.012	12	12	
Anchor_01 to PT_04	1.050			Anchor_01 to PT_04	1.050		0.000	0	0	
BOX_32_01 to BOX_32_02	0.415			BOX_32_01 to BOX_32_02	0.427		-0.012	-12	12	
BOX_38_01 to BOX_38_02	0.416			BOX_38_01 to BOX_38_02	0.428		-0.012	-12	12	
Anchor_01 to BOX_32_01	0.466			Anchor_01 to BOX_32_01	0.465		0.001	1	1	
Anchor_01 to BOX_32_02	0.869			Anchor_01 to BOX_32_02	0.858		0.011	11	11	
Anchor_01 to BOX_38_01	0.630			Anchor_01 to BOX_38_01	0.626		0.004	4	4	
Anchor_01 to BOX_38_02	0.982			Anchor_01 to BOX_38_02	0.974		0.008	8	8	
Coordinates (Agisoft)	**X**	**Y**	**Z**	**ERROR**	**X**	**Y**	**Z**			
Anchor_01	2.4974	2.9867	0.8035	ANCHOR_01	-0.0032	-0.0077	-0.0003			
Anchor_02	2.9733	2.8238	0.4290	ANCHOR_02	-0.0036	-0.0113	0.0052			
Anchor_03	2.7651	2.1197	0.4404	ANCHOR_03	-0.0006	0.0016	-0.0020			
PT_01	2.2565	3.5628	0.4187	PT_01	-0.0008	-0.0015	-0.0003			
PT_02	3.1078	3.5343	0.4169	PT_02	0.0001	0.0012	0.0003			
PT_03	3.2268	1.9974	0.4262	PT_03	0.0004	-0.0022	-0.0003			
PT_04	2.2534	2.0341	0.4239	PT_04	0.0003	0.0026	0.0003			
BOX_32_01	2.4799	2.5261	0.7426	BOX_32_01	0.0002	-0.0027	0.0002			
BOX_32_02	2.3419	2.1346	0.7317	BOX_32_02	0.0031	0.0005	-0.0050			
BOX_38_01	3.0204	2.6414	0.7442	BOX_38_01	0.0001	0.0059	0.0005			
BOX_38_02	3.1331	2.2413	0.7365	BOX_38_02	0.0046	-0.0010	0.0014			
				ERROR	**X (+ve)**	**Y (+ve)**	**Z (+ve)**			
TS Coordinates	**X**	**Y**	**Z**	ANCHOR_01	0.0032	0.0077	0.0003			
ANCHOR_01	2.5006	2.9944	0.8038	ANCHOR_02	0.0036	0.0113	0.0052			
ANCHOR_02	2.9769	2.8351	0.4238	ANCHOR_03	0.0006	0.0016	0.0020			
ANCHOR_03	2.7657	2.1181	0.4424	PT_01	0.0008	0.0015	0.0003			
PT_01	2.2573	3.5643	0.4190	PT_02	0.0001	0.0012	0.0003			
PT_02	3.1077	3.5331	0.4166	PT_03	0.0004	0.0022	0.0003			
PT_03	3.2264	1.9996	0.4265	PT_04	0.0003	0.0026	0.0003			
PT_04	2.2531	2.0315	0.4236	BOX_32_01	0.0002	0.0027	0.0002			
BOX_32_01	2.4797	2.5288	0.7424	BOX_32_02	0.0031	0.0005	0.0050			**SUM ERROR (MM)**
BOX_32_02	2.3388	2.1341	0.7367	BOX_38_01	0.0001	0.0059	0.0005			**71**
BOX_38_01	3.0203	2.6355	0.7437	BOX_38_02	0.0046	0.0010	0.0014			
BOX_38_02	3.1285	2.2423	0.7351							**MEAN ERROR (MM)**
				ERROR (SUM)	0.0171	0.0382	0.0157	71	71	**2**

Detail Points										
Scaling	**X**	**Y**	**Z**							
PT_01	2.2573	3.5643	0.4190							
PT_02	3.1077	3.5331	0.4166							
PT_03	3.2264	1.9996	0.4265							
PT_04	2.2531	2.0315	0.4236							
ANCHOR_01	2.5006	2.9944	0.8038							
ANCHOR_02	2.9769	2.8351	0.4238							
ANCHOR_03	2.7657	2.1181	0.4424							
BOX_32_01	2.4797	2.5288	0.7424							
BOX_32_02	2.3388	2.1341	0.7367							
BOX_38_01	3.0203	2.6355	0.7437							
BOX_38_02	3.1285	2.2423	0.7351							
Measurements				**Check Measurements**		**ERROR**		**ERROR (MM)**	**ERROR (MM) +ve**	**SUM ERROR (MM)**
PT_01 to PT_02	0.854			PT_01 to PT_02	0.851	0.003		3	3	**94**
PT_02 to PT_03	1.540			PT_02 to PT_03	1.539	0.001		1	1	
PT_03 to PT_04	0.976			PT_03 to PT_04	0.974	0.002		2	2	**MEAN ERROR (MM)**
PT_01 to PT_04	1.530			PT_01 to PT_04	1.532	-0.002		-2	2	**6**
Anchor_02 to Anchor_03	0.734			Anchor_02 to Anchor_03	0.732	0.002		2	2	
Anchor_01 to PT_01	0.735			Anchor_01 to PT_01	0.742	-0.007		-7	7	
Anchor_01 to PT_02	0.908			Anchor_01 to PT_02	0.913	-0.005		-5	5	
Anchor_01 to PT_03	1.290			Anchor_01 to PT_03	1.278	0.012		12	12	
Anchor_01 to PT_04	1.060			Anchor_01 to PT_04	1.050	0.010		10	10	
BOX_32_01 to BOX_32_02	0.416			BOX_32_01 to BOX_32_02	0.427	-0.011		-11	11	
BOX_38_01 to BOX_38_02	0.416			BOX_38_01 to BOX_38_02	0.428	-0.012		-12	12	
Anchor_01 to BOX_32_01	0.466			Anchor_01 to BOX_32_01	0.465	0.001		1	1	
Anchor_01 to BOX_32_02	0.870			Anchor_01 to BOX_32_02	0.858	0.012		12	12	
Anchor_01 to BOX_38_01	0.631			Anchor_01 to BOX_38_01	0.626	0.005		5	5	
Anchor_01 to BOX_38_02	0.983			Anchor_01 to BOX_38_02	0.974	0.009		9	9	
Coordinates (Agisoft)	**X**	**Y**	**Z**	**ERROR**	**X**	**Y**	**Z**			
Anchor_01	2.4979	2.9891	0.8038	ANCHOR_01	-0.0027	-0.0053	0.0000			
Anchor_02	2.9736	2.8250	0.4281	ANCHOR_02	-0.0033	-0.0101	0.0043			
Anchor_03	2.7642	2.1202	0.4407	ANCHOR_03	-0.0015	0.0021	-0.0017			
PT_01	2.2568	3.5657	0.4183	PT_01	-0.0005	0.0014	-0.0007			
PT_02	3.1091	3.5362	0.4151	PT_02	0.0014	0.0031	-0.0015			
PT_03	3.2264	1.9972	0.4258	PT_03	0.0000	-0.0024	-0.0007			
PT_04	2.2518	2.0352	0.4251	PT_04	-0.0013	0.0037	0.0015			
BOX_32_01	2.4798	2.5278	0.7433	BOX_32_01	0.0001	-0.0010	0.0009			
BOX_32_02	2.3410	2.1360	0.7331	BOX_32_02	0.0022	0.0019	-0.0036			
BOX_38_01	3.0211	2.6426	0.7439	BOX_38_01	0.0008	0.0071	0.0002			
BOX_38_02	3.1334	2.2419	0.7363	BOX_38_02	0.0049	-0.0004	0.0012			
				ERROR	**X (+ve)**	**Y (+ve)**	**Z (+ve)**			
TS Coordinates	**X**	**Y**	**Z**	ANCHOR_01	0.0027	0.0053	0.0000			
ANCHOR_01	2.5006	2.9944	0.8038	ANCHOR_02	0.0033	0.0101	0.0043			
ANCHOR_02	2.9769	2.8351	0.4238	ANCHOR_03	0.0015	0.0021	0.0017			
ANCHOR_03	2.7657	2.1181	0.4424	PT_01	0.0005	0.0014	0.0007			
PT_01	2.2573	3.5643	0.4190	PT_02	0.0014	0.0031	0.0015			
PT_02	3.1077	3.5331	0.4166	PT_03	0.0000	0.0024	0.0007			
PT_03	3.2264	1.9996	0.4265	PT_04	0.0013	0.0037	0.0015			
PT_04	2.2531	2.0315	0.4236	BOX_32_01	0.0001	0.0010	0.0009			
BOX_32_01	2.4797	2.5288	0.7424	BOX_32_02	0.0022	0.0019	0.0036			**SUM ERROR (MM)**
BOX_32_02	2.3388	2.1341	0.7367	BOX_38_01	0.0008	0.0071	0.0002			**74**
BOX_38_01	3.0203	2.6355	0.7437	BOX_38_02	0.0049	0.0004	0.0012			
BOX_38_02	3.1285	2.2423	0.7351							**MEAN ERROR (MM)**
				ERROR (SUM)	0.0187	0.0386	0.0164	74	74	**2**

Appendix 5: MFV *Sanu* Exported Data

MFV_Sanu Output Data				
Number of Photographs	349			
Image Quality	Lowest	Lowest Aligned	Highest	
	0.440567	0.440567	0.919927	
Number Aligned	349			
Tie Points	213,694			
Dense Cloud	15,120,124			
3D Model	1,008,007			
		SUM ERROR (MM)	MEAN ERROR (MM)	
Scale Bar (1)		60	4	
Scale Bar (2)		52	4	
Enclosure		57	4	
CP (Measurements)		64	5	
CP (Coordinates)		64	2	
DP (Measurements)		66	5	
DP (Coordinates)		71	2	
DSM CP (Measurements)		61	4	
DSM CP (Coordinates)		313	10	
DSM DP (Measurements)		63	5	
DSM CP (Coordinates)		397	13	

ScaleBar_1								
Scaling								
ScaleBar_1_1 to ScaleBar_1_2	1.000							
Measurements			**Check Measurements**			**ERROR**	**ERROR (MM)**	**ERROR (MM) +ve**
ScaleBar_1_1	ScaleBar_1_2	1.000	ScaleBar_1_1	ScaleBar_1_2	1.000	0.000	0	0
ScaleBar_2_1	ScaleBar_2_2	0.987	ScaleBar_2_1	ScaleBar_2_2	0.986	0.001	1	1
PT_07	PT_08	3.470	PT_07	PT_08	3.464	0.006	6	6
PT_08	PT_09	1.810	PT_08	PT_09	1.804	0.006	6	6
PT_09	PT_10	3.440	PT_09	PT_10	3.435	0.005	5	5
PT_07	PT_10	1.870	PT_07	PT_10	1.873	-0.003	-3	3
PT_07	PT_02	1.700	PT_07	PT_02	1.690	0.010	10	10
PT_07	PT_04	1.250	PT_07	PT_04	1.253	-0.003	-3	3
PT_06	PT_05	1.890	PT_06	PT_05	1.891	-0.001	-1	1
PT_06	PT_09	1.020	PT_06	PT_09	1.016	0.004	4	4
Keel_1	Keel_2	0.329	Keel_1	Keel_2	0.330	-0.001	-1	1
U_Section_1	U_Section_2	0.579	U_Section_1	U_Section_2	0.568	0.011	11	11
S_Plank_02_Upper_1	S_Plank_02_Upper_2	1.190	S_Plank_02_Upper_1	S_Plank_02_Upper_2	1.193	-0.003	-3	3
S_Plank_03_Recess_1	S_Plank_03_Recess_2	0.118	S_Plank_03_Recess_1	S_Plank_03_Recess_2	0.112	0.006	6	6
~~Second_Section_1~~	~~Second_Section_2~~	~~0.651~~	~~Second_Section_1~~	~~Second_Section_2~~	~~0.716~~	~~-0.065~~	~~-65~~	~~65~~
							SUM ERROR (MM)	**60**
							MEAN ERROR (MM)	**4**

ScaleBar_1+2								
Scaling								
ScaleBar_1_1 to ScaleBar_1_	1.000							
ScaleBar_2_1 to ScaleBar_2_	0.986							
Measurements			**Check Measurements**			**ERROR**	**ERROR (MM)**	**ERROR (MM) +ve**
ScaleBar_1_1	ScaleBar_1_2	0.999	ScaleBar_1_1	ScaleBar_1_2	1.000	-0.001	-1	1
ScaleBar_2_1	ScaleBar_2_2	0.988	ScaleBar_2_1	ScaleBar_2_2	0.986	0.002	2	2
PT_07	PT_08	3.470	PT_07	PT_08	3.464	0.006	6	6
PT_08	PT_09	1.810	PT_08	PT_09	1.804	0.006	6	6
PT_09	PT_10	3.440	PT_09	PT_10	3.435	0.005	5	5
PT_07	PT_10	1.870	PT_07	PT_10	1.873	-0.003	-3	3
PT_07	PT_02	1.690	PT_07	PT_02	1.690	0.000	0	0
PT_07	PT_04	1.250	PT_07	PT_04	1.253	-0.003	-3	3
PT_06	PT_05	1.890	PT_06	PT_05	1.891	-0.001	-1	1
PT_06	PT_09	1.020	PT_06	PT_09	1.016	0.004	4	4
Keel_1	Keel_2	0.330	Keel_1	Keel_2	0.330	0.000	0	0
U_Section_1	U_Section_2	0.578	U_Section_1	U_Section_2	0.568	0.010	10	10
S_Plank_02_Upper_1	S_Plank_02_Upper_2	1.190	S_Plank_02_Upper_1	S_Plank_02_Upper_2	1.193	-0.003	-3	3
S_Plank_03_Recess_1	S_Plank_03_Recess_2	0.104	S_Plank_03_Recess_1	S_Plank_03_Recess_2	0.112	-0.008	-8	8
~~Second_Section_1~~	~~Second_Section_2~~	~~0.651~~	~~Second_Section_1~~	~~Second_Section_2~~	~~0.716~~	~~-0.065~~	~~-65~~	~~65~~
							SUM ERROR (MM)	**52**
							MEAN ERROR (MM)	**4**

Enclosure								
Scaling								
PT_07 to PT_08	3.464							
PT_07 to PT_10	1.873							
PT_08 to PT_09	1.804							
PT_09 to PT_10	3.435							
Measurements			**Check Measurements**			**ERROR**	**ERROR (MM)**	**ERROR (MM) +ve**
ScaleBar_1_1	ScaleBar_1_2	0.999	ScaleBar_1_1	ScaleBar_1_2	1.000	-0.001	-1	1
ScaleBar_2_1	ScaleBar_2_2	0.984	ScaleBar_2_1	ScaleBar_2_2	0.986	-0.002	-2	2
PT_07	PT_08	3.470	PT_07	PT_08	3.464	0.006	6	6
PT_08	PT_09	1.810	PT_08	PT_09	1.804	0.006	6	6
PT_09	PT_10	3.440	PT_09	PT_10	3.435	0.005	5	5
PT_07	PT_10	1.870	PT_07	PT_10	1.873	-0.003	-3	3
PT_07	PT_02	1.690	PT_07	PT_02	1.690	0.000	0	0
PT_07	PT_04	1.250	PT_07	PT_04	1.253	-0.003	-3	3
PT_06	PT_05	1.890	PT_06	PT_05	1.891	-0.001	-1	1
PT_06	PT_09	1.010	PT_06	PT_09	1.016	-0.006	-6	6
Keel_1	Keel_2	0.329	Keel_1	Keel_2	0.330	-0.001	-1	1
U_Section_1	U_Section_2	0.579	U_Section_1	U_Section_2	0.568	0.011	11	11
S_Plank_02_Upper_1	S_Plank_02_Upper_2	1.190	S_Plank_02_Upper_1	S_Plank_02_Upper_2	1.193	-0.003	-3	3
S_Plank_03_Recess_1	S_Plank_03_Recess_2	0.103	S_Plank_03_Recess_1	S_Plank_03_Recess_2	0.112	-0.009	-9	9
~~Second_Section_1~~	~~Second_Section_2~~	~~0.651~~	~~Second_Section_1~~	~~Second_Section_2~~	~~0.716~~	~~-0.065~~	~~-65~~	~~65~~
							SUM ERROR (MM)	**57**
							MEAN ERROR (MM)	**4**

Control Points									
									SUM ERROR (MM)
Scaling	**X**	**Y**	**Z**						64
PT_07	1.6370	0.5030	0.1371						
PT_08	1.8267	3.9618	0.1413						**MEAN ERROR (MM)**
PT_09	3.6279	3.8647	0.1389						5
PT_10	3.5090	0.4315	0.1266						
Measurements				**Check Measurements**			**ERROR**	**ERROR (MM)**	**ERROR (MM) +ve**
ScaleBar_1_1	ScaleBar_1_2	0.999		ScaleBar_1_1	ScaleBar_1_2	1.000	-0.001	-1	1
ScaleBar_2_1	ScaleBar_2_2	0.986		ScaleBar_2_1	ScaleBar_2_2	0.986	0.000	0	0
PT_07	PT_08	3.470		PT_07	PT_08	3.464	0.006	6	6
PT_08	PT_09	1.810		PT_08	PT_09	1.804	0.006	6	6
PT_09	PT_10	3.440		PT_09	PT_10	3.435	0.005	5	5
PT_07	PT_10	1.860		PT_07	PT_10	1.873	-0.013	-13	13
PT_07	PT_02	1.690		PT_07	PT_02	1.690	0.000	0	0
PT_07	PT_04	1.250		PT_07	PT_04	1.253	-0.003	-3	3
PT_06	PT_05	1.890		PT_06	PT_05	1.891	-0.001	-1	1
PT_06	PT_09	1.020		PT_06	PT_09	1.016	0.004	4	4
Keel_1	Keel_2	0.327		Keel_1	Keel_2	0.330	-0.003	-3	3
U_Section_1	U_Section_2	0.579		U_Section_1	U_Section_2	0.568	0.011	11	11
S_Plank_02_Upper_1	S_Plank_02_Upper_2	1.190		S_Plank_02_Upper_1	S_Plank_02_Uppe	1.193	-0.003	-3	3
S_Plank_03_Recess_1	S_Plank_03_Recess_2	0.104		S_Plank_03_Recess_1	S_Plank_03_Rece	0.112	-0.008	-8	8
~~Second_Section_1~~	~~Second_Section_2~~	~~0.651~~		~~Second_Section_1~~	~~Second_Section_2~~	~~0.716~~	~~-0.065~~	~~-65~~	~~65~~
Coordinates (Agisoft)	**X**	**Y**	**Z**	**ERROR**	**X**	**Y**	**Z**		
PT_01	2.027641	3.774743	0.414805	PT_01	-0.010959	-0.007357	-0.002295		
PT_02	2.645730	1.833487	0.413990	PT_02	-0.007870	-0.005013	-0.000210		
PT_03	2.808219	0.864958	0.239411	PT_03	0.001519	0.000758	-0.001189		
PT_04	2.892569	0.494899	0.202701	PT_04	-0.000031	-0.003601	-0.002499		
PT_05	2.902689	1.708015	0.358604	PT_05	0.000689	0.000115	0.000504		
PT_06	2.662299	3.581403	0.254870	PT_06	0.001499	0.000003	0.000370		
PT_07	1.641275	0.501225	0.136402	PT_07	0.004275	-0.001775	-0.000698		
PT_08	1.825622	3.962916	0.142000	PT_08	-0.001078	0.001116	0.000700		
PT_09	3.629361	3.865328	0.138197	PT_09	0.001461	0.000628	-0.000703		
PT_10	3.504342	0.431530	0.127302	PT_10	-0.004658	0.000030	0.000702		
				ERROR	**X (+ve)**	**Y (+ve)**	**Z (+ve)**		
TS Coordinates	**X**	**Y**	**Z**	PT_01	0.010959	0.007357	0.002295		
PT_01	2.0386	3.7821	0.4171	PT_02	0.007870	0.005013	0.000210		
PT_02	2.6536	1.8385	0.4142	PT_03	0.001519	0.000758	0.001189		
PT_03	2.8067	0.8642	0.2406	PT_04	0.000031	0.003601	0.002499		
PT_04	2.8926	0.4985	0.2052	PT_05	0.000689	0.000115	0.000504		**SUM ERROR (MM)**
PT_05	2.9020	1.7079	0.3581	PT_06	0.001499	0.000003	0.000370		64
PT_06	2.6608	3.5814	0.2545	PT_07	0.004275	0.001775	0.000698		
PT_07	1.6370	0.5030	0.1371	PT_08	0.001078	0.001116	0.000700		**MEAN ERROR (MM)**
PT_08	1.8267	3.9618	0.1413	PT_09	0.001461	0.000628	0.000703		2
PT_09	3.6279	3.8647	0.1389	PT_10	0.004658	0.000030	0.000702		
PT_10	3.5090	0.4315	0.1266						
				ERROR (SUM)	0.034039	0.020396	0.009870	64	64

Detail Points									
									SUM ERROR (MM)
Scaling	**X**	**Y**	**Z**						**66**
PT_01	2.0386	3.7821	0.4171						
PT_02	2.6536	1.8385	0.4142						**MEAN ERROR (MM)**
PT_03	2.8067	0.8642	0.2406						**5**
PT_04	2.8926	0.4985	0.2052						
PT_05	2.9020	1.7079	0.3581						
PT_06	2.6608	3.5814	0.2545						
PT_07	1.6370	0.5030	0.1371						
PT_08	1.8267	3.9618	0.1413						
PT_09	3.6279	3.8647	0.1389						
PT_10	3.5090	0.4315	0.1266						
Measurements				**Check Measurements**			**ERROR**	**ERROR (MM)**	**ERROR (MM) +ve**
ScaleBar_1_1	ScaleBar_1_2	0.998		ScaleBar_1_1	ScaleBar_1_2	1.000	-0.002	-2	2
ScaleBar_2_1	ScaleBar_2_2	0.986		ScaleBar_2_1	ScaleBar_2_2	0.986	0.000	0	0
PT_07	PT_08	3.470		PT_07	PT_08	3.464	0.006	6	6
PT_08	PT_09	1.810		PT_08	PT_09	1.804	0.006	6	6
PT_09	PT_10	3.440		PT_09	PT_10	3.435	0.005	5	5
PT_07	PT_10	1.860		PT_07	PT_10	1.873	-0.013	-13	13
PT_07	PT_02	1.690		PT_07	PT_02	1.690	0.000	0	0
PT_07	PT_04	1.250		PT_07	PT_04	1.253	-0.003	-3	3
PT_06	PT_05	1.890		PT_06	PT_05	1.891	-0.001	-1	1
PT_06	PT_09	1.010		PT_06	PT_09	1.016	-0.006	-6	6
Keel_1	Keel_2	0.327		Keel_1	Keel_2	0.330	-0.003	-3	3
U_Section_1	U_Section_2	0.578		U_Section_1	U_Section_2	0.568	0.010	10	10
S_Plank_02_Upper_1	S_Plank_02_Upper_2	1.190		S_Plank_02_Upper_1	S_Plank_02_Upper_2	1.193	-0.003	-3	3
S_Plank_03_Recess_1	S_Plank_03_Recess_2	0.104		S_Plank_03_Recess_1	S_Plank_03_Recess_2	0.112	-0.008	-8	8
~~Second_Section_1~~	~~Second_Section_2~~	~~0.651~~		~~Second_Section_1~~	~~Second_Section_2~~	~~0.716~~	~~-0.065~~	~~-65~~	~~65~~
Coordinates (Agisoft)	**X**	**Y**	**Z**	**ERROR**	**X**	**Y**	**Z**		
PT_01	2.030663	3.776725	0.415543	PT_01	-0.007937	-0.005375	-0.001557		
PT_02	2.647206	1.835055	0.414590	PT_02	-0.006394	-0.003445	0.000390		
PT_03	2.808755	0.866390	0.240094	PT_03	0.002055	0.002190	-0.000506		
PT_04	2.892775	0.496270	0.203393	PT_04	0.000175	-0.002230	-0.001807		
PT_05	2.904002	1.709372	0.358981	PT_05	0.002002	0.001472	0.000881		
PT_06	2.664986	3.582855	0.255028	PT_06	0.004186	0.001455	0.000528		
PT_07	1.641466	0.503561	0.138344	PT_07	0.004466	0.000561	0.001244		
PT_08	1.828527	3.964983	0.142904	PT_08	0.001827	0.003183	0.001604		
PT_09	3.632119	3.865983	0.137323	PT_09	0.004219	0.001283	-0.001577		
PT_10	3.504400	0.432405	0.127401	PT_10	-0.004600	0.000905	0.000801		
				ERROR	**X (+ve)**	**Y (+ve)**	**Z (+ve)**		
TS Coordinates	**X**	**Y**	**Z**	PT_01	0.007937	0.005375	0.001557		
PT_01	2.0386	3.7821	0.4171	PT_02	0.006394	0.003445	0.000390		
PT_02	2.6536	1.8385	0.4142	PT_03	0.002055	0.002190	0.000506		
PT_03	2.8067	0.8642	0.2406	PT_04	0.000175	0.002230	0.001807		
PT_04	2.8926	0.4985	0.2052	PT_05	0.002002	0.001472	0.000881		**SUM ERROR (MM)**
PT_05	2.9020	1.7079	0.3581	PT_06	0.004186	0.001455	0.000528		**71**
PT_06	2.6608	3.5814	0.2545	PT_07	0.004466	0.000561	0.001244		
PT_07	1.6370	0.5030	0.1371	PT_08	0.001827	0.003183	0.001604		**MEAN ERROR (MM)**
PT_08	1.8267	3.9618	0.1413	PT_09	0.004219	0.001283	0.001577		**2**
PT_09	3.6279	3.8647	0.1389	PT_10	0.004600	0.000905	0.000801		
PT_10	3.5090	0.4315	0.1266						
				ERROR (SUM)	0.037861	0.022099	0.010895	71	71

DSM Control Points									
									SUM ERROR (MM)
Scaling	**X**	**Y**	**Z**						**61**
PT_07	1.660	0.496	0.137						
PT_08	1.840	3.951	0.145						**MEAN ERROR (MM)**
PT_09	3.638	3.856	0.148						**4**
PT_10	3.509	0.410	0.150						
Measurements				**Check Measurements**			**ERROR**	**ERROR (MM)**	**ERROR (MM) +ve**
ScaleBar_1_1	ScaleBar_1_2	1.000		ScaleBar_1_1	ScaleBar_1_2	1.000	0.000	0	0
ScaleBar_2_1	ScaleBar_2_2	0.986		ScaleBar_2_1	ScaleBar_2_2	0.986	0.000	0	0
PT_07	PT_08	3.460		PT_07	PT_08	3.464	-0.004	-4	4
PT_08	PT_09	1.800		PT_08	PT_09	1.804	-0.004	-4	4
PT_09	PT_10	3.440		PT_09	PT_10	3.435	0.005	5	5
PT_07	PT_10	1.860		PT_07	PT_10	1.873	-0.013	-13	13
PT_07	PT_02	1.690		PT_07	PT_02	1.690	0.000	0	0
PT_07	PT_04	1.250		PT_07	PT_04	1.253	-0.003	-3	3
PT_06	PT_05	1.890		PT_06	PT_05	1.891	-0.001	-1	1
PT_06	PT_09	1.010		PT_06	PT_09	1.016	-0.006	-6	6
Keel_1	Keel_2	0.327		Keel_1	Keel_2	0.330	-0.003	-3	3
U_Section_1	U_Section_2	0.578		U_Section_1	U_Section_2	0.568	0.010	10	10
S_Plank_02_Upper_1	S_Plank_02_Upper_2	1.190		S_Plank_02_Upper_1	S_Plank_02_Upper_2	1.193	-0.003	-3	3
S_Plank_03_Recess_1	S_Plank_03_Recess_2	0.103		S_Plank_03_Recess_1	S_Plank_03_Recess_2	0.112	-0.009	-9	9
~~Second_Section_1~~	~~Second_Section_2~~	~~0.649~~		~~Second_Section_1~~	~~Second_Section_2~~	~~0.716~~	~~-0.067~~	~~-67~~	~~67~~
Coordinates (Agisoft)	**X**	**Y**	**Z**	**ERROR**	**X**	**Y**	**Z**		
PT_01	2.038737	3.762904	0.415809	PT_01	0.000137	-0.019196	-0.001291		
PT_02	2.654842	1.822207	0.423483	PT_02	0.001242	-0.016293	0.009283		
PT_03	2.817799	0.853752	0.252091	PT_03	0.011099	-0.010448	0.011491		
PT_04	2.902079	0.483759	0.216757	PT_04	0.009479	-0.014741	0.011557		
PT_05	2.911983	1.696489	0.370388	PT_05	0.009983	-0.011411	0.012288		
PT_06	2.674124	3.568848	0.261329	PT_06	0.013324	-0.012552	0.006829		
PT_07	1.652039	0.490991	0.140624	PT_07	0.015039	-0.012009	0.003524		
PT_08	1.839143	3.950630	0.141220	PT_08	0.012443	-0.011170	-0.000080		
PT_09	3.641782	3.851600	0.151815	PT_09	0.013882	-0.013100	0.012915		
PT_10	3.514037	0.419779	0.146341	PT_10	0.005037	-0.011721	0.019741		
				ERROR	**X (+ve)**	**Y (+ve)**	**Z (+ve)**		
TS Coordinates	**X**	**Y**	**Z**	PT_01	0.000137	0.019196	0.001291		
PT_01	2.0386	3.7821	0.4171	PT_02	0.001242	0.016293	0.009283		
PT_02	2.6536	1.8385	0.4142	PT_03	0.011099	0.010448	0.011491		
PT_03	2.8067	0.8642	0.2406	PT_04	0.009479	0.014741	0.011557		
PT_04	2.8926	0.4985	0.2052	PT_05	0.009983	0.011411	0.012288		**SUM ERROR (MM)**
PT_05	2.9020	1.7079	0.3581	PT_06	0.013324	0.012552	0.006829		**313**
PT_06	2.6608	3.5814	0.2545	PT_07	0.015039	0.012009	0.003524		
PT_07	1.6370	0.5030	0.1371	PT_08	0.012443	0.011170	0.000080		**MEAN ERROR (MM)**
PT_08	1.8267	3.9618	0.1413	PT_09	0.013882	0.013100	0.012915		**10**
PT_09	3.6279	3.8647	0.1389	PT_10	0.005037	0.011721	0.019741		
PT_10	3.5090	0.4315	0.1266						
				ERROR (SUM)	0.091665	0.132641	0.088999	313	313

DSM Detail Points									
									SUM ERROR (MM)
Scaling	**X**	**Y**	**Z**						**63**
PT_01	2.041	3.774	0.431						
PT_02	2.663	1.834	0.460						**MEAN ERROR (MM)**
PT_03	2.826	0.851	0.265						**5**
PT_04	2.918	0.513	0.230						
PT_05	2.918	1.699	0.384						
PT_06	2.669	3.567	0.271						
PT_07	1.660	0.496	0.137						
PT_08	1.840	3.951	0.145						
PT_09	3.638	3.856	0.148						
PT_10	3.509	0.410	0.150						
Measurements				**Check Measurements**			**ERROR**	**ERROR (MM)**	**ERROR (MM) +ve**
ScaleBar_1_1	ScaleBar_1_2	0.998		ScaleBar_1_1	ScaleBar_1_2	1.000	-0.002	-2	2
ScaleBar_2_1	ScaleBar_2_2	0.985		ScaleBar_2_1	ScaleBar_2_2	0.986	-0.001	-1	1
PT_07	PT_08	3.460		PT_07	PT_08	3.464	-0.004	-4	4
PT_08	PT_09	1.800		PT_08	PT_09	1.804	-0.004	-4	4
PT_09	PT_10	3.430		PT_09	PT_10	3.435	-0.005	-5	5
PT_07	PT_10	1.860		PT_07	PT_10	1.873	-0.013	-13	13
PT_07	PT_02	1.690		PT_07	PT_02	1.690	0.000	0	0
PT_07	PT_04	1.250		PT_07	PT_04	1.253	-0.003	-3	3
PT_06	PT_05	1.890		PT_06	PT_05	1.891	-0.001	-1	1
PT_06	PT_09	1.010		PT_06	PT_09	1.016	-0.006	-6	6
Keel_1	Keel_2	0.328		Keel_1	Keel_2	0.330	-0.002	-2	2
U_Section_1	U_Section_2	0.578		U_Section_1	U_Section_2	0.568	0.010	10	10
S_Plank_02_Upper_1	S_Plank_02_Upper_2	1.190		S_Plank_02_Upper_1	S_Plank_02_Upper_2	1.193	-0.003	-3	3
S_Plank_03_Recess_1	S_Plank_03_Recess_2	0.103		S_Plank_03_Recess_1	S_Plank_03_Recess_2	0.112	-0.009	-9	9
~~Second_Section_1~~	~~Second_Section_2~~	~~0.648~~		~~Second_Section_1~~	~~Second_Section_2~~	~~0.716~~	~~-0.068~~	~~-68~~	68
Coordinates (Agisoft)	**X**	**Y**	**Z**	**ERROR**	**X**	**Y**	**Z**		
PT_01	2.039931	3.765816	0.425173	PT_01	0.001331	-0.016284	0.008073		
PT_02	2.659064	1.827514	0.433712	PT_02	0.005464	-0.010986	0.019512		
PT_03	2.823426	0.859855	0.263036	PT_03	0.016726	-0.004345	0.022436		
PT_04	2.908262	0.490230	0.227929	PT_04	0.015662	-0.008270	0.022729		
PT_05	2.916193	1.702290	0.380459	PT_05	0.014193	-0.005610	0.022359		
PT_06	2.675058	3.572886	0.270222	PT_06	0.014258	-0.008514	0.015722		
PT_07	1.658960	0.495185	0.153281	PT_07	0.021960	-0.007815	0.016181		
PT_08	1.839823	3.952839	0.150845	PT_08	0.013123	-0.008961	0.009545		
PT_09	3.641441	3.857069	0.159436	PT_09	0.013541	-0.007631	0.020536		
PT_10	3.519842	0.427316	0.156907	PT_10	0.010842	-0.004184	0.030307		
				ERROR	**X (+ve)**	**Y (+ve)**	**Z (+ve)**		
TS Coordinates	**X**	**Y**	**Z**	PT_01	0.001331	0.016284	0.008073		
PT_01	2.0386	3.7821	0.4171	PT_02	0.005464	0.010986	0.019512		
PT_02	2.6536	1.8385	0.4142	PT_03	0.016726	0.004345	0.022436		
PT_03	2.8067	0.8642	0.2406	PT_04	0.015662	0.008270	0.022729		
PT_04	2.8926	0.4985	0.2052	PT_05	0.014193	0.005610	0.022359		**SUM ERROR (MM)**
PT_05	2.9020	1.7079	0.3581	PT_06	0.014258	0.008514	0.015722		**397**
PT_06	2.6608	3.5814	0.2545	PT_07	0.021960	0.007815	0.016181		
PT_07	1.6370	0.5030	0.1371	PT_08	0.013123	0.008961	0.009545		**MEAN ERROR (MM)**
PT_08	1.8267	3.9618	0.1413	PT_09	0.013541	0.007631	0.020536		**13**
PT_09	3.6279	3.8647	0.1389	PT_10	0.010842	0.004184	0.030307		
PT_10	3.5090	0.4315	0.1266						
				ERROR (SUM)	0.127100	0.082600	0.187400	397	397

Appendix 6: *PhotoScan* Report: Anchor (Scale-Bar)

Anchor_ScaleBar

Processing Report

24 February 2019

Survey Data

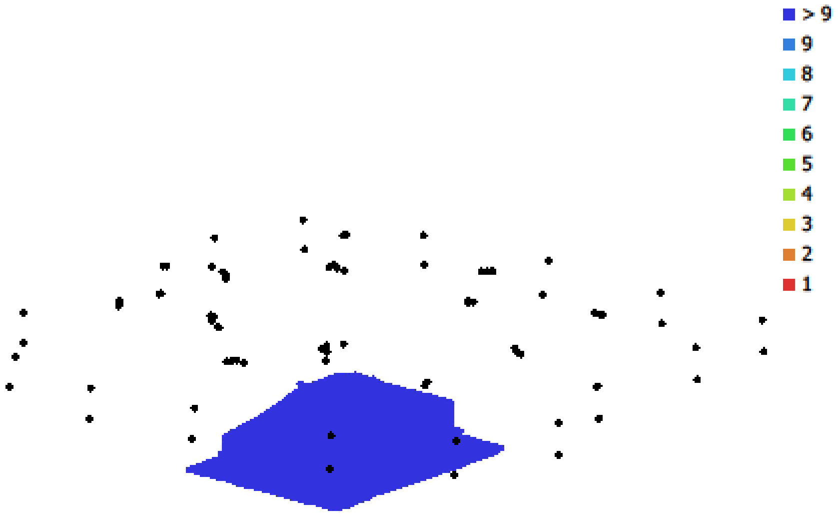

Fig. 1. Camera locations and image overlap.

Number of images:	82	Camera stations:	81
		Tie points:	106,924
		Projections:	255,311
		Reprojection error:	0.805 pix

Camera Model	Resolution	Focal Length	Pixel Size	Precalibrated
Canon EOS 50D (28mm)	4752 x 3168	28 mm	4.78 x 4.78 μm	No
Canon EOS 50D (32mm)	4752 x 3168	32 mm	4.78 x 4.78 μm	No
Canon EOS 50D (35mm)	4752 x 3168	35 mm	4.78 x 4.78 μm	No

Table 1. Cameras.

Page 2

Camera Calibration

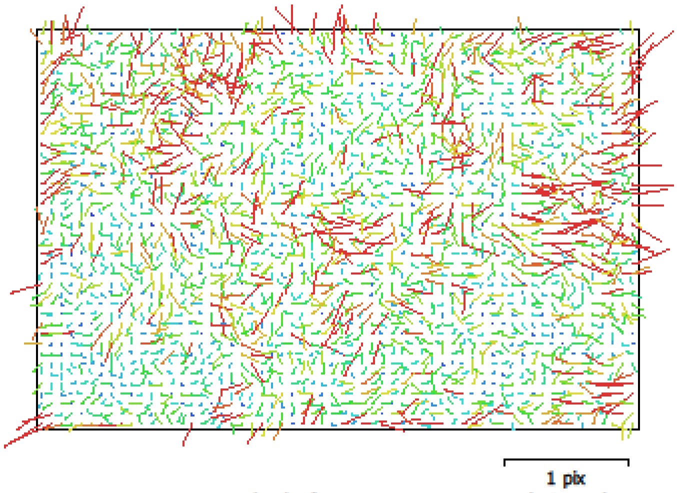

Fig. 2. Image residuals for Canon EOS 50D (28mm).

Canon EOS 50D (28mm)
72 images

Type	Resolution	Focal Length	Pixel Size
Frame	**4752 x 3168**	**28 mm**	**4.78 x 4.78 µm**

	Value	Error	F	Cx	Cy	B1	B2	K1	K2	P1	P2
F	6112.75	0.27	1.00	0.08	-0.09	0.01	-0.05	-0.07	0.15	0.04	-0.03
Cx	57.8902	0.47		1.00	-0.07	0.19	-0.14	-0.05	0.05	0.85	0.07
Cy	38.0324	0.42			1.00	-0.01	0.24	0.05	-0.04	-0.11	0.64
B1	2.20486	0.079				1.00	-0.03	-0.04	0.05	0.24	0.05
B2	0.406843	0.07					1.00	-0.01	0.00	-0.22	0.24
K1	-0.151905	0.00016						1.00	-0.94	-0.06	0.01
K2	0.106627	0.00065							1.00	0.08	-0.04
P1	0.00300403	1.6e-05								1.00	0.07
P2	0.000221751	1.4e-05									1.00

Table 2. Calibration coefficients and correlation matrix.

Page 3

Camera Calibration

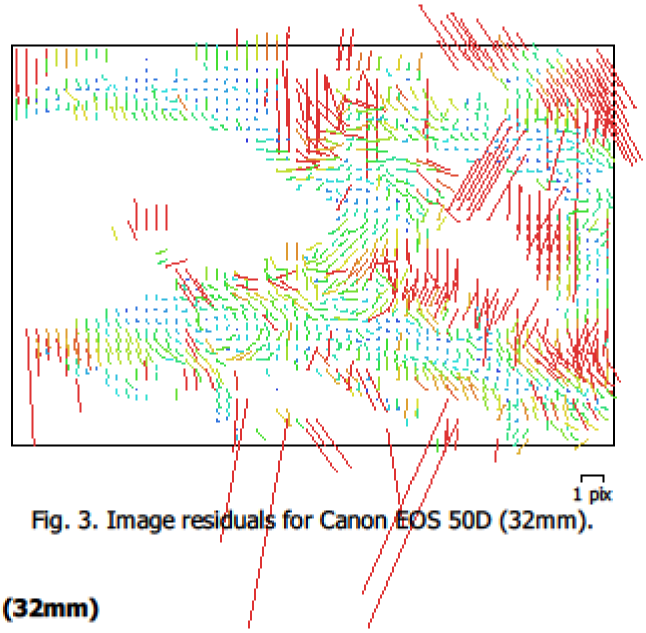

Fig. 3. Image residuals for Canon EOS 50D (32mm).

Canon EOS 50D (32mm)
3 images

Type	Resolution	Focal Length	Pixel Size
Frame	**4752 x 3168**	**32 mm**	**4.78 x 4.78 µm**

	Value	Error	B1	B2	K1	P1	P2
F	**6691**						
B1	**-23.2352**	0.36	1.00	0.39	0.05	-0.16	0.30
B2	**-7.27174**	0.4		1.00	0.11	-0.34	-0.20
K1	**-0.10389**	0.00022			1.00	-0.34	-0.19
P1	**0.00681563**	4.3e-05				1.00	0.47
P2	**0.00585931**	4.6e-05					1.00

Table 3. Calibration coefficients and correlation matrix.

Page 4

Camera Calibration

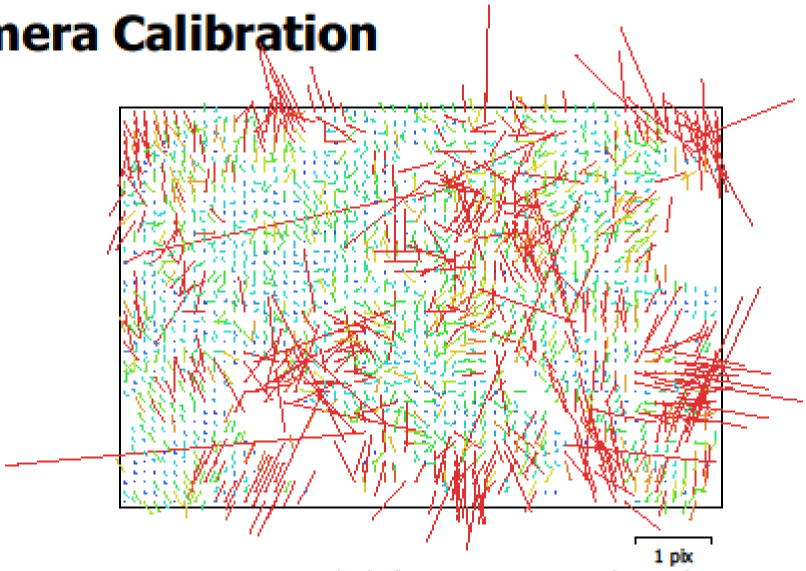

Fig. 4. Image residuals for Canon EOS 50D (35mm).

Canon EOS 50D (35mm)
7 images

Type	Resolution	Focal Length	Pixel Size
Frame	**4752 x 3168**	**35 mm**	**4.78 x 4.78 µm**

	Value	Error	B1	K1	P1	P2
F	7318.28					
B1	14.7033	0.56	1.00	-0.01	-0.03	0.37
K1	-0.0560273	0.00029		1.00	0.30	-0.09
P1	0.00198479	5e-05			1.00	-0.31
P2	-0.00151882	5.2e-05				1.00

Table 4. Calibration coefficients and correlation matrix.

Digital Elevation Model

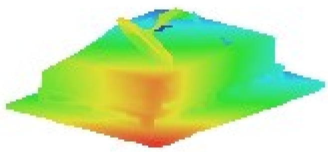

Fig. 5. Reconstructed digital elevation model.

Page 6

Processing Parameters

General	
Cameras	82
Aligned cameras	81
Markers	9
Coordinate system	Local Coordinates (m)
Rotation angles	Yaw, Pitch, Roll
Point Cloud	
Points	106,924 of 123,800
RMS reprojection error	0.185367 (0.804608 pix)
Max reprojection error	0.590333 (16.8737 pix)
Mean key point size	4.11019 pix
Point colors	3 bands, uint8
Key points	No
Average tie point multiplicity	2.52524
Alignment parameters	
Accuracy	High
Generic preselection	Yes
Key point limit	40,000
Tie point limit	4,000
Adaptive camera model fitting	Yes
Matching time	36 minutes 58 seconds
Alignment time	7 minutes 31 seconds
Dense Point Cloud	
Points	4,864,278
Point colors	3 bands, uint8
Reconstruction parameters	
Quality	Medium
Depth filtering	Aggressive
Depth maps generation time	1 hours 37 minutes
Dense cloud generation time	3 hours 4 minutes
Model	
Faces	324,285
Vertices	163,123
Vertex colors	3 bands, uint8
Texture	4,096 x 4,096, 4 bands, uint8
Reconstruction parameters	
Surface type	Arbitrary
Source data	Dense
Interpolation	Enabled
Quality	Medium
Depth filtering	Aggressive
Face count	324,285
Processing time	3 minutes 24 seconds
Texturing parameters	
Mapping mode	Generic
Blending mode	Mosaic
Texture size	4,096 x 4,096
Enable hole filling	Yes
Enable ghosting filter	Yes
UV mapping time	49 seconds
Blending time	7 minutes 53 seconds
Software	
Version	1.4.5 build 7354
Platform	Windows 64

Page 7

Appendix 7: *PhotoScan* Report: Anchor (Box)

Anchor_Boxes

Processing Report

24 February 2019

Survey Data

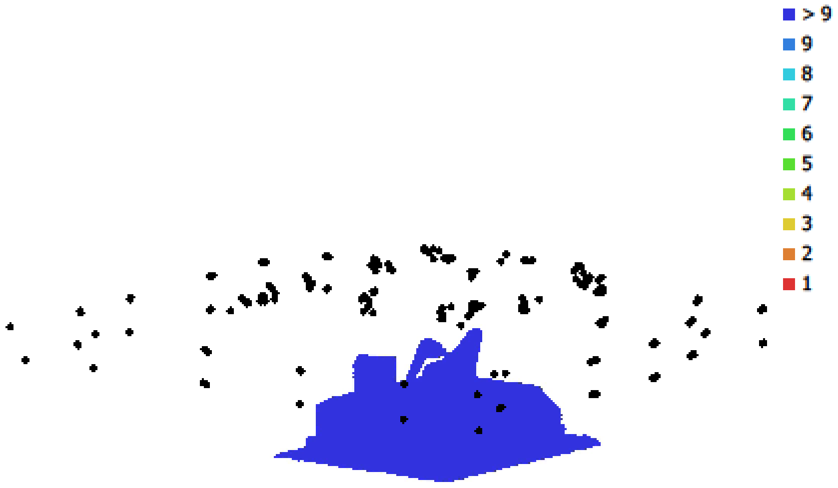

Fig. 1. Camera locations and image overlap.

Number of images:	184	Camera stations:	184
		Tie points:	199,913
		Projections:	567,680
		Reprojection error:	1.01 pix

Camera Model	Resolution	Focal Length	Pixel Size	Precalibrated
Canon EOS 50D (28mm)	4752 x 3168	28 mm	4.78 x 4.78 μm	No
Canon EOS 50D (32mm)	4752 x 3168	32 mm	4.78 x 4.78 μm	No

Table 1. Cameras.

Camera Calibration

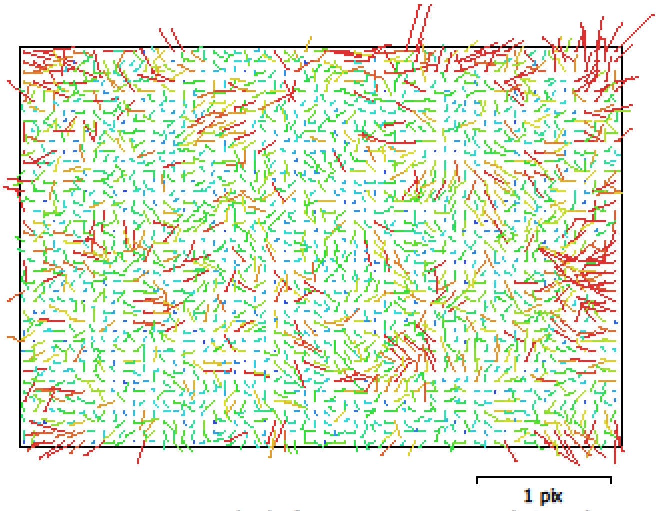

Fig. 2. Image residuals for Canon EOS 50D (28mm).

Canon EOS 50D (28mm)
141 images

Type	Resolution	Focal Length	Pixel Size
Frame	**4752 x 3168**	**28 mm**	**4.78 x 4.78 µm**

	Value	Error	F	Cx	Cy	B1	B2	K1	K2	K3	P1	P2
F	**6063.32**	0.21	1.00	0.03	-0.12	-0.17	-0.01	-0.15	0.18	-0.17	0.05	-0.13
Cx	**51.0713**	0.31		1.00	-0.02	0.06	0.04	0.00	0.00	0.00	0.84	-0.03
Cy	**28.5347**	0.27			1.00	0.02	-0.02	-0.02	0.02	-0.03	-0.02	0.67
B1	**2.14579**	0.057				1.00	-0.04	0.02	-0.02	0.03	0.06	0.11
B2	**-1.25299**	0.052					1.00	-0.03	0.03	-0.04	-0.09	-0.01
K1	**-0.166891**	0.00024						1.00	-0.97	0.92	0.01	0.01
K2	**0.232907**	0.0024							1.00	-0.98	-0.02	-0.02
K3	**-0.382788**	0.0071								1.00	0.03	0.01
P1	**0.00267613**	8.8e-06									1.00	-0.02
P2	**-0.000269744**	7.3e-06										1.00

Table 2. Calibration coefficients and correlation matrix.

Page 3

Camera Calibration

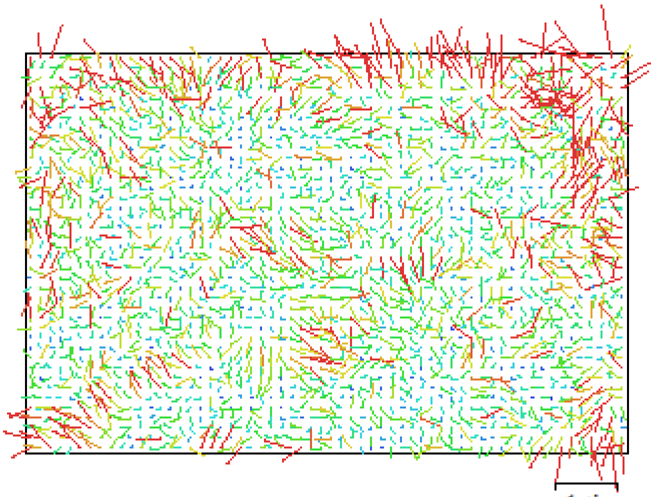

Fig. 3. Image residuals for Canon EOS 50D (32mm).

Canon EOS 50D (32mm)
43 images

Type	Resolution	Focal Length	Pixel Size
Frame	**4752 x 3168**	**32 mm**	**4.78 x 4.78 µm**

	Value	Error	F	B1	B2	K1	K2	P1	P2
F	**6545.05**	0.34	1.00	-0.23	-0.11	-0.10	0.17	-0.03	0.05
B1	**-5.81995**	0.11		1.00	-0.07	-0.08	0.06	0.02	0.10
B2	**-3.46465**	0.11			1.00	-0.01	-0.00	-0.27	0.03
K1	**-0.128279**	0.00024				1.00	-0.96	0.01	-0.00
K2	**0.142838**	0.0013					1.00	-0.02	-0.07
P1	**0.001388**	9.7e-06						1.00	0.01
P2	**-0.0018057**	1.1e-05							1.00

Table 3. Calibration coefficients and correlation matrix.

Page 4

Digital Elevation Model

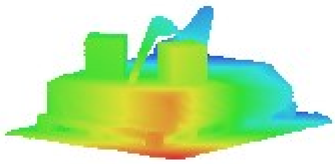

Fig. 4. Reconstructed digital elevation model.

Page 5

Processing Parameters

General	
Cameras	184
Aligned cameras	184
Markers	11
Coordinate system	Local Coordinates (m)
Rotation angles	Yaw, Pitch, Roll
Point Cloud	
Points	199,913 of 239,001
RMS reprojection error	0.2407 (1.00929 pix)
Max reprojection error	0.773658 (32.9923 pix)
Mean key point size	4.01682 pix
Point colors	3 bands, uint8
Key points	No
Average tie point multiplicity	3.08147
Alignment parameters	
Accuracy	High
Generic preselection	Yes
Key point limit	40,000
Tie point limit	4,000
Adaptive camera model fitting	Yes
Matching time	6 minutes 5 seconds
Alignment time	3 minutes 33 seconds
Dense Point Cloud	
Points	9,435,319
Point colors	3 bands, uint8
Reconstruction parameters	
Quality	Medium
Depth filtering	Aggressive
Depth maps generation time	7 minutes 41 seconds
Dense cloud generation time	34 minutes 52 seconds
Model	
Faces	628,874
Vertices	315,705
Vertex colors	3 bands, uint8
Texture	4,096 x 4,096, 4 bands, uint8
Reconstruction parameters	
Surface type	Arbitrary
Source data	Dense
Interpolation	Enabled
Quality	Medium
Depth filtering	Aggressive
Face count	629,105
Processing time	5 minutes 46 seconds
Texturing parameters	
Mapping mode	Generic
Blending mode	Mosaic
Texture size	4,096 x 4,096
Enable hole filling	Yes
Enable ghosting filter	Yes
UV mapping time	40 seconds
Blending time	9 minutes 45 seconds
Software	
Version	1.4.5 build 7354
Platform	Windows 64

Page 6

Appendix 8: *PhotoScan* Report: MFV *Sanu*

MFV_Sanu

Processing Report
24 February 2019

Survey Data

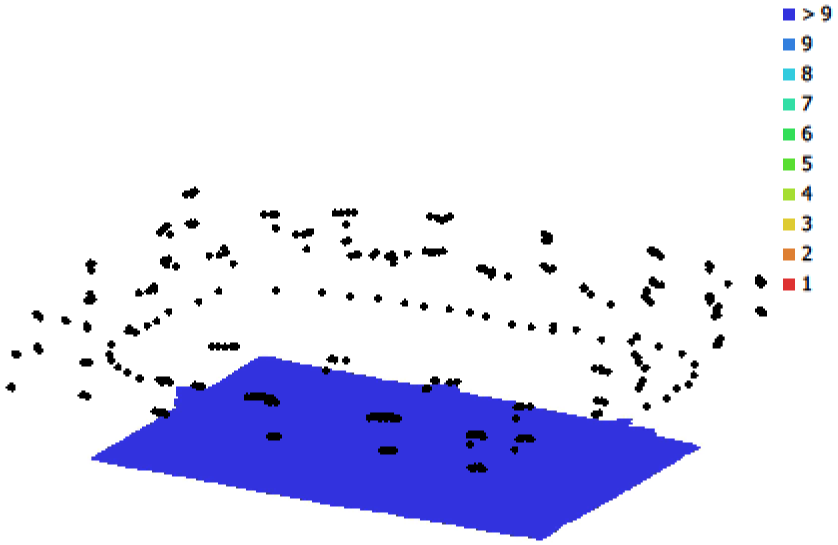

Fig. 1. Camera locations and image overlap.

Number of images:	349	Camera stations:	349
		Tie points:	213,694
		Projections:	891,154
		Reprojection error:	1.32 pix

Camera Model	Resolution	Focal Length	Pixel Size	Precalibrated
Canon EOS 50D (28mm)	4752 x 3168	28 mm	4.78 x 4.78 μm	No
Canon EOS 50D (32mm)	4752 x 3168	32 mm	4.78 x 4.78 μm	No
Canon EOS 50D (40mm)	4752 x 3168	40 mm	4.78 x 4.78 μm	No

Table 1. Cameras.

Page 2

Camera Calibration

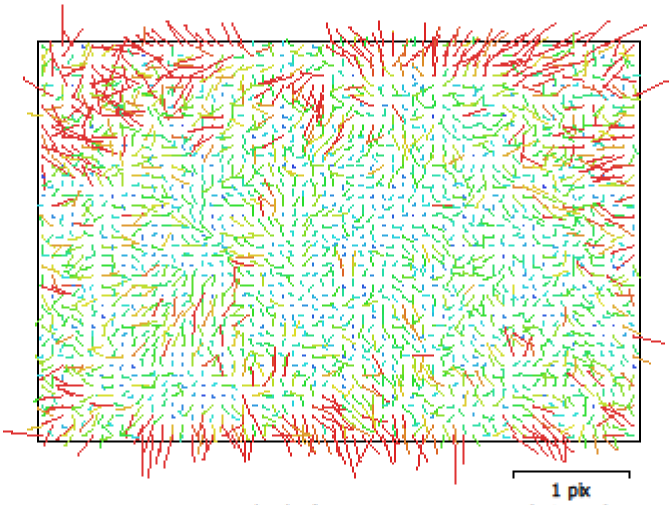

Fig. 2. Image residuals for Canon EOS 50D (28mm).

Canon EOS 50D (28mm)
242 images

Type	Resolution	Focal Length	Pixel Size
Frame	**4752 x 3168**	**28 mm**	**4.78 x 4.78 μm**

	Value	Error	F	Cx	Cy	B1	B2	K1	K2	K3	P1	P2
F	6099.59	0.14	1.00	0.08	-0.30	-0.25	-0.02	-0.16	0.17	-0.15	0.08	-0.12
Cx	62.987	0.29		1.00	-0.02	0.04	0.02	0.01	-0.00	0.01	0.89	-0.05
Cy	40.9085	0.24			1.00	-0.11	0.04	-0.03	0.02	-0.02	-0.04	0.57
B1	2.33029	0.048				1.00	0.03	-0.01	-0.01	0.01	0.03	0.21
B2	-1.28855	0.048					1.00	0.01	-0.01	0.01	-0.16	0.01
K1	-0.162382	0.00018						1.00	-0.97	0.91	0.01	-0.03
K2	0.225839	0.0019							1.00	-0.98	-0.01	0.01
K3	-0.367667	0.0059								1.00	0.02	-0.01
P1	0.00262811	8.3e-06									1.00	-0.03
P2	-0.000452937	6.3e-06										1.00

Table 2. Calibration coefficients and correlation matrix.

Page 3

Camera Calibration

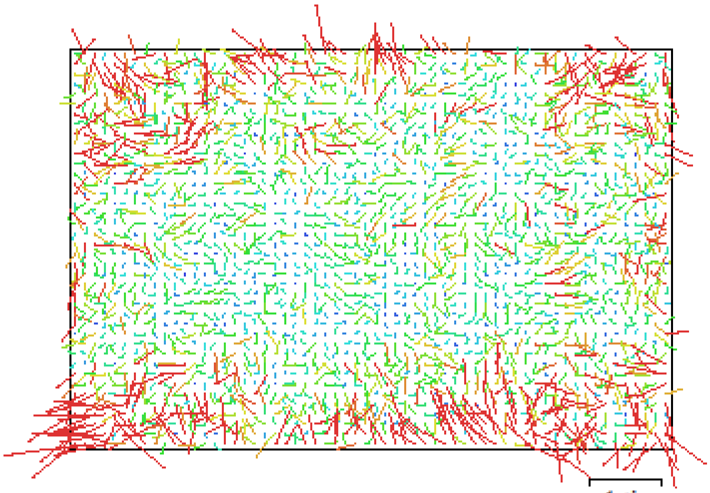

Fig. 3. Image residuals for Canon EOS 50D (32mm).

Canon EOS 50D (32mm)
97 images

Type	Resolution	Focal Length	Pixel Size
Frame	**4752 x 3168**	**32 mm**	**4.78 x 4.78 µm**

	Value	**Error**	**F**	**Cx**	**Cy**	**B1**	**B2**	**K1**	**K2**	**P1**	**P2**
F	**6712**	0.2	1.00	0.09	-0.24	-0.20	-0.00	-0.14	0.15	0.07	-0.03
Cx	**57.6227**	0.45		1.00	-0.04	0.09	0.02	0.05	-0.05	0.93	-0.05
Cy	**45.8965**	0.33			1.00	-0.06	0.01	-0.01	0.01	-0.04	0.65
B1	**3.76427**	0.062				1.00	0.02	-0.05	0.03	0.10	0.03
B2	**-1.64458**	0.062					1.00	0.01	-0.00	-0.06	0.10
K1	**-0.114876**	0.00017						1.00	-0.96	0.03	-0.01
K2	**0.148281**	0.001							1.00	-0.02	0.00
P1	**0.00304867**	1.6e-05								1.00	-0.06
P2	**-0.000452709**	1.1e-05									1.00

Table 3. Calibration coefficients and correlation matrix.

Page 4

Camera Calibration

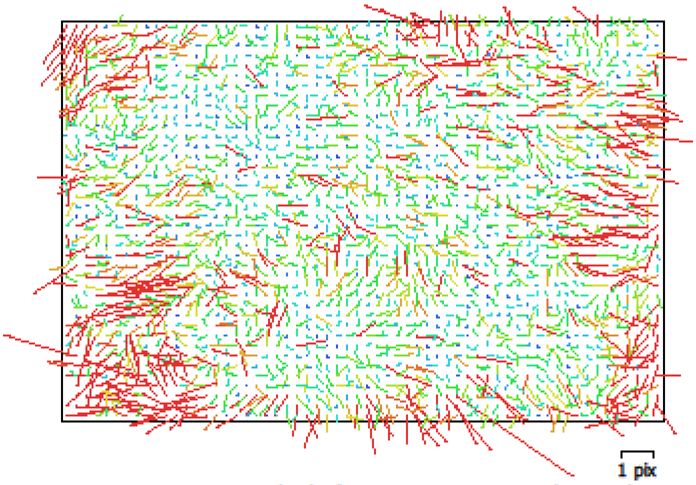

Fig. 4. Image residuals for Canon EOS 50D (40mm).

Canon EOS 50D (40mm)
10 images

Type	Resolution	Focal Length	Pixel Size
Frame	**4752 x 3168**	**40 mm**	**4.78 x 4.78 µm**

	Value	Error	F	B1	B2	K1	P1	P2
F	8903.89	0.71	1.00	-0.34	0.25	0.16	0.27	0.21
B1	0.544269	0.21		1.00	0.03	-0.13	-0.15	0.02
B2	-2.03798	0.24			1.00	-0.12	-0.20	-0.18
K1	0.0447888	0.0002				1.00	-0.02	0.11
P1	0.00130995	2.1e-05					1.00	0.14
P2	-0.00272876	2.5e-05						1.00

Table 4. Calibration coefficients and correlation matrix.

Digital Elevation Model

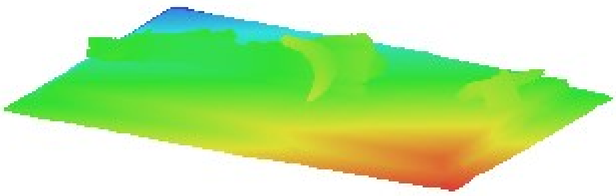

Fig. 5. Reconstructed digital elevation model.

Processing Parameters

General	
Cameras	349
Aligned cameras	349
Markers	24
Coordinate system	Local Coordinates (m)
Rotation angles	Yaw, Pitch, Roll
Point Cloud	
Points	213,694 of 284,945
RMS reprojection error	0.287652 (1.32397 pix)
Max reprojection error	0.931456 (49.4037 pix)
Mean key point size	4.31593 pix
Point colors	3 bands, uint8
Key points	No
Average tie point multiplicity	5.48681
Alignment parameters	
Accuracy	High
Generic preselection	Yes
Key point limit	40,000
Tie point limit	4,000
Adaptive camera model fitting	Yes
Matching time	25 minutes 3 seconds
Alignment time	9 minutes 5 seconds
Dense Point Cloud	
Points	15,120,124
Point colors	3 bands, uint8
Reconstruction parameters	
Quality	Medium
Depth filtering	Aggressive
Depth maps generation time	48 minutes 14 seconds
Dense cloud generation time	3 hours 34 minutes
Model	
Faces	1,008,007
Vertices	505,472
Vertex colors	3 bands, uint8
Texture	4,096 x 4,096, 4 bands, uint8
Reconstruction parameters	
Surface type	Arbitrary
Source data	Dense
Interpolation	Enabled
Quality	Medium
Depth filtering	Aggressive
Face count	1,008,008
Processing time	8 minutes 58 seconds
Texturing parameters	
Mapping mode	Generic
Blending mode	Mosaic
Texture size	4,096 x 4,096
Enable hole filling	Yes
Enable ghosting filter	Yes
UV mapping time	42 seconds
Blending time	15 minutes 29 seconds
Software	
Version	1.4.5 build 7354
Platform	Windows 64

Page 7

Appendix 9: TotalStation Raw Data

ANCHOR_TS_MASTER

PtID	East	North	Height
JOB_1			
TS_01	2.1536	0.4812	-0.0077
PT_01	2.2547	3.5601	0.4172
PT_02	3.1055	3.5307	0.4149
PT_03	3.2236	1.9963	0.4246
PT_04	2.2500	2.0286	0.4224
ANCHOR_01	2.4958	2.9749	0.8051
ANCHOR_02	2.9674	2.8237	0.4262
ANCHOR_03	2.7658	2.1203	0.4295
BOX_32_01	2.4735	2.5149	0.7432
BOX_32_02	2.3384	2.1345	0.7363
BOX_38_01	3.0186	2.6368	0.7394
BOX_38_02	3.1276	2.2376	0.7324
JOB_2			
TS_01	1.9896	0.7126	-0.0045
PT_01	2.2573	3.5643	0.4190
PT_02	3.1077	3.5331	0.4166
PT_03	3.2264	1.9996	0.4265
PT_04	2.2531	2.0315	0.4236
ANCHOR_01	2.5006	2.9944	0.8038
ANCHOR_02	2.9769	2.8351	0.4238
ANCHOR_03	2.7657	2.1181	0.4424
BOX_32_01	2.4797	2.5288	0.7424
BOX_32_02	2.3388	2.1341	0.7367
BOX_38_01	3.0203	2.6355	0.7437
BOX_38_02	3.1285	2.2423	0.7351

MFV_SANU_TS_MASTER

PtID	East	North	Height
TS_01	0.5678	1.0506	-0.0031
TS_01_PT_01	2.0386	3.7821	0.4171
TS_01_PT_02	2.6536	1.8385	0.4142
TS_01_PT_04	2.8926	0.4985	0.2052
TS_01_PT_07	1.6434	0.5092	0.1398
TS_01_PT_08	1.8350	3.9663	0.1447
TS_01_PT_09	3.6392	3.8665	0.1428
TS_02	4.4216	3.0245	-0.0168
TS_02_PT_03	2.8067	0.8642	0.2406
TS_02_PT_05	2.9020	1.7079	0.3581
TS_02_PT_06	2.6608	3.5814	0.2545
TS_02_PT_07	1.6370	0.5030	0.1371
TS_02_PT_08	1.8267	3.9618	0.1413
TS_02_PT_09	3.6279	3.8647	0.1389
TS_02_PT_10	3.5090	0.4315	0.1266

Appendix 10: DSM Raw Data

MFV Sanu DSM Measurements

Lines of Sight Checklist

	CP_01	CP_02	CP_03	CP_04	CP_05	CP_06	CP_07	CP_08
PT_01	YES	YES	?	NO	NO	NO	YES	YES
PT_02	YES	YES	NO	?	NO	NO	NO	YES
PT_03	NO	?	YES	?	YES	YES	NO	NO
PT_04	YES	YES	NO	NO	NO	NO	YES	YES
PT_05	NO	NO	NO	YES	YES	YES	YES	?
PT_06	NO	NO	NO	YES	YES	YES	YES	NO
PT_07	YES	YES	YES	YES	NO	YES	YES	YES
PT_08	YES	YES	YES	YES	YES	NO	YES	YES
PT_09	YES	YES	YES	YES	YES	YES	YES	YES
PT_10	YES	NO	YES	YES	YES	YES	YES	YES

CP Measurements

	CP_01	CP_02	CP_03	CP_04	CP_05	CP_06	CP_07	CP_08
CP_01		2166	4844	7016	7050	5342	4554	2458
CP-02			3088	5652	6808	6058	6268	4584
CP_03				3054	5308	6126	7700	7040
CP_04					4030	6012	8598	8854
CP_05						3196	6336	7932
CP-06							3274	5332
CP-07								NULL
CP-08								

PT Measurements

	CP_01	CP_02	CP_03	CP_04	CP_05	CP_06	CP_07	CP_08
PT_01	4346	3698	2538	NULL	NULL	NULL	5660	5930
PT_02	3300	3764	NULL	NULL	NULL	NULL	NULL	4184
PT_03	NULL	4076	5014	6296	4696	NULL	NULL	NULL
PT_04	3084	4268	NULL	NULL	NULL	NULL	2576	3198
PT_05	3458	NULL	NULL	5492	3910	NULL	3476	4174
PT_06	NULL	NULL	NULL	3774	2780	NULL	5276	NO CP_06
PT_07	1998	3162	4714	6542	NULL	NULL	3466	2826
PT_08	4472	3694	2312	3338	3396	NULL	5954	6130
PT_09	5392	NULL	4054	4000	1896	NULL	5354	6442
PT_10	3682	NULL	NULL	6900	4834	NULL	2282	3508

Elevation Measurements

CP_01	1.15
CP-02	0.99
CP_03	0.52
CP_04	1.86
CP_05	0.85
CP-06	1.62
CP-07	1.37
CP-08	1.33
PT_01	0.43
PT_02	0.46
PT_03	0.27
PT_04	0.22
PT_05	0.40
PT_06	0.27
PT_07	0.15
PT_08	0.15
PT_09	0.15
PT_10	0.15

MFV_Sanu_DSM_Master

Name	Layer	Easting	Northing	Height
CP_01_TS	2019 Control	-0.005	0.006	1.155
CP_02_TS	2019 Control	-1.053	1.869	1.081
CP_03_TS	2019 Control	-0.295	4.788	0.522
CP_04_TS	2019 Control	1.570	6.806	1.839
CP_05_TS	2019 Control	4.988	4.970	0.836
CP_06_TS	2019 Control	4.978	1.876	1.611
CP_07_TS	2019 Control	4.343	-1.296	1.342
CP_08_TS	2019 Control	1.333	-1.994	1.315
PT_01_TS	2019 Detail	2.039	3.782	0.417
PT_02_TS	2019 Detail	2.654	1.839	0.414
PT_03_TS	2019 Detail	2.807	0.864	0.241
PT_04_TS	2019 Detail	2.893	0.499	0.205
PT_05_TS	2019 Detail	2.902	1.708	0.358
PT_06_TS	2019 Detail	2.661	3.581	0.255
PT_07_TS	2019 Detail	1.637	0.503	0.137
PT_08_TS	2019 Detail	1.827	3.962	0.141
PT_09_TS	2019 Detail	3.628	3.865	0.139
PT_10_TS	2019 Detail	3.509	0.431	0.127
CP_01_DSM	2019 DSM CP	0.004	-0.011	1.150
CP_02_DSM	2019 DSM CP	-1.055	1.848	1.004
CP_03_DSM	2019 DSM CP	-0.293	4.776	0.503
CP_04_DSM	2019 DSM CP	1.541	6.798	1.863
CP_05_DSM	2019 DSM CP	4.993	4.977	0.853
CP_06_DSM	2019 DSM CP	4.977	1.876	1.625
CP_07_DSM	2019 DSM CP	4.351	-1.313	1.362
CP_08_DSM	2019 DSM CP	1.357	-2.038	1.330
PT_01_DSM	2019 DSM PT	2.041	3.774	0.431
PT_02_DSM	2019 DSM PT	2.663	1.834	0.460
PT_03_DSM	2019 DSM PT	2.826	0.851	0.265
PT_04_DSM	2019 DSM PT	2.918	0.513	0.230
PT_05_DSM	2019 DSM PT	2.918	1.699	0.384
PT_06_DSM	2019 DSM PT	2.669	3.567	0.271
PT_07_DSM	2019 DSM PT	1.660	0.496	0.137
PT_08_DSM	2019 DSM PT	1.840	3.951	0.145
PT_09_DSM	2019 DSM PT	3.638	3.856	0.148
PT_10_DSM	2019 DSM PT	3.509	0.410	0.150

MFV_Sanu_PT_DSM

Name	Easting	Northing	Height
PT_01	2.041	3.774	0.431
PT_02	2.663	1.834	0.460
PT_03	2.826	0.851	0.265
PT_04	2.918	0.513	0.230
PT_05	2.918	1.699	0.384
PT_06	2.669	3.567	0.271
PT_07	1.660	0.496	0.137
PT_08	1.840	3.951	0.145
PT_09	3.638	3.856	0.148
PT_10	3.509	0.410	0.150

MFV_SANU_DSM_CP_TS

PtID	East	North	Height
TS_01	-0.1426	2.0076	-0.0076
CP_01	-0.0053	0.0056	1.1546
CP_02	-1.0526	1.8686	1.0814
CP_03	-0.2950	4.7882	0.5217
CP_04	1.5698	6.8060	1.8391
CP_05	4.9884	4.9703	0.8364
CP_06	4.9776	1.8764	1.6110
CP_07	4.3430	-1.2962	1.3422
CP_08	1.3331	-1.9936	1.3153

Appendix 11: *Site Recorder* DSM Report

Site Recorder Demo Copyright (C) 3H Consulting Ltd 1998 - 2017

Report Generated : 12/02/2019 02:21:33

Site

Site Name : MFV_Sanu_DSM

Site Code :

Date Created : 11/02/2019 23:52:01

Last Modified : 12/02/2019 02:19:51

Site Notes : This is a new Site

Units : m

Statistics

Total RMS Residuals : 0.009 m

Distance RMS Resid. : 0.008 m

Height RMS Resid. : 0.013 m

Position RMS Resid. : 0.000 m

Maximum Position Error: PT_10_DSM 10.000

Maximum Height Error : PT_10_DSM 1.000

Unit Variance : 0.052

Redundancy : 0

Distance error (1 SD) : 0.050

Height error (1 SD) : 0.100

Position error (1 SD) : 1.000

Auto Reject : On

Points Used : 17

Points Ignored : 0

Observations Used : 6

Observations Ignored : 0

Observations Rejected : 0

Points :

Name	X	Y	Z	Major	Minor	Theta	Z Error	St.	Layer
PT_03_DSM	2.826	0.851	-0.265	0.000	0.000	0	0.000	F	2019 DSM PT
PT_04_DSM	2.918	0.513	-0.230	0.000	0.000	0	0.000	F	2019 DSM PT
PT_05_DSM	2.918	1.699	-0.384	0.000	0.000	0	0.000	F	2019 DSM PT
PT_06_DSM	2.669	3.567	-0.271	0.000	0.000	0	0.000	F	2019 DSM PT
PT_07_DSM	1.660	0.496	-0.137	0.000	0.000	0	0.000	F	2019 DSM PT
CP_01_DSM	0.004	-0.011	-1.150	0.000	0.000	0	0.000	F	2019 DSM CP
CP_01_TS	-0.005	0.006	-1.155	0.000	0.000	0	0.000	F	2019 Control
CP_02_DSM	-1.055	1.848	-1.004	0.000	0.000	0	0.000	F	2019 DSM CP
CP_02_TS	-1.053	1.869	-1.081	0.000	0.000	0	0.000	F	2019 Control
CP_03_DSM	-0.293	4.776	-0.503	0.000	0.000	0	0.000	F	2019 DSM CP
CP_03_TS	-0.295	4.788	-0.522	0.000	0.000	0	0.000	F	2019 Control
CP_04_DSM	1.541	6.798	-1.863	0.000	0.000	0	0.000	F	2019 DSM CP
CP_04_TS	1.570	6.806	-1.839	0.000	0.000	0	0.000	F	2019 Control
CP_05_DSM	4.993	4.977	-0.853	0.000	0.000	0	0.000	F	2019 DSM CP
CP_05_TS	4.988	4.970	-0.836	0.000	0.000	0	0.000	F	2019 Control
CP_06_DSM	4.977	1.876	-1.625	0.000	0.000	0	0.000	F	2019 DSM CP
CP_06_TS	4.978	1.876	-1.611	0.000	0.000	0	0.000	F	2019 Control
CP_07_DSM	4.351	-1.313	-1.362	0.000	0.000	0	0.000	F	2019 DSM CP
CP_07_TS	4.343	-1.296	-1.342	0.000	0.000	0	0.000	F	2019 Control
CP_08_DSM	1.357	-2.038	-1.330	0.000	0.000	0	0.000	F	2019 DSM CP
CP_08_TS	1.333	-1.994	-1.315	0.000	0.000	0	0.000	F	2019 Control
PT_01_DSM	2.041	3.774	-0.431	0.000	0.000	0	0.000	F	2019 DSM PT
PT_01_TS	2.039	3.782	-0.417	0.000	0.000	0	0.000	F	2019 Detail
PT_02_DSM	2.663	1.834	-0.460	0.000	0.000	0	0.000	F	2019 DSM PT
PT_02_TS	2.654	1.839	-0.414	0.000	0.000	0	0.000	F	2019 Detail
PT_03_TS	2.807	0.864	-0.241	0.000	0.000	0	0.000	F	2019 Detail
PT_04_TS	2.893	0.499	-0.205	0.000	0.000	0	0.000	F	2019 Detail
PT_05_TS	2.902	1.708	-0.358	0.000	0.000	0	0.000	F	2019 Detail
PT_06_TS	2.661	3.581	-0.255	0.000	0.000	0	0.000	F	2019 Detail
PT_07_TS	1.637	0.503	-0.137	0.000	0.000	0	0.000	F	2019 Detail
PT_08_DSM	1.840	3.951	-0.145	0.000	0.000	0	0.000	F	2019 DSM PT
PT_08_TS	1.827	3.962	-0.141	0.000	0.000	0	0.000	F	2019 Detail
PT_09_DSM	3.638	3.856	-0.148	0.000	0.000	0	0.000	F	2019 DSM PT
PT_09_TS	3.628	3.865	-0.139	0.000	0.000	0	0.000	F	2019 Detail

PT_10_DSM	3.509	0.410	-0.150	10.000	10.000	0	1.000		2019 DSM PT
PT_10_TS	3.509	0.431	-0.127	0.000	0.000	0	0.000	F	2019 Detail
PT_03_DSM	2.826	0.851	-0.265	0.000	0.000	0	0.000	F	2019 DSM PT
PT_04_DSM	2.918	0.513	-0.230	0.000	0.000	0	0.000	F	2019 DSM PT
PT_05_DSM	2.918	1.699	-0.384	0.000	0.000	0	0.000	F	2019 DSM PT
PT_06_DSM	2.669	3.567	-0.271	0.000	0.000	0	0.000	F	2019 DSM PT
PT_07_DSM	1.660	0.496	-0.137	0.000	0.000	0	0.000	F	2019 DSM PT
CP_01_DSM	0.004	-0.011	-1.150	0.000	0.000	0	0.000	F	2019 DSM CP
CP_01_TS	-0.005	0.006	-1.155	0.000	0.000	0	0.000	F	2019 Control
CP_02_DSM	-1.055	1.848	-1.004	0.000	0.000	0	0.000	F	2019 DSM CP
CP_02_TS	-1.053	1.869	-1.081	0.000	0.000	0	0.000	F	2019 Control
CP_03_DSM	-0.293	4.776	-0.503	0.000	0.000	0	0.000	F	2019 DSM CP
CP_03_TS	-0.295	4.788	-0.522	0.000	0.000	0	0.000	F	2019 Control
CP_04_DSM	1.541	6.798	-1.863	0.000	0.000	0	0.000	F	2019 DSM CP
CP_04_TS	1.570	6.806	-1.839	0.000	0.000	0	0.000	F	2019 Control
CP_05_DSM	4.993	4.977	-0.853	0.000	0.000	0	0.000	F	2019 DSM CP
CP_05_TS	4.988	4.970	-0.836	0.000	0.000	0	0.000	F	2019 Control
CP_06_DSM	4.977	1.876	-1.625	0.000	0.000	0	0.000	F	2019 DSM CP
CP_06_TS	4.978	1.876	-1.611	0.000	0.000	0	0.000	F	2019 Control
CP_07_DSM	4.351	-1.313	-1.362	0.000	0.000	0	0.000	F	2019 DSM CP
CP_07_TS	4.343	-1.296	-1.342	0.000	0.000	0	0.000	F	2019 Control
CP_08_DSM	1.357	-2.038	-1.330	0.000	0.000	0	0.000	F	2019 DSM CP
CP_08_TS	1.333	-1.994	-1.315	0.000	0.000	0	0.000	F	2019 Control
PT_01_DSM	2.041	3.774	-0.431	0.000	0.000	0	0.000	F	2019 DSM PT
PT_01_TS	2.039	3.782	-0.417	0.000	0.000	0	0.000	F	2019 Detail
PT_02_DSM	2.663	1.834	-0.460	0.000	0.000	0	0.000	F	2019 DSM PT
PT_02_TS	2.654	1.839	-0.414	0.000	0.000	0	0.000	F	2019 Detail
PT_03_TS	2.807	0.864	-0.241	0.000	0.000	0	0.000	F	2019 Detail
PT_04_TS	2.893	0.499	-0.205	0.000	0.000	0	0.000	F	2019 Detail
PT_05_TS	2.902	1.708	-0.358	0.000	0.000	0	0.000	F	2019 Detail
PT_06_TS	2.661	3.581	-0.255	0.000	0.000	0	0.000	F	2019 Detail
PT_07_TS	1.637	0.503	-0.137	0.000	0.000	0	0.000	F	2019 Detail
PT_08_DSM	1.840	3.951	-0.145	0.000	0.000	0	0.000	F	2019 DSM PT
PT_08_TS	1.827	3.962	-0.141	0.000	0.000	0	0.000	F	2019 Detail
PT_09_DSM	3.638	3.856	-0.148	0.000	0.000	0	0.000	F	2019 DSM PT
PT_09_TS	3.628	3.865	-0.139	0.000	0.000	0	0.000	F	2019 Detail
PT_10_DSM	3.509	0.410	-0.150	10.000	10.000	0	1.000		2019 DSM PT

PT_10_TS	3.509	0.431	-0.127	0.000	0.000	0	0.000	F 2019 Detail

Measurements :

Baselines :

From	To.	Meas.	O-C	Error	w-Test	Comment
CP_05_DSM	PT_06_DSM	2.780	-0.000	0.050	0.005	F
CP_04_DSM	CP_08_DSM	8.854	-0.000	0.050	0.006	F
CP_07_DSM	PT_06_DSM	5.276	-0.000	0.050	0.014	F
CP_04_DSM	PT_06_DSM	3.774	-0.000	0.050	0.014	F
CP_07_DSM	PT_05_DSM	3.476	-0.000	0.050	0.014	F
CP_04_DSM	PT_08_DSM	3.338	-0.001	0.050	0.017	F
CP_07_DSM	PT_07_DSM	3.466	-0.001	0.050	0.022	F
CP_04_DSM	PT_10_DSM	6.900	-0.001	0.050	0.204	
CP_04_DSM	PT_09_DSM	4.000	0.001	0.050	0.025	F
CP_05_DSM	CP_06_DSM	3.196	0.001	0.050	0.025	F
CP_01_DSM	CP_04_DSM	7.016	-0.001	0.050	0.025	F
CP_05_DSM	PT_09_DSM	1.896	0.001	0.050	0.028	F
CP_03_DSM	PT_09_DSM	4.054	0.001	0.050	0.030	F
CP_04_DSM	CP_07_DSM	8.598	-0.001	0.050	0.031	F
CP_01_DSM	CP_06_DSM	5.342	0.001	0.050	0.036	F
CP_02_DSM	CP_08_DSM	4.584	-0.001	0.050	0.038	F
CP_05_DSM	PT_03_DSM	4.696	-0.001	0.050	0.046	F
CP_02_DSM	PT_03_DSM	4.076	0.002	0.050	0.053	F
CP_04_DSM	CP_05_DSM	4.030	-0.002	0.050	0.076	F
CP_05_DSM	PT_05_DSM	3.910	0.003	0.050	0.075	F
CP_03_DSM	PT_01_DSM	2.538	-0.003	0.050	0.099	F
CP_02_DSM	CP_05_DSM	6.808	-0.003	0.050	0.099	F
CP_02_DSM	CP_04_DSM	5.652	-0.004	0.050	0.107	F
CP_03_DSM	PT_08_DSM	2.312	-0.004	0.050	0.093	F
CP_03_DSM	CP_04_DSM	3.054	0.004	0.050	0.148	F
CP_07_DSM	PT_09_DSM	5.354	-0.004	0.050	0.104	F
CP_01_DSM	CP_03_DSM	4.844	0.004	0.050	0.112	F
CP_07_DSM	PT_01_DSM	5.660	-0.004	0.050	0.109	F
CP_04_DSM	CP_06_DSM	6.012	0.004	0.050	0.132	F
CP_07_DSM	PT_08_DSM	5.954	-0.005	0.050	0.113	F
CP_03_DSM	PT_07_DSM	4.714	-0.005	0.050	0.115	F

CP_02_DSM	CP_07_DSM	6.268	-0.005	0.050	0.138	F
CP_08_DSM	PT_08_DSM	6.130	0.005	0.050	0.122	F
CP_04_DSM	PT_03_DSM	6.296	0.005	0.050	0.136	F
CP_03_DSM	PT_03_DSM	5.014	-0.005	0.050	0.145	F
CP_05_DSM	PT_08_DSM	3.396	0.006	0.050	0.153	F
CP_03_DSM	CP_05_DSM	5.308	0.006	0.050	0.190	F
CP_08_DSM	PT_02_DSM	4.184	0.006	0.050	0.257	F
CP_02_DSM	PT_02_DSM	3.764	0.006	0.050	0.257	F
CP_02_DSM	PT_04_DSM	4.268	0.006	0.050	0.176	F
CP_03_DSM	CP_06_DSM	6.126	0.006	0.050	0.183	F
CP_02_DSM	CP_06_DSM	6.058	-0.006	0.050	0.183	F
CP_03_DSM	CP_07_DSM	7.700	-0.007	0.050	0.178	F
CP_07_DSM	PT_04_DSM	2.576	-0.007	0.050	0.219	F
CP_04_DSM	PT_07_DSM	6.542	0.007	0.050	0.202	F
CP_02_DSM	PT_01_DSM	3.698	0.007	0.050	0.187	F
CP_05_DSM	CP_07_DSM	6.336	-0.007	0.050	0.210	F
CP_01_DSM	PT_05_DSM	3.458	-0.007	0.050	0.213	F
CP_04_DSM	PT_05_DSM	5.492	0.007	0.050	0.223	F
CP_06_DSM	CP_08_DSM	5.332	-0.008	0.050	0.249	F
CP_01_DSM	PT_07_DSM	1.998	-0.008	0.050	0.229	F
CP_02_DSM	PT_07_DSM	3.162	0.008	0.050	0.203	F
CP_01_DSM	PT_09_DSM	5.392	-0.009	0.050	0.208	F
CP_08_DSM	PT_07_DSM	2.826	0.009	0.050	0.234	F
CP_08_DSM	PT_01_DSM	5.930	0.009	0.050	0.228	F
CP_01_DSM	PT_02_DSM	3.300	-0.010	0.050	0.257	F
CP_01_DSM	PT_08_DSM	4.472	-0.010	0.050	0.230	F
CP_01_DSM	CP_07_DSM	4.554	0.011	0.050	0.336	F
CP_01_DSM	CP_05_DSM	7.050	-0.011	0.050	0.313	F
CP_08_DSM	PT_04_DSM	3.198	0.012	0.050	0.431	F
CP_01_DSM	PT_01_DSM	4.346	-0.012	0.050	0.295	F
CP_08_DSM	PT_09_DSM	6.442	0.012	0.050	0.301	F
CP_06_DSM	CP_07_DSM	3.274	0.013	0.050	0.389	F
CP_01_DSM	PT_10_DSM	3.682	0.013	0.050	0.330	
CP_02_DSM	PT_08_DSM	3.694	0.013	0.050	0.321	F
CP_07_DSM	PT_10_DSM	2.282	0.013	0.050	0.019	
CP_01_DSM	CP_08_DSM	2.458	0.014	0.050	0.390	F
CP_08_DSM	PT_05_DSM	4.174	0.015	0.050	0.355	F

CP_01_DSM	PT_04_DSM	3.084	-0.016	0.050	0.430	F
CP_05_DSM	CP_08_DSM	7.932	0.017	0.050	0.476	F
CP_05_DSM	PT_10_DSM	4.834	-0.020	0.050	0.031	
CP_03_DSM	CP_08_DSM	7.040	-0.020	0.050	0.518	F
CP_02_DSM	CP_03_DSM	3.088	0.021	0.050	0.609	F
CP_01_DSM	CP_02_DSM	2.166	0.022	0.050	0.571	F
CP_08_DSM	PT_10_DSM	3.508	0.042	0.050	0.345	
CP_05_DSM	PT_06_DSM	2.780	-0.000	0.050	0.005	F
CP_04_DSM	CP_08_DSM	8.854	-0.000	0.050	0.006	F
CP_07_DSM	PT_06_DSM	5.276	-0.000	0.050	0.014	F
CP_04_DSM	PT_06_DSM	3.774	-0.000	0.050	0.014	F
CP_07_DSM	PT_05_DSM	3.476	-0.000	0.050	0.014	F
CP_04_DSM	PT_08_DSM	3.338	-0.001	0.050	0.017	F
CP_07_DSM	PT_07_DSM	3.466	-0.001	0.050	0.022	F
CP_04_DSM	PT_10_DSM	6.900	-0.001	0.050	0.204	
CP_04_DSM	PT_09_DSM	4.000	0.001	0.050	0.025	F
CP_05_DSM	CP_06_DSM	3.196	0.001	0.050	0.025	F
CP_01_DSM	CP_04_DSM	7.016	-0.001	0.050	0.025	F
CP_05_DSM	PT_09_DSM	1.896	0.001	0.050	0.028	F
CP_03_DSM	PT_09_DSM	4.054	0.001	0.050	0.030	F
CP_04_DSM	CP_07_DSM	8.598	-0.001	0.050	0.031	F
CP_01_DSM	CP_06_DSM	5.342	0.001	0.050	0.036	F
CP_02_DSM	CP_08_DSM	4.584	-0.001	0.050	0.038	F
CP_05_DSM	PT_03_DSM	4.696	-0.001	0.050	0.046	F
CP_02_DSM	PT_03_DSM	4.076	0.002	0.050	0.053	F
CP_04_DSM	CP_05_DSM	4.030	-0.002	0.050	0.076	F
CP_05_DSM	PT_05_DSM	3.910	0.003	0.050	0.075	F
CP_03_DSM	PT_01_DSM	2.538	-0.003	0.050	0.099	F
CP_02_DSM	CP_05_DSM	6.808	-0.003	0.050	0.099	F
CP_02_DSM	CP_04_DSM	5.652	-0.004	0.050	0.107	F
CP_03_DSM	PT_08_DSM	2.312	-0.004	0.050	0.093	F
CP_03_DSM	CP_04_DSM	3.054	0.004	0.050	0.148	F
CP_07_DSM	PT_09_DSM	5.354	-0.004	0.050	0.104	F
CP_01_DSM	CP_03_DSM	4.844	0.004	0.050	0.112	F
CP_07_DSM	PT_01_DSM	5.660	-0.004	0.050	0.109	F
CP_04_DSM	CP_06_DSM	6.012	0.004	0.050	0.132	F
CP_07_DSM	PT_08_DSM	5.954	-0.005	0.050	0.113	F

CP_03_DSM	PT_07_DSM	4.714	-0.005	0.050	0.115	F
CP_02_DSM	CP_07_DSM	6.268	-0.005	0.050	0.138	F
CP_08_DSM	PT_08_DSM	6.130	0.005	0.050	0.122	F
CP_04_DSM	PT_03_DSM	6.296	0.005	0.050	0.136	F
CP_03_DSM	PT_03_DSM	5.014	-0.005	0.050	0.145	F
CP_05_DSM	PT_08_DSM	3.396	0.006	0.050	0.153	F
CP_03_DSM	CP_05_DSM	5.308	0.006	0.050	0.190	F
CP_08_DSM	PT_02_DSM	4.184	0.006	0.050	0.257	F
CP_02_DSM	PT_02_DSM	3.764	0.006	0.050	0.257	F
CP_02_DSM	PT_04_DSM	4.268	0.006	0.050	0.176	F
CP_03_DSM	CP_06_DSM	6.126	0.006	0.050	0.183	F
CP_02_DSM	CP_06_DSM	6.058	-0.006	0.050	0.183	F
CP_03_DSM	CP_07_DSM	7.700	-0.007	0.050	0.178	F
CP_07_DSM	PT_04_DSM	2.576	-0.007	0.050	0.219	F
CP_04_DSM	PT_07_DSM	6.542	0.007	0.050	0.202	F
CP_02_DSM	PT_01_DSM	3.698	0.007	0.050	0.187	F
CP_05_DSM	CP_07_DSM	6.336	-0.007	0.050	0.210	F
CP_01_DSM	PT_05_DSM	3.458	-0.007	0.050	0.213	F
CP_04_DSM	PT_05_DSM	5.492	0.007	0.050	0.223	F
CP_06_DSM	CP_08_DSM	5.332	-0.008	0.050	0.249	F
CP_01_DSM	PT_07_DSM	1.998	-0.008	0.050	0.229	F
CP_02_DSM	PT_07_DSM	3.162	0.008	0.050	0.203	F
CP_01_DSM	PT_09_DSM	5.392	-0.009	0.050	0.208	F
CP_08_DSM	PT_07_DSM	2.826	0.009	0.050	0.234	F
CP_08_DSM	PT_01_DSM	5.930	0.009	0.050	0.228	F
CP_01_DSM	PT_02_DSM	3.300	-0.010	0.050	0.257	F
CP_01_DSM	PT_08_DSM	4.472	-0.010	0.050	0.230	F
CP_01_DSM	CP_07_DSM	4.554	0.011	0.050	0.336	F
CP_01_DSM	CP_05_DSM	7.050	-0.011	0.050	0.313	F
CP_08_DSM	PT_04_DSM	3.198	0.012	0.050	0.431	F
CP_01_DSM	PT_01_DSM	4.346	-0.012	0.050	0.295	F
CP_08_DSM	PT_09_DSM	6.442	0.012	0.050	0.301	F
CP_06_DSM	CP_07_DSM	3.274	0.013	0.050	0.389	F
CP_01_DSM	PT_10_DSM	3.682	0.013	0.050	0.330	
CP_02_DSM	PT_08_DSM	3.694	0.013	0.050	0.321	F
CP_07_DSM	PT_10_DSM	2.282	0.013	0.050	0.019	
CP_01_DSM	CP_08_DSM	2.458	0.014	0.050	0.390	F

CP_08_DSM	PT_05_DSM	4.174	0.015	0.050	0.355	F
CP_01_DSM	PT_04_DSM	3.084	-0.016	0.050	0.430	F
CP_05_DSM	CP_08_DSM	7.932	0.017	0.050	0.476	F
CP_05_DSM	PT_10_DSM	4.834	-0.020	0.050	0.031	
CP_03_DSM	CP_08_DSM	7.040	-0.020	0.050	0.518	F
CP_02_DSM	CP_03_DSM	3.088	0.021	0.050	0.609	F
CP_01_DSM	CP_02_DSM	2.166	0.022	0.050	0.571	F
CP_08_DSM	PT_10_DSM	3.508	0.042	0.050	0.345	

Heights :

Point	Meas.	O-C	Error	w-Test	Comment
PT_10_DSM		-0.150	0.000	0.100	0.163
CP_01_DSM		-1.150	0.000	0.100	0.004
CP_08_DSM		-1.330	0.000	0.100	0.007
PT_02_DSM		-0.460	-0.000	0.100	0.187
PT_06_DSM		-0.270	0.001	0.100	0.014
PT_01_DSM		-0.430	0.001	0.100	0.088
PT_09_DSM		-0.150	-0.002	0.100	0.031
CP_04_DSM		-1.860	0.003	0.100	0.057
CP_05_DSM		-0.850	0.003	0.100	0.074
PT_03_DSM		-0.270	-0.005	0.100	0.152
CP_06_DSM		-1.620	0.005	0.100	0.126
PT_08_DSM		-0.150	-0.005	0.100	0.066
CP_07_DSM		-1.370	-0.008	0.100	0.324
PT_04_DSM		-0.220	0.010	0.100	0.205
PT_07_DSM		-0.150	-0.013	0.100	0.152
CP_02_DSM		-0.990	0.014	0.100	0.399
PT_05_DSM		-0.400	-0.016	0.100	0.226
CP_03_DSM		-0.520	-0.017	0.100	0.317
PT_07_TS		-0.137	0.000	0.100	0.000
PT_09_TS		-0.139	0.000	0.100	0.000
PT_03_TS		-0.241	0.000	0.100	0.000
CP_04_TS		-1.839	0.000	0.100	0.000
CP_07_TS		-1.342	0.000	0.100	0.000
PT_08_TS		-0.141	0.000	0.100	0.000
CP_06_TS		-1.611	0.000	0.100	0.000
PT_04_TS		-0.205	0.000	0.100	0.000

PT_02_TS	-0.414	0.000	0.100	0.000
CP_08_TS	-1.315	0.000	0.100	0.000
CP_02_TS	-1.081	0.000	0.100	0.000
PT_10_TS	-0.127	0.000	0.100	0.000
PT_06_TS	-0.255	0.000	0.100	0.000
PT_05_TS	-0.358	0.000	0.100	0.000
CP_05_TS	-0.836	0.000	0.100	0.000
PT_01_TS	-0.417	0.000	0.100	0.000
CP_03_TS	-0.522	0.000	0.100	0.000
CP_01_TS	1.155	2.310	0.100	0.000
PT_10_DSM	-0.150	0.000	0.100	0.163
CP_01_DSM	-1.150	0.000	0.100	0.004
CP_08_DSM	-1.330	0.000	0.100	0.007
PT_02_DSM	-0.460	-0.000	0.100	0.187
PT_06_DSM	-0.270	0.001	0.100	0.014
PT_01_DSM	-0.430	0.001	0.100	0.088
PT_09_DSM	-0.150	-0.002	0.100	0.031
CP_04_DSM	-1.860	0.003	0.100	0.057
CP_05_DSM	-0.850	0.003	0.100	0.074
PT_03_DSM	-0.270	-0.005	0.100	0.152
CP_06_DSM	-1.620	0.005	0.100	0.126
PT_08_DSM	-0.150	-0.005	0.100	0.066
CP_07_DSM	-1.370	-0.008	0.100	0.324
PT_04_DSM	-0.220	0.010	0.100	0.205
PT_07_DSM	-0.150	-0.013	0.100	0.152
CP_02_DSM	-0.990	0.014	0.100	0.399
PT_05_DSM	-0.400	-0.016	0.100	0.226
CP_03_DSM	-0.520	-0.017	0.100	0.317
PT_07_TS	-0.137	0.000	0.100	0.000
PT_09_TS	-0.139	0.000	0.100	0.000
PT_03_TS	-0.241	0.000	0.100	0.000
CP_04_TS	-1.839	0.000	0.100	0.000
CP_07_TS	-1.342	0.000	0.100	0.000
PT_08_TS	-0.141	0.000	0.100	0.000
CP_06_TS	-1.611	0.000	0.100	0.000
PT_04_TS	-0.205	0.000	0.100	0.000
PT_02_TS	-0.414	0.000	0.100	0.000

CP_08_TS	-1.315	0.000	0.100	0.000
CP_02_TS	-1.081	0.000	0.100	0.000
PT_10_TS	-0.127	0.000	0.100	0.000
PT_06_TS	-0.255	0.000	0.100	0.000
PT_05_TS	-0.358	0.000	0.100	0.000
CP_05_TS	-0.836	0.000	0.100	0.000
PT_01_TS	-0.417	0.000	0.100	0.000
CP_03_TS	-0.522	0.000	0.100	0.000
CP_01_TS	1.155	2.310	0.100	0.000

Positions :

Point	Type	Meas.	O-C	Error	w-Test	Comment

Offsets :

Name	Along	Offset	Side	Comment

Ties :

Name	Along1	Offset1	Along2	Offset2	AlongC	OffsetC	Side	Residual	Comment

Radial :

From	To.	Dist.	Azim.	Comment